6-30-2016

Emodin Regulates Macrophage Polarization: Application In Breast Cancer Treatment

Stephen Iwanowycz
University of South Carolina

EMODIN REGULATES MACROPHAGE POLARIZATION: APPLICATION IN BREAST CANCER TREATMENT

By

Stephen Iwanowycz

Bachelor of Science
Bob Jones University, 2011

Submitted in Partial Fulfillment of the Requirements

For the Degree of Doctor of Philosophy in

Biomedical Science

School of Medicine

University of South Carolina

2016

Accepted by:

Daping Fan, Major Professor

Jay Potts, Committee Member

Angela Murphy, Committee Member

Narendra Singh, Committee Member

Hexin Chen, Committee Member

Lacy Ford, Senior Vice Provost and Dean of Graduate Studies

DEDICATION

To my wife, Trisha, whose loving support made this work possible. Thank you for putting up with all the long nights. Thank you for taking care of so much at home and allowing me to put so much time and energy into research. Thank you for the constant encouragement and for not letting me dwell on the many failed experiments. Thank you for how you care for our son, Matthias.

ACKNOWLEDGEMENTS

I would like to thank those who have spent time in the lab of Dr. Daping Fan for the countless conversations and advice that they provided. I would particularly like to acknowledge Xuemei Jia and Junfeng Wang for their encouragement along the way and the training they provided. I would also like to thank Yuezhen Wang for her help with all of the immunohistochemical staining and Yvonne Hui for her help with protein and nucleic acid analysis. I also thank the staff of the University of South Carolina's IRF for their training and guidance in microscopy and flow cytometry. I also thank Diego Altomare for his help with the microarray experiments. I also would like to thank those who served on my advisory committee, Jay Potts, Angela Murphy, Narendra Singh, and Hexin Chen for their invaluable advice in designing and carrying out this study. Finally I would like to thank my mentor Dr. Daping Fan for his guidance and support, and also for his constant encouragement for working smarter.

This work was supported, in whole or in part, by National Institutes of Health Grants HL116626 and AT003961-8455.

ABSTRACT

Macrophages are pleiotropic cells capable of performing a broad spectrum of functions. Their phenotypes are classified along a continuum between the extremes of pro-inflammatory M1 macrophages and anti-inflammatory M2 macrophages. The seemingly opposing functions of M1 and M2 macrophages must be tightly regulated for an effective inflammatory response to foreign molecules or damaged tissue. Excessive activation of either M1 or M2 macrophages contributes to the pathology of many diseases. Infiltration of macrophages into breast tumors correlates with increased metastasis and decreased patient survival. Tumors recruit macrophages to the primary site as well as pre-metastatic niches, and educate them to adopt an M2-like phenotype, thereby creating a growth-promoting immunosuppressive microenvironment. Emodin is a Chinese herb-derived single compound and has shown potential to inhibit macrophage activation and to prevent tumor growth. In this study, the effects of emodin on macrophage response to M1 or M2 stimuli were investigated. Further, emodin was used to treat mice bearing breast tumors and its effect on tumor cell-macrophage interactions was examined. Emodin was found to bi-directionally tune the activation of macrophages induced by LPS/IFNγ or IL4 through inhibiting NFkB/IRF5/STAT1 or IRF4/STAT6 signaling pathways respectively. Furthermore, emodin inhibited the removal of H3K27m3 and the placement of H3K27ac histone modifications on genes associated with macrophage activation. In mice bearing breast cancer, emodin treatment attenuated tumor growth by reducing macrophage infiltration into the primary tumors and subsequent M2-

like polarization. Reduced accumulation of M2-like macrophages in the tumors leads to increased T cell activation and decreased angiogenesis. Emodin was shown to suppress infiltration and M2-like polarization of TAMs by targeting the TAM-tumor interaction. Emodin inhibited macrophage M2-like polarization in response to tumor cell secreted molecules, inhibited tumor cell recruitment of macrophages through reducing CCL2 and CSF1 expression, and block tumor cell-macrophage adhesion. In conclusion, our data suggest that emodin is uniquely able to suppress excessive response of macrophages to both M1 and M2 stimuli, and that emodin has potential as a new anti-breast cancer therapy.

TABLE OF CONTENTS

Dedication ii

Acknowledgements iii

Abstract iv

List of tables viii

List of figures ix

Chapter 1: Introduction 1

1.1 Macrophages and their Phenotypes 1

1.2 Macrophages in disease 3

1.3 Macrophages and cancer 7

1.4 Emodin and inflammatory disease 11

1.5 Emodin and Cancer 15

Chapter 2: Emodin is a bidirectional modulator of macrophage activation 19

2.1 Background 19

2.2 Detailed Methods 20

2.3 Results 27

2.4 Discussion 34

Chapter 3: Emodin inhibits breast cancer growth by modulating the tumor microenvironment 54

3.1 Background 54

3.2 Detailed Methods 55

3.3 Results 63

3.4 Discussion 69

Chapter 4: Conclusions and future perspectives 83

References 88

LIST OF TABLES

Table 2.1 Antibodies used for western blots and ChIP procedures. 40

Table 2.2 Primers for RT-qPCR 41

Table 2.3 Primers for ChIP-qPCR. 41

Table 2.4 List of genes reciprocally regulated by emodin 42

Table 2.5 List of histone modifying enzymes regulated by emodin 43

Table 3.1 Primers for RT-qPCR. 73

LIST OF FIGURES

Figure 1.1 Structure of Emodin 18

Figure 1.2 Serum Concentration of Emodin 18

Figure 2.1 DNA fragmentation for ChIP assays 44

Figure 2.2 Emodin inhibits LPS/IFNγ and IL4 induced transcriptional changes in macrophages 45

Figure 2.3 Emodin inhibits the induction of signaling pathways associated with macrophage polarization and function 46

Figure 2.4 Effects of emodin on the expression of genes that regulate macrophage activation 47

Figure 2.5 Emodin inhibits expression of M1 and M2 genes 49

Figure 2.6 Emodin modulates functions of activated macrophages 50

Figure 2.7 Emodin inhibits LPS/IFNγ and IL4 induced activation of signaling pathways 51

Figure 2.8 Emodin inhibits LPS/IFNγ and IL4 induced histone modifications in macrophages 52

Figure 2.9 Emodin inhibits macrophage memory 53

Figure 3.1 Emodin inhibits growth of breast tumors 74

Figure 3.2 Emodin inhibits macrophage infiltration into tumors and activation 75

Figure 3.3 Emodin inhibits macrophage response to tumor cell secreted factors 77

Figure 3.4 Emodin inhibits macrophage suppression of T cell activation and support of angiogenesis 78

Figure 3.5 Emodin inhibits tumor cell recruitment of macrophages 80

Figure 3.6 Emodin inhibits macrophage adhesion to tumor cells 81

Figure 3.7 Emodin induces T cell apoptosis.....82

CHAPTER 1

INTRODUCTION

1.1 MACROPHAGES AND THEIR PHENOTYPES

Macrophages are a heterogeneous population of innate immune cells that reside in most tissues in the body (1,2). Tissue populations of macrophages were once thought to be entirely derived from blood monocytes; however, recent research has shown that most populations of macrophage originate from yoke sac precursors, with the exception of those in the gastrointestinal tract (3-5). Under normal physiological conditions, tissue populations are maintained through local proliferation without the need for monocyte recruitment. Following injury or infection blood monocytes can be recruited to bolster the local population; however, the role of tissue resident and monocyte derived macrophages in different tissues is still under debate (6-9). Macrophages were first identified by their ability to eat invading organisms, and initial research on macrophages was focused on their functions in tissue defense. However, it has since been discovered that macrophages also play substantial roles in normal tissue homeostasis as well as wound repair (10-12). Macrophages are highly plastic cells which are constantly sampling their environment and adapting their phenotype to the signals that they encounter. Macrophages display a spectrum of phenotypes at either end of which are M1 macrophages and M2 macrophages which mirror the Th1/Th2 classification system of T cells (13-15). M1 macrophages are classical pro-inflammatory macrophages which support tissue defense. M2 macrophages are non-classical “alternatively” activated cells which include a wide

range of phenotypes such as immune regulatory or tissue growth promoting. These seemingly opposing functions of defense and repair need to be tightly regulated for a proper response.

Macrophage polarization is regulated by a large number of transcriptional and epigenetic signaling pathways which coordinate to fine tune the response to environmental signals (14,16). Th1 cytokines (such as IFNγ and TNFα) and bacterial products (such as LPS) induce macrophages to adopt a pro-inflammatory (M1) phenotype characterized by the secretion of high amounts of inflammatory cytokines and reactive oxygen and nitrogen species. IFNγ and TNFα activate the JAK/STAT cascade and lead to STAT1 activation, while LPS activates the NFκB and MAPK cascade upon ligation with TLR4. M1 macrophages can kill invading organisms through secretion of proinflammatory mediators, phagocytic engulfment, or production of reactive species. M1 macrophages also express costimulatory molecules and can activate $CD4^+$ T cells. A combination of stimuli including Th2 cytokines (such as IL4, IL10, and IL13), growth factors (such as TGFβ, CSF1), glucocorticoids, and immune complexes, can polarize macrophages toward an anti-inflammatory M2 phenotype (17). M2 macrophages have major roles in tissue homeostasis and repair, inflammation resolution, and immune regulation. M2 macrophages are characterized by high expression of Arg1, YM1, Mrc1, and IL10, and low expression of pro-inflammatory cytokines (11). IL4/IL13 signal through the common IL4ra receptor and lead to STAT6 phosphorylation and activation which, along with several other secondary transcription factors, including IRF4, PPARγ and KLF4, fine tune transcriptional responses in the cells (16,18-21). IRF4 induces the M2 phenotype in response to parasite infections, and is regulated through the removal of

H3K27m3 by the histone demethylase JMJD3 (22,23). Many of these signaling pathways have shown to be antagonistic, which promotes the exclusive nature of the M1 and M2 phenotypes. STAT6 and STAT1 can competitively bind to the same DNA sequence to inhibit each other (16,24). STAT6 can also inhibit NFκB DNA binding (25). IRF5 is activated by TLR4 ligation and promotes the transcription of pro-inflammatory genes (IL12b) while also suppressing the expression of anti-inflammatory genes (IL10) (16,26). IRF4 competitively binds to MyD88 and is a negative regulator of IRF5 signaling (27). Macrophage are also able to retain a memory for the signals that they have been exposed to through epigenetic modification, which results in increased transcription (priming) or repressed transcription (tolerance) upon future exposure (28-31). Cytokines cause the addition of positive histone modifications H3K4m3 or H3K27ac to gene promoters which lead to increased expression (32,33). The mechanisms of tolerance are incompletely understood but could involve the loss of positive histone modifications and/or an increase in negative histone modifications (such as H3K27m3) (31).

1.2 MACROPHAGES IN DISEASE

An imbalance in macrophage phenotypes has been shown to contribute to the pathology of a large number of diseases (34-36).The same mechanisms by which M1 macrophages kill invading pathogens can also damage host cells. Excessive or chronic M1 macrophage activation promotes tissue damage in neurodegenerative disorders, arthritis, and autoimmune diseases (34,37,38). M1 macrophages are necessary to the initial stages of the wound healing response to remove debris from the area; however, prolonged M1 activation inhibits the healing of damaged tissue through excessive matrix degradation and inhibition of tissue regeneration (39,40). Inflammatory mediators

released from M1 macrophages inhibit the secretion of ECM proteins and increase the secretion of proteases. This effect has been seen in many pathologies including ischemia/reperfusion injury in the myocardium, diabetic chronic wounds, and central nervous system injuries (37,39,41,42). Further, increased inflammatory monocyte/macrophage infiltration has been shown to correlate with disease severity in patients with myocardial infarction, atherosclerosis, and metabolic disorders (43-46). Chronic M1 activation has also been shown to promote the development of cancer (34,47,48) through creating mutagenic environments. Patients with inflammatory bowel disease or chronic lung inflammation, caused by infections or particulate inhalation, have been shown to have greatly increased risks for colon or lung cancer respectively (49,50). Shifting the balance toward M2 macrophages has been shown to be beneficial in some experimental models; however, prolonged or excessive M2 macrophage activation can also be detrimental.

M2 macrophages contribute to allergic inflammation and lung damage through the secretion of Th2 cytokines IL4 and IL13, (35,36), and the recruitment of eosinophils (51). Macrophages have also been shown to impair functions of many organs including the lungs, liver, and pancreas through promoting fibrosis (52). M2 macrophages can indirectly increase ECM deposition by recruiting fibroblasts and inducing them to become myofibroblasts through secretion of growth factors TGF-β and PDGF and can directly regulate ECM turnover through production of MMPs and TIMPs (53). Further, M2 macrophage infiltration correlates with increased cancer growth and metastasis in multiple types of cancer (36,54). While M1 macrophages have been shown to promote tumor initiation, as tumors develop, tumor associated macrophages (TAMs) are educated

to adopt a pro-tumor M2-like phenotype (55). Macrophages are the largest population of tumor infiltrating immune cells in many solid tumors (56). Tumor cells recruit and educate macrophages toward an M2-like phenotype through secretion of soluble mediators (such as CSF1, CCL2, IL10, and TGFβ), and through direct cell-cell interactions (57-59). TAMs in turn create a niche to support tumor stem cells growth and survival (60). TAMs protect tumors from immune response through secreting anti-inflammatory cytokines (such as IL10) and the depletion of metabolites (through Arg1 and iNOS) (61,62). Further, TAMs promote angiogenesis through secreting VEGF and proteases (MMPs) to remodel the extra cellular matrix (63,64). TAMs also promote tumor cell migration toward blood vessels and intravasation (65). Macrophages at distant sites have also been shown to be trained by signals released from the primary tumor to create environments receptive to circulating tumor cells termed pre-"metastatic niche"(66). These macrophages support tumor cell extravasation and colonization of the tissue through remodeling the ECM and promoting angiogenesis.

Many strategies have been developed to target macrophage-driven inflammation in experimental disease models including: macrophage recruitment, survival, and activation. However, translating therapies from experimental models to clinical settings has had mixed results. Inhibiting macrophage recruitment to tumors through blocking CCL2/CCR2 signaling has shown great potential in pre-clinical studies and has advanced to clinical studies for treatment of bone metastasis and pancreatic cancer (67). Similarly, inhibition of macrophage adhesion molecules (CD11/CD18) reduced macrophage infiltration into the myocardium post MI and improved healing in animal models; however, it was not effective in clinical trials (68). Monoclonal antibodies have been

developed to block macrophage activation by targeting cytokines/chemokines (or their receptors) such as TNFα and IL1. Anti-TNFα therapy has shown to be effective in treating arthritis, but not other inflammatory conditions including multiple sclerosis and I/R injury (69). Targeting the CSF1 axis has shown strong potential in cancer treatment. CSF1/r1 inhibition greatly decreased macrophage infiltration into mouse mammary tumors which led to an increase T cell response (70). CSFr1 also sensitized pancreatic tumors to T cell check point blockade (71). Inhibition of macrophage activation by HDAC inhibitors has also shown therapeutic potential for a variety of inflammatory diseases and cancers (72,73).

There have been many challenges in developing macrophage-targeting therapies for clinical use (69). If treatment is administered too late during the disease, irreversible tissue damage can occur; therefore, targeting the macrophage/inflammatory component of disease would likely require chronic therapies to be administered early during disease progression. Further, most current treatments target one molecule or pathway, but there are many redundant and compensatory pathways built into the inflammatory responses. Therefore, there is much interest in herb derived compounds since they can modulate multiple inflammatory pathways, are inexpensive, and have low toxicity for chronic treatment (74). Many compounds have shown potential to inhibit macrophage activation; however, experimental studies with these compounds has focused on responses to stimuli which induce a narrow range of activation (either M1 or M2 phenotypes but not both) (74-77). A compound which could inhibit a broad range of macrophage phenotypes through regulation of multiple signaling pathways would have great clinical potential.

1.3 MACROPHAGES AND CANCER

M1 macrophages have been shown to promote tumor initiation by contributing to chronic inflammation. Approximately 25% of cancers are related to chronic infections and inflammation (49). However, as tumors grow the phenotype of macrophages switches toward a M2-like tissue growth-promoting phenotype (47,55). Tumor cells recruit and educate macrophages toward a M2-like phenotype through secreting a spectrum of chemokines and cytokines (with CCL2 and CSF1 being two of the most important (59)), through direct cell-cell interactions, and through the creation of a hypoxic microenvironment (57,78-80). Tumor signals trigger M2-like phenotype through activating multiple signaling pathways including STAT1, 3, and 6, C/EBPβ, PPARγ, and IRF4 (55,81-84). Macrophages in turn secrete growth factors (such as EGF and VEGF) which promote tumor cell growth and migration toward and into blood vessels, promote angiogenesis, and inhibit immune response (65,85). TAMs generally express high levels of scavenger, mannose, and galactose receptors; low levels of co-stimulatory molecules, and their metabolism is shifted to ornithine and polyamine production (67).

M1 macrophages have the potential to inhibit tumor growth and help mediate the effectiveness of immunotherapies. Infiltration of M1 macrophages has been correlated with a favorable prognosis in numerous cancers, including colon, cervical, and lung cancer (86-88). Macrophage cytotoxicity toward cancer cells has been known for nearly four decades. Tagliabue and colleagues found that adherent phagocytic cells isolated from the peripheral blood or the peritoneal cavity of mice were selectively able to kill tumor cells (89). These cells were specifically identified as macrophages and not natural killer cells. Similarly Urban et al. showed that activated macrophages were able to

directly kill tumor cells in a TNFα dependent manner (90). More recent studies have shown the therapeutic benefit of activating tumor associated macrophages toward an M1 phenotype. Stimulating macrophages with tumor cell lysate enhanced their expression of co-stimulatory molecules (91). Vaccination of mice with these macrophages attenuated tumor growth and increased T cell activation. Guiducci and colleagues reported that adenoviral delivery of chemoattractant CCL16 and activation of macrophages with CpG and an IL10 receptor antagonistic antibody shifted TAM phenotype toward M1 and led to rapid de-bulking of breast and colon tumors in mice (92). Tumor regression was dependent on direct killing of tumor cells by macrophages and activation of T cells by dendritic cells. Many experimental studies have demonstrated similar results, revealing that tumor regression requires the interplay between M1 macrophages and T cells. In myeloma models, Th1 stimulated macrophages are necessary for the killing of tumor cells (93). Furthermore, M1 macrophages have been shown to play a major role in the effectiveness of immunotherapies. Injection of tumor bearing mice with a synthetic vaccine led to tumor regression which was dependent on recruitment and activated of M1 macrophages by $CD8^+$ T cells (94). Similarly, macrophages have been shown to mediate tumor killing following monoclonal antibody therapy (95-97).

However, in spite of macrophage's natural cytotoxic potential, macrophage infiltration into tumors is most often associated with worse clinical outcomes. Over 80% of immunohistochemical studies performed on human tumors have shown that increased TAM infiltration is associated with worse clinical prognosis (98). This is likely because the majority of TAM's adopt a pro-tumor M2-like phenotype (98). Particularly in breast cancer, studies have shown that macrophage infiltration and M2-like polarization are

associated with increased angiogenesis and metastasis and reduced survival (54,99,100). Macrophage chemoattractant MCP1/CCL2 has been correlated with increased TAM infiltration and was a significant indicator in early relapse (101). DeNardo and colleagues revealed that there was an inverse association between $CD68^+$ macrophages and $CD8^+$ T lymphocytes in human breast cancer tissues and that there was increased macrophage infiltration into the tumors from patients who had received neoadjuvant chemotherapy compared to those treated with surgery alone (102). Further, the ratio of $CD68^+$ to $CD8^+$ cells predicted patient response to neoadjuvant chemotherapy.

TAMs are essential to breast cancer pathogenesis. TAMs have been reported to comprise up to 80% of infiltrating leukocytes in late stage mouse mammary tumors (56). TAMs are necessary for immune suppression, angiogenesis, ECM remodeling and tumor cell migration and metastasis. Resident macrophages support stem cell activity in the mammary glands and their depletion from mammary fat pads prevents stem cell repopulation of de-epithelialized mammary glands (103). Similarly macrophages also support the growth of breast cancer stem cells through juxtacrine signaling; macrophage depletion is able to almost completely block tumor initiation following implantation of cancer stem cells into the mammary fat pad (60). Infiltration of macrophages into breast tumors depends on CSF1 signaling, and overexpression of the macrophage of CSF-1 and its receptor (CSF-1R) in macrophages correlates with poor prognosis in humans (67). In experimental models of breast cancer, genetic overexpression or inhibition of CSF1 led to increased or decreased macrophage infiltration, respectively, and concomitantly led to exacerbated or attenuated tumor growth (104). Similarly, blocking CCL2 signaling resulted in significantly reduced macrophage infiltration and tumor size, although

cessation of treatment resulted in a rebound with increased macrophage infiltration and tumor growth (102). Co-injection of M2 macrophages with tumor cells into the mammary fat pad significantly increased tumor growth (105). In agreement with these findings, Galmbacher and colleagues treated mice which had breast cancer with an attenuated strain of *Shigella flexneri* which selectively killed macrophages (106), and found that a single injection with *S. flexneri* resulted in complete regression of tumors. Similarly, tumor cell migration and intravasation have been shown to be dependent on TAM signaling (107). Further, pre-clinical studies have shown that inhibition of TAM's immune suppressive phenotype, without changing the overall number of TAMs or vascularity of tumors, is sufficient to reduce breast cancer growth (108). TAMs have also been shown to promote chemotherapy resistance, and can support tumor relapse following radiotherapy (109,110).

The dependence of breast tumors on macrophages makes TAMs a strong therapeutic target, and several strategies for targeting TAMs have been developed including: inhibition of recruitment, M2-like activation, survival, and polarization (67,111). Many of these therapies have advanced to clinical trials. Among the most promising treatments is blocking CSF1 signaling through inhibiting CSFr1. Interfering with the CSF1/r1 axis has been shown to inhibit macrophage recruitment and TAM activation in many preclinical studies. CSF1/r1 inhibition greatly decreased macrophage infiltration into mouse mammary tumors which led to an increase T cell response (70). CSFr1 also sensitized pancreatic tumors to T cell check point blockade (71). CSF1 inhibition also could sensitize tumors to other therapies. Clinical trials are also being performed on inhibition of CCL2 signaling which can potently block macrophage

recruitment (67). Another promising strategy is re-polarizing TAMs towards an anti-tumor M1 phenotype. CD40 agonists are able to induce macrophages toward tumor-lytic phenotypes and can promote the development of T-cell–dependent antitumor immunity (112,113). CD40 agonists are showing promising clinical activity and can increase the survival of melanoma patients. Similarly anti-CD47 antibodies, which bind to CD47 a "don't eat me signal" on tumor cells, are able to improve macrophage phagocytosis and the priming of T cells and are showing encouraging results in clinic trials (114). Zoledronic acid is a compound which has shown selective toxicity for macrophages (115). Pre-clinical studies have shown that ZA can inhibit spontaneous mammary cancerogenesis by reducing the number of TAMs (116,117). A phase 3 clinical trial has shown that ZA treatment could improve disease free survival in premenopausal patients with estrogen-responsive early breast cancer when added to adjuvant endocrine therapy (118,119).

1.4 EMODIN AND INFLAMMATORY DISEASE

Natural compounds and their derivatives comprise the main source of new drugs (120). Herb derived compounds provide many benefits over purely synthetic structures. Their potential toxicity is often better known, especially in compounds isolated from traditional medicine (121). Further, natural products are more frequently found to bind to clinical targets than synthetic compounds since they more closely resemble natural ligands or metabolites found in human cells (121-123). Recently, increasing numbers of compounds have been purified from traditional medicines and shown to have biological activity. Chinese traditional medicine, which has demonstrated efficacy in patients for thousands of years, is a particularly rich source of potential new therapies (120,124). One

of the main obstacles preventing the development of many herb derived compounds into modern drugs is the lack of information on their distinct mode of action (121).

Emodin is a trihydroxy-anthraquinone (Figure 1.1) and is the active ingredient of several Chinese herbs including Chinese rhubarb and has been used to treat a variety of inflammatory diseases (125). Emodin has generated much interest because of its strong anti-inflammatory and anti-cancer properties as well as its low cost and low toxicity. Prior studies performed on emodin hint at its potential to be a broad acting regulator of macrophage activation. The NIH's National Toxicity Program (NTP) performed an in-depth evaluation of emodin's toxicity by administering emodin in the feed of rats and mice for up to two years (126). There was no effect on survival of the animals even at doses up to 1000 mg/kg/day for rats and 70 mg/kg/day for mice. Further, emodin showed little to no evidence of carcinogenic activity. Emodin has low water solubility and is cleared from the blood stream fairly quickly. The NTP study found that emodin had a half life of about 23 min in mice following a single dose (10 mg/kg) intravenous injection. Our lab has found that one hour following a single intraperitoneal injection of emodin (40 mg/kg) the serum concentration of emodin (including its conjugated forms) is just under 30 μM, but by 24 hour the serum concentration is almost undetectable (Figure 1.2).

Emodin has a strong potential to target the macrophage component in many diseases. Excessive M1 macrophage activation causes tissue damages and exacerbates numerous pathologies. Emodin has been shown to attenuate inflammation and reduce the severity of many experimental disease models including arthritis, hepatic steatosis, atherosclerosis, myocarditis, pancreatitis, and cancer (125). Hwang et. al. reported that IP

administration of emodin (10 mg/kg) inhibited joint destruction in a mouse model of arthritis (127). Emodin decreased TNFα and IL1β levels in the serum and joint by decreasing NFκB signaling. Similarly Wu et. al. found that emodin treatment dose dependently attenuated myocardial damage following coronary artery occlusion in mice (128). Emodin decreased NFκB activation in the myocardium which led to decreased TNF-α expression. Emodin treatment significantly inhibited tissue damage in numerous acute inflammatory models including LPS induced Kidney and Lung inflammation through decreasing the production of inflammatory cytokines (TNFα, IL1β, and IL6) and the infiltration of inflammatory cells (129,130). Emodin decreased inflammatory cell infiltration and LPS induced activation of NFκB signaling. Our lab and others have shown that emodin can protect the liver from injury from numerous different inflammatory insults. Liu et. al treated ethanol fed mice with emodin (50 mg/kg administered by oral gavage) and found that emodin improved liver function and decreased hepatic oxidative stress (131). Orally delivered emodin was also able to protect mice from concavalin A induced T cell-mediated hepatitis (132). Emodin substantially reduced hepatic expression of pro-inflammatory cytokines and chemokines (TNFα, IFNγ, IL1β, IL-6, IL-12, iNOS, ITGAM, CCL2, MIP-2 and CXCR2) and dramatically reduced the number of hepatic infiltrating T cells and macrophages through blocking NFκB and P38 signaling. Our lab found that IP administered emodin attenuated systemic and hepatic inflammation in high fat diet fed mice administered with LPS (133). Emodin significantly reduced macrophage infiltration into the liver, and mechanistic studies revealed that emodin inhibited P38 and ERK phosphorylation in LPS treated macrophages.

In spite of the many model systems which have been used to study emodin's therapeutic potential, the detailed molecular mechanisms of emodin's benefits have not been fully elucidated; however, emodin has been shown to target a variety of signaling pathways in different cell populations. Emodin has been described as a promiscuous kinase inhibitor (134). Yang et. al. revealed that emodin could induce the differentiation of fibroblasts to adipocytes by binding to and activating PPARγ (135). Emodin was also able to inhibit inflammatory cytokine release by hypertrophic scar fibroblasts through blocking PI3K and AKT phosphorylation (136). In synoviocytes, emodin inhibited LPS-induced activation by reducing HDAC1 expression and activity but had no effect on NFκB or Erk signaling (137). However, emodin has been shown to inhibit NFκB nuclear translocation and DNA binding in endothelial cells through blocking IkB degradation (138). Emodin is also able to inhibit NFκB signaling induced by IgE in mast cells along with mobilization of intracellular Ca2+ and activation of the mitogen-activated protein kinase and phosphatidylinositol 3-kinase (PI3K) pathways through blocking the phosphorylation of Syk (139). Further, emodin has been shown to be a potent regulator of macrophage activation in numerous different animal models by blocking NFκB and MAP kinase signaling as well as inhibiting the NRLP3 inflammasome (125,140).

Macrophages are plastic cells capable of displaying a large number of different phenotypes. However, studies with emodin haven been focused on response to stimuli which induce a narrow range of activation (either M1 or M2 phenotypes but not both). Evidence does exist, however, which hints that emodin might be able to inhibit a broad spectrum of phenotypes depending on the environment of the cells. Emodin has already been shown to suppress M1 macrophage activation and push Th1 inflammation to Th2 by

decreasing the expression of IL1, iNOS, TNF, IFN and IL12 and increasing the expression of TGFβ, IL4, IL10, and PPARγ (74,131,141-144). In other studies, however, emodin has decreased Th2 inflammatory mediators and increased Th1. Chu et. al showed that emodin could attenuate Th2 driven hyper-responsiveness in the lungs of mice sensitized and challenged with OVA (145). Emodin substantially decreased BALF levels of IL4, IL5, and IL13 and suppressed the number of infiltrating macrophages. Other studies have shown that emodin is able to inhibit PPARγ and TGFβ expression (146,147). Recently, our lab has shown that emodin could inhibit breast cancer metastasis through blocking infiltration of M2-like macrophages (148).

1.5 EMODIN AND CANCER

There is increasing interest in using herb derived compounds to complement modern therapies by modulating the inflammatory component of tumors. Emodin's ability to regulate macrophage activation makes it a strong candidate as therapy for breast cancer. Emodin treatments have shown benefits in many different pre-clinical animal models, including cancers of the gastric system, respiratory system, reproductive system, and blood system, and emodin has been shown to repress tumor growth in many clinical situations (125,149). The vast majority of these studies have focused on emodin's direct effects on tumor cells; however, the detailed mechanisms have not been fully elucidated. Various different mechanisms have been proposed for emodin's anti-tumor properties in different tumor types. Emodin has been shown to inhibit DNA repair enzymes, induce ROS generation, and inhibit NFκB, ERK 1/2, p38, JUNK and PI3K/AKT signaling pathways in different cell lines (125). Emodin has been reported to trigger apoptosis in both caspase dependent and independent manners (150-152). In many cancer cell lines,

emodin induced apoptosis by increasing ROS production (150,153,154). Emodin has also been shown to inhibit NFκB signaling in a wide variety of cancer cells (152,153,155-157). Emodin inhibited myeloma growth by blocking JAK2 activation and the subsequent activation of STAT3, but had no effect on the phosphorylation of AKT, ERK 1/2, or P38 (158). However, emodin was shown to inhibit ERK 1/2 signaling in human non-small cell lung cancer cells and sensitize them to EGFR inhibitor gefitinib (159). Emodin also inhibited ERK 1/2 activity in MDA-MB-231 and reduced their migration (160). Emodin can induce apoptosis in HER2/neu breast cancer cell lines by inhibiting HER2/neu tyrosine kinase (161,162). Huang et. al. reported that emodin induced apoptosis in Bcap-37 breast cancer cells by decreasing the Bcl-2/Bax ratio and increasing cytoplasm cytochrome c (163). MCF-7/Adr breast cancer cells are resistant to Adriamycin and cisplatin. Emodin treatment can reverse drug resistance in MCF-7 cells by down-regulate the expression of DNA repair protein ERCC1 (164). However, for many tumor cells emodin is only cytotoxic at high doses, which can be difficult to achieve in vivo.

In spite of emodin's demonstrated anti-inflammatory properties, most studies with emodin have taken a narrow approach in determining emodin's mechanisms and have focused only on emodin's direct effects on tumor cells. However, a few studies have found that emodin is able to attenuate tumor growth by modulating the tumor microenvironment. Recently, emodin was found to inhibit pancreatic cancer growth by targeting both the tumor cells and the microenvironment (165). Emodin was able to reduce angiogenesis by inhibiting NFκB signaling, and its regulated factors VEGF, MMP-2, MMP-9, and eNOS. MMP2 and 9 promote tumor angiogenesis by cleavage of ECM proteins (166). Emodin is able to inhibit MM2/9 secretion from colon cancer cells

possibly by blocking VEGFR signaling (167). Emodin has also been shown to inhibit MMP9 production in breast cancer and tongue cancer (160,168). Further, emodin has been reported to directly inhibit angiogenesis by attenuating endothelial cell proliferation, migration and tube formation through blocking VEGF-A receptor-2 (KDR/Flk-1) signaling and downstream effector molecules, including focal adhesion kinase, Erk 1/2, p38 mitogen-, Akt and eNOS (169,170). Our lab was the first to show that emodin treatment could inhibit tumor growth by targeting macrophages (148). Emodin treatment of mice bearing established breast tumors inhibited pulmonary metastasis by reducing infiltration of M2-like macrophages into the lungs of the mice. Mechanistic studies showed that emodin inhibited macrophage migration toward tumor cell derived factors, and blocked M2-like polarization by inhibiting C/EBPβ and STAT6 signaling. However, emodin had no effect on the growth of the established primary breast tumors. Emodin's ability to target both cancer cells and macrophages confers it good potential as a therapy to inhibit tumor cell-macrophage signaling loop which supports the tumor promoting microenvironment. Therefore, for this study I will comprehensively study emodin's effects on macrophage activation and investigate its therapeutic potential for breast cancer treatment.

Figures

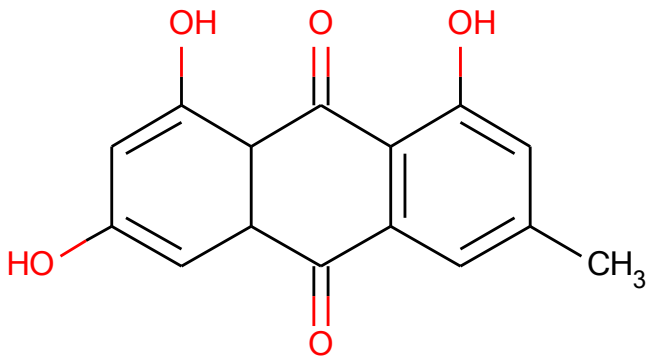

Figure 1.1-Molecular structure of emodin.

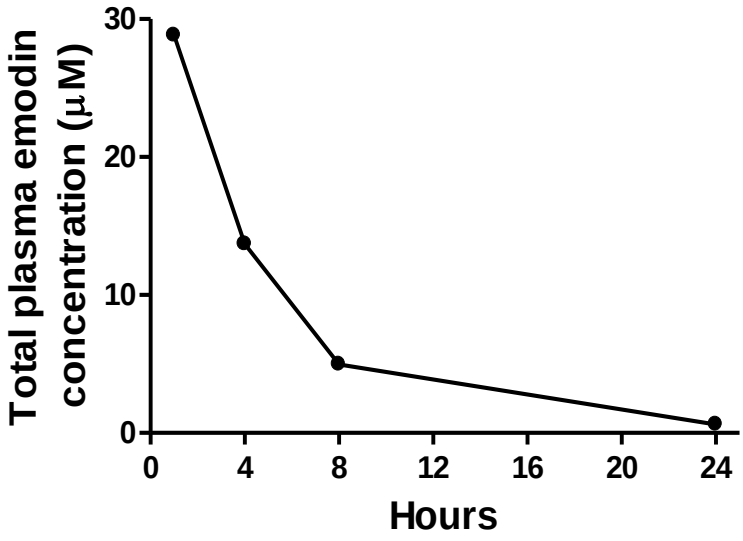

Figure 1.2- Total plasma emodin concentration. Total bioactive emodin concentration was calculated in the plasma of mice following IP administration of emodin 40 mg/kg. Adapted from Jia et al (133).

CHAPTER 2

EMODIN IS A BIDIRECTIONAL MODULATOR OF MACROPHAGE ACTIVATION.

2.1 BACKGROUND

The diversity of macrophage phenotypes presents a major obstacle to the development of macrophage targeted therapies. There is much interest in using herb derived compounds to inhibit macrophage activation since they can modulate multiple inflammatory pathways, are inexpensive, and have low toxicity for chronic treatment (74). However, experimental studies with these compounds haven been focused on responses to stimuli which induce a narrow range of activation (either M1 or M2 phenotypes but not both) (74-77). A compound which could inhibit a broad range of macrophage phenotypes through regulation of multiple signaling pathways would have great clinical potential. Studies in our lab and others have shown that emodin has potential to regulate both Th1 and Th2 driven inflammation (133,145,148,171), which indicates that emodin is able to regulate a broad spectrum of macrophage phenotypes. However, emodin's mechanism has not been fully discovered.

Therefore, we tested the ability of emodin to regulate both M1 and M2 macrophage activation in order to comprehensively characterize emodin's effects on macrophages and attempt to elucidate its mechanism of action. Primary mouse macrophages were stimulated with LPS/IFNγ as an M1 stimulus or IL4 as a M2 stimulus

and emodin's mechanism of action was investigated using a whole genome microarray. Emodin was able to inhibit the change in expression of a large percentage of both M1 and M2 associated genes. Emodin inhibited the NFkB, IRF5 and STAT1 pathways following LPS and IFNγ stimulation and the STAT6 and IRF4 signaling pathways following IL4 stimulation. Finally our data showed for the first time that emodin is able to regulate macrophage memory by inhibiting changes in H3K27m3 and H3K27ac at the promoter regions of several key genes. Taken together, our data shows that emodin has the ability to bi-directionally modulate macrophage activation by targeting multiple pathways.

2.2 DETAILED METHODS

Peritoneal Macrophage isolation and culture—

Primary macrophages were collected from the peritoneal cavity of mice. Three milliliters of 4% Thioglycolate (Hi media Laboratories Ltd; Mumbai, India) solution was injected intraperitoneally into 8-12 week old C57BL/6 mice. Three days later, macrophages were collected by lavaging the peritoneal cavity with 20 mls of PBS. The cells were then resuspended in high-glucose Dulbecco's modified Eagle's medium (DMEM, Invitrogen, Grand Island, NY) containing 10% fetal bovine serum (FBS), 100 U/mL penicillin (Sigma-Aldrich, St. Louis, MO), and 100 μg/mL streptomycin (Sigma-Aldrich) and seeded into culture plates. They were cultured at 37 °C in a humidified CO_2 incubator for 2 h, and then non-adherent cells were washed away with PBS and the macrophages were cultured overnight in serum free DMEM containing penicillin and streptomycin. The macrophages were then treated with DMEM containing IL4 (10 ng/ml, BioAbChem Inc. Ladson, SC) or LPS (100 ng/ml, Sigma-Aldrich) and IFNγ (20 ng/ml, BioAbChem Inc) with or without emodin. Emodin was purchase from Nanjing Langze

Medicine and Technology Co. Ltd (Nanjing, China) and verified by NMR spectroscopy and mass spectrometry as we previously described (28). Emodin was dissolved in DMSO at a concentration of 10 mg/ml.

For macrophage memory experiments, macrophages were stimulated overnight with IL4 or IFNγ with or without emodin. Then the cells were washed 3x with PBS and cultured for 2 or 5 days in DMEM with 2% FBS. The media were changed every 2 days. The cells were then restimulated with IL4 or LPS for 6 h.

Microarray analysis—

Microarray analysis was carried out as described previously (172), with a few alterations. Macrophages were stimulated with IL4 for 6 h or LPS+IFNγ for 24 h with or without emodin (50 μM). Samples were prepared in biological replicates of 4. Cells were lysed with Qiazol and RNA was extracted using Qiagen's miRNeasy kit. Next Agilent's 2100 Bioanalyzer was used to determine the quality and quantity of the RNA. All RNA samples had a RIN of 9.2 or higher. The RNA was amplified and labeled with Agilent's Low Input Quick Amp Labeling Kit (Agilent) according to the manufacturer's instructions. Labeled RNA was then purified using Qiagen's RNeasy Mini Kit (Qiagen, Valencia, CA) and dye incorporation and cRNA yield were assessed. Labeled samples were hybridized to Agilent Whole Mouse Genome Microarrays 8x60K (Agilent) using Agilent's Gene Expression Hybridization Kit (Agilent) according to the manufacturer's instructions. Microarray analysis was performed using an Agilent DNA Microarray Scanner System (Cat. #G2565CA). A heatmap of genes from relevant pathways identified by Ingenuity pathway analysis was generated using R function heatmap.2. A

principle component analysis was performed using all genes differentially expressed in at least one of the treatment groups using the R function prcomp.

Phagocytosis assay—

Macrophages were seeded into a 96-well plate ($2x10^5$ cells/well) and were stimulated with IL4 or LPS+IFNγ for 24 h with or without emodin. Then phagocytotic activity was measured using a Vybrant Phagocytosis assay kit (Molecular Probes). The medium was removed and the cells were washed with PBS. The fluorescent BioParticle suspension was added to the cells and incubated up to 6 h. After the indicated time, the BioParticle suspension was removed and any extracellular fluorescence was quenched with trypan blue. The intracellular fluorescence was then detected using a Spectramax M5 microplate reader (Molecular Devices, Sunnyvale, CA).

Macrophage migration assay—

Macrophages were stimulated with IL4 or LPS+IFNγ for 24 h with or without emodin. The media was then removed and the cells were washed with PBS. The cells were then resuspended in DMEM with scraping and $2x10^5$ macrophages were seeded in triplicate into the top chamber of transwell inserts with 8 μm pores (Corning) and placed in 24 well plates. Serum free DMEM with 20 ng/ml MCP1 (BioAbChem Inc, Ladson, SC) was placed in the bottom of the wells. After 4 h, inserts were fixed in 4% paraformaldehyde for 20 min; the cells in upper inserts were swabbed using cotton buds, and the cells left on the membrane were stained with DAPI (5 μg/ml) for 1 min. The inserts were then cut out, mounted onto slides and imaged under a Nikon Eclipse NI-U fluorescence microscope (Nikon Inc. Melville, NY) at 20 × magnification (5 fields/insert). DAPI stained cells were quantified using Nikon NIS-Elements software.

NO production assay—

Macrophages were stimulated with LPS+IFNγ for 24 h with various concentrations of emodin (0-50 µM) in triplicate. The culture media was then collected and the NO content was detected using a Griess assay performed with a Nitrite/Nitrate colormetric kit (Sigma-Aldrich) according to the manufacturer's instructions. Briefly, the supernatant was centrifuged at 1000xg for 15 minutes to remove any cells. Then 80 µl of sample was placed in a 96 well plate and 50 µl of Greiss reagent A was added to the samples and incubated for 5 minutes. Then 50 µl of Greiss reagent B was added to the samples and incubated for 10 min. The assay was read using a Spectramax M5 microplate reader (Molecular Devices, Sunnyvale, CA) at 540 nm.

Western blotting and Real time PCR—

Following stimulation with IL4 or LPS+IFNγ with or without emodin for varying periods, macrophages were lysed with cell signaling lysis buffer (Millipore) in order to collect protein from whole cell lysates. The cells were incubated in lysis buffer for 20 min on ice, then mechanically homogenized and collected. In order to examine nuclear factor translocation, cytoplasmic and nuclear extracts were prepared using the Epiquik Nuclear Extraction kit (Epigentek, Farmingdale, NY). Macrophages were washed with PBS following treatment and collected by scraping. Then the cells were incubated in lysis buffer 1 for 15 min. The nuclei were pelleted by centrifugation at 2000xg for 5 min and the supernatant containing cytoplasmic proteins was collected. The nuclei were resuspended in nuclear lysis buffer. The cells were incubated for 15 minutes, and then sonicated using a Diagnode Bioruptor Pico for 3 cycles of 30 s on/30 s off. The samples

were centrifuged again for 10 minutes at 20,000xg and the supernatant was placed in a new tube.

In order to detect genome wide levels of histone H3 modifications, histones were isolated from macrophages using EpiQuik total histone extraction kits (Epigentek, Farmingdale, NY) according to the manufacturer's directions. Briefly, macrophages were washed with PBS following treatments and collected by scraping. Macrophages were resuspended in pre-lysis buffer and incubated on ice for 10 min. The nuclei was then pelleted by centrifugation and resuspended in approximately 40µl lysis buffer and incubated on ice for 30 min. The lysate was centrifuged at 20,000xg for 5 min and the supernatant was collected. The lysate was then neutralized with balance buffer.

Total protein in the lysates was quantified using a BioRad colormetric DC Protein Assay (Bio-Rad Laboratories, Hercules, California). Total protein (40-50 µg for whole cell lysates, 40 µg for cytoplasmic lysates, 20-30 µg for nuclear lysates, and 10-15 µg for histone extracts) was separated on 4-20% Tris-glycine pre-cast gels (Pierce) and transferred onto Nitrocellulose membranes (Bio-Rad Life Science, Hercules, CA). Antibodies are shown in table 2.1. The membranes were then probed with HRP conjugated secondary antibodies (Table 2.1), and signals were detected using Pierce ECL Western Blotting Substrate (Pierce). For a loading control, nuclear fraction blots were stained with Ponceau S (0.5% (w/v) Ponceau S in 1% (v/v) acetic acid) and destained with water. Densitometry analysis was performed using Image Studio Lite version 5.0 (LiCOR Biosciences).

For qPCR, macrophages were washed with PBS following treatments, then lysed with Qiazol. RNA was extracted using Zymo research Direct-zol RNA isolation kit.

cDNA was then made from 1 microgram of RNA using iScript cDNA Synthesis Kit (Bio-Rad Life Science). Primers are listed in table 2.2; run conditions were 95°C for 10 s, 58°C for 15 s, 70°C for 15 s. Samples were run in duplicate on a Bio-rad CFX Real Time thermocycler. Relative expression was determined using the ΔΔCt method.

ChIP Assay

Macrophages were stimulated with IL4 or LPS+IFNγ for 24 h with or without emodin. They were then fixed in 1% formaldehyde. Excess formaldehyde was quenched with glycine and the cells were collected in PBS by scraping. The cells were incubated in lysis buffer (0.5% IGEPAL, 4 mM HEPES) for 15 min on ice. The nuclei were centrifuged at 1000xg for 5 min and were resuspended in nuclear lysis buffer (1% SDS, 10 mM EDTA, and 50 mM Tris, pH 8.1). The DNA was sheared by sonication using a Diagnode Bioruptor Pico for 15 cycles of 30 s on/30 s off. A small fraction of DNA was taken from each sample and eluted from the protein by incubating the sample with Proteinase K at 62°C for 2 h in elution buffer. The DNA was purified using Zymo research's ChIP DNA Clean and Concentrator kit. The efficiency of shearing was evaluated by running the samples on a 1% agarose gel and the amount of DNA in each sample was quantified by detecting absorbance at 260 and 280 nm. Samples containing a DNA smear between 1000-200 BP were used for the ChIP assay, a representative gel is shown in figure 2.1. For the ChIP assays, 10 µg chromatin was diluted 1:10 (0.01% SDS, 1.1% Triton X- 100, 1.2 mM EDTA, 16.7 mM Tris-HCl, pH 8.1, 167 mM NaCl) and 2% of the input was removed from each sample and saved for analysis. Anti-H3K27m3 or anti-H3K27ac (Abcam) was added to each sample along with 20 µl of protein A+G magnetic beads (Millipore) and the samples were incubated overnight at 4 °C on a

rocking platform. The beads were washed with low salt, high salt, LiCl, and TE wash buffers sequentially for 5 min each and the DNA was eluted off the beads with Proteinase K at 62 °C for 2 h (elution buffer: 200 mM NaCl, 1% SDS and 50 mM Tris). The DNA was purified using Zymo research's ChIP DNA Clean and Concentrator kit; 50 µl of water was used to elute the DNA off of the columns. The DNA was then analyzed by real time PCR using primers listed in table 2.3.

Statistical analysis—

For microarray analysis, data was extracted from images with Feature Extractor Software version 10.7.3.1 (Agilent); background correction using detrending algorithms was performed. Subsequently, background-corrected data was uploaded into GeneSpring GX version 11.5.1 for analysis. In this process, data was log2 transformed, quantile normalized and baseline transformed using the median of all samples. Then, data was filtered by flags in a way that 3 out of the 4 biological replicates have a "detected" flag in at least one of the three treatment groups. Differentially expressed genes were determined by analysis of the data using the Mann-Whitney unpaired statistics. A cutoff p-value of 0.05 and a fold change cutoff value of 2.0 were used to filter the data. Pathway analysis was performed using Ingenuity Pathway Analysis software.

For all other experiments, data were presented as mean ± standard error of the mean (SEM). Statistical significance was calculated by 2-tailed Student's *t* test (two-group comparison) using the GraphPad Prism statistical program (GraphPad Software Inc., San Diego, CA). $p \leq 0.05$ was considered significant.

2.3 RESULTS

Emodin affects the activation of different transcriptional programs depending on the nature of the stimuli.

LPS/IFNγ and IL4 induce macrophages to adopt opposing pro-inflammatory or anti-inflammatory phenotypes, respectively, through the activation of different, often mutually exclusive, signaling cascades. Therefore, we tested the ability of emodin to inhibit macrophage response to these signals and analyzed gene expression using a whole genome microarray. Mouse peritoneal macrophages were stimulated with LPS/IFNγ or IL4 with or without emodin. We found that LPS/IFNγ stimulation changed the expression of over 4,400 genes and IL4 changed the expression of over 700 genes (≥2 fold, p-value ≤ 0.05) (GEO accession number GSE73311). Figure 2.2A shows the effect of emodin treatment on the expression of genes that are significantly increased (upper panel) or decreased (lower panel) by LPS/IFNγ**.** Emodin treatment attenuated the LPS/IFNγ induced changes in about 31% of the LPS/IFNγ responsive genes. Similarly, emodin inhibited IL4 induced changes in almost 60% of IL4 responsive genes (Fig. 2.2B). These results indicate that emodin significantly inhibited the transcription programs induced by both M1 and M2 stimuli.

LPS/IFNγ and IL4 induce macrophage activation through competing signaling pathways (STAT1 vs STAT6, IRF4 vs IRF5), resulting in very little overlap between the transcriptional programs that they induce. Of the over 4,400 genes changed by LPS/IFNγ and the 719 genes changed by IL4, only 387 genes could be found in both datasets (Fig. 2.2C, upper). The expression of almost 6,500 genes was changed by emodin in at least one of the conditions; among them only 1,575 were changed in both groups (Fig. 2.2C,

lower). Therefore, emodin treatment predominately affected different transcriptional programs under the two different conditions. These results were confirmed with a principle component analysis (PCA) of the genes that were significantly changed in at least one of the treatment groups (~10,000 genes) **(**Fig. 2.2D**)**. The samples within each group cluster near each other with LPS/IFNγ treated cells clustering much further from naïve cells than IL4 treated cells, indicating that M1 activation involves much greater transcriptional changes than M2, in agreement with previous studies (173). Similarly, there is significant distance between the two emodin treatment groups, indicating that emodin treatment differentially affected the expression of transcriptional programs under the different conditions.

Emodin inhibits the induction of signaling pathways associated with macrophage polarization and function.

Next, we investigated which cell signaling pathways might be targeted by emodin by performing a canonical signaling pathway analysis using Ingenuity IPA. The genes influenced by emodin treatment were enriched for genes associated with immune cell signaling, inflammation, cell adhesion, and metabolism. Figure 2.3 shows a list of pathways with the highest significance. Several pathways were targeted by emodin under both conditions, including: communication between immune cells, granulocyte adhesion, NFκB signaling, and Toll-like receptor signaling. However, most of the pathways targeted by emodin were unique to the different conditions. The genes changed by emodin under LPS/IFNγ stimulation were enriched for M1 associated pathways: antigen presentation, IL1 signaling, and iNOS signaling; whereas, the genes changed by emodin

under IL4 stimulation were enriched for M2 associated pathways: IL4, JAK/STAT, TGFβ, and VEGF signaling.

The expression of genes in these pathways is shown in Figure 2.4. Emodin significantly attenuated the LPS/IFNγ induced changes in a large number of genes including canonical M1 associated genes: proinflammatory cytokines IL1β, TNFα, and IL6 (13.64, 2.01, and 3.25 fold reduction, respectively); proteases MMP2/9 (11.86 and 28.87 fold reduction, respectively); and antigen presentation genes CD86 and H2-Oa/b (7.74, 3.85, and 6.42 fold reduction, respectively) (Fig. 2.4A). Similarly, emodin inhibited the IL4 induced expression of canonical M2 genes Arg1, Mrc1, and Ch3l3 (7.69, 2.29, and 4.24 fold reduction, respectively); and transcription factors SOCS1 and IRF4 (22.9 and 97.43 fold reduction, respectively) both of which are necessary for M2 activation (21,22,174) (Fig. 2.4B). Emodin also increased the expression of CDKN1A (p21) which has been shown to inhibit macrophage proliferation and activation (175,176).

Interestingly, we also found that emodin treatment had inverse effects on a subset of 86 genes under the two different stimuli (Table 2.4**)**. For examples, emodin increased the expression of some proinflammatory genes including TNFα, CXCL2, and CXCL10 (2.7, 60.6, and 15.5 fold, respectively) under IL4 stimulation while significantly decreasing them (-2.47, -10.31, and -2.01 fold, respectively) under LPS/IFNγ stimulation (Fig. 6**).** Similarly, emodin increased the expression of M2 genes YM1 and Mrc1 under LPS/IFNγ stimulation (2.04 and 8.72 fold, respectively), while reducing them in IL4-stimulated cells (Fig. 2.4 and Table 2.4**)**. These results show emodin's ability to tune

macrophage phenotype back towards the center between the extremes of the M1 or M2 activation states.

The expression of several important genes for macrophage activation was confirmed by qPCR (Figs. 2.5A and B**).** Emodin inversely regulated M1 genes TNFα, CXCL2 and CXCL10, and M2 gene Mrc1, in the two settings. Interestingly, emodin inhibited the expression of transcription factors IRF5 and SOCS1, and chemoattractant CCL2 under both IL4 and LPS/IFNγ stimulation. In agreement with the microarray results, emodin inhibited the expression of many pro-inflammatory mediators including IL1β, iNOS, and IL6 as well as proteases MMP2 and 9 under LPS/IFNγ stimulation, and inhibited M2 genes Arg1 and Chi3l3 under IL4 stimulation. Emodin also inhibited the expression of receptors TLR4 and CSFr1 under LPS/IFNγ or IL4 stimulation, respectively, which could further inhibit macrophages from detecting activation signals in the environment. IRF4, a major regulator of M2 macrophage activation, was the most down regulated gene by emodin under IL4 stimulation in the microarray dataset. We examined the production of IRF4 protein and found that emodin dose dependently inhibited IRF4 production (Fig. 2.5C).

Emodin inhibits functions of activated macrophages.

Next we investigated the effects of emodin on the functions of macrophages, which were predicted to be inhibited by emodin in one or both of the groups based on pathway analysis of the microarray results. We examined the phagocytic ability of activated macrophages. Macrophages were pretreated with LPS/IFNγ or IL4 with or without emodin for 24 h; then the cells were incubated with Fitc labeled *E. coli* bioparticles. In agreement with previous studies (150,177), emodin treatment alone was

able to increase phagocytic activity of naïve cells at the 6 h time point; however, emodin decreased both LPS/IFNγ and IL4 induced phagocytosis. Both IL4 and LPS/IFNγ stimulated macrophages showed time dependent increases in bioparticle uptake (6-8 fold increase at 6 h). However, emodin significantly inhibited particle uptake under both conditions (by almost 2 fold) (Fig. 2.6A). Next, macrophages were stimulated with LPS/IFNγ or IL4 with or without emodin then their migration potential was detected. Macrophages were seeded into the top chamber of transwell inserts and media containing MCP1 (20 ng/ml) was placed in the bottom. Emodin significantly reduced macrophage migration under both conditions (Fig. 2.6B). M1 macrophage expression of iNOS leads to the synthesis of large amounts of NO which is cytotoxic and is effectively used to kill invading organisms. However, excessive NO production can also damage surrounding cell populations. Since the expression of iNOS was significantly decreased by emodin, we then verified emodin's ability to inhibit M1 activation by detecting NO production. Macrophage production of NO was measured in the culture media following stimulation with LPS/IFNγ for 24 h. The result showed that emodin dose dependently inhibited NO production decreasing NO levels by 57% at 25 µM and 96% at 50 µM (Fig. 2.6C).

Emodin modulates IL4 and LPS/IFNγ induced activation of cell signaling pathways.

We next attempted to identify the cell signaling pathways targeted by emodin under the different conditions. Ingenuity's Upstream regulator analysis of the microarray date set was unable to identify a single high probability molecular target or casual network for emodin under the different conditions, but instead provided many different possible targets. Macrophage polarization is controlled by multiple different signaling pathways which coordinate to fine tune the functional phenotype. LPS promotes M1

macrophage activation by signaling through NFκB and MAPK pathways while IFNγ mainly signals through the STAT1 pathway. IL4 stimulation leads to STAT6 pathway activation along with several secondary transcription factors including IRF4. Nuclear and cytoplasmic fractions of macrophages treated with LPS/IFNγ or IL4 and emodin were analyzed using western blotting to detect nuclear translocation of transcription factors. In agreement with previously published results (125,133,148), emodin was able to drastically inhibit NFκB p65 nuclear translocation in response to LPS/IFNγ stimulation (Fig. 2.7A) and STAT6 nuclear translocation in response to IL4 stimulation (Fig. 2.7B). Emodin also inhibited nuclear accumulation of IRF4 (Fig. 2.7B), in agreement with our gene expression data. Further, we found that emodin inhibited STAT1 and IRF5 nuclear translocation (Fig. 2.7A). These results indicate that emodin is able to inhibit the key signaling pathways necessary for macrophage polarization.

Emodin inhibits IL4 and LPS/IFNγ induced changes in the epigenetic landscape in macrophages.

The microarray revealed that emodin changed the expression of several histone modifying enzymes including those that regulate H3K27 methylation and acetylation under both IL4 and LPS/IFNγ stimulation (Table 2.5). H3K27me3 attenuates M2 polarization by inhibiting the expression of IRF4; therefore, its removal by demethylase JMJD3 promotes M2 activation (22,23). H3K27ac has been shown to prime both M1 and M2 genes for expression upon subsequent stimulation (23,178). Therefore, we next investigated emodin's effects on these histone modifications in macrophages. We investigated the global expression of these histone modifications using western blotting and found that emodin had no effect on the global expression of either H3K27m3 or

H3K27ac (Fig. 2.8A**)**. We then examined gene specific changes in histone modifications using ChIP assays. We found that emodin attenuated the LPS/IFNγ-induced decrease of H3K27m3 in the promoter of iNOS, TNFα and IL6 genes, and reversed the IL4-induced decrease of H3K27m3 in the promoter of IRF4, Arg1 and YM1 genes. Emodin also suppressed LPS/IFNγ-induced increase of H3K27ac in the promoters of iNOS, TNFα and IL6 genes, and IL4-induced increase of H3K27ac in the promoter of IRF4 and YM1 genes (Figs. 2.8B and C). These data for the first time show that emodin epigenetically regulates macrophage activation. Further, unlike emodin's effects on signaling pathways, emodin's effects on histone modification are not stimuli dependent, but gene specific.

Recent studies have revealed that macrophages are able to retain a memory of the environmental signals to which they have been exposed, allowing them to alter their response upon subsequent stimulation. Therefore, we then investigated how emodin's effects on histone modifications affect macrophage memory. Macrophages were stimulated with IFNγ or IL4 for 24 h with or without emodin. Then they were cultured in fresh media for 2-5 d before being stimulated again with LPS or IL4, respectively, for 6 h without emodin. There was no difference in the expression of iNOS after 2 d post stimulation with IFNγ, while the expression of Arg1 was still slightly elevated 2 d post IL4 treatment compared to the emodin treatment group (Figure 2.9D and E). However, re-stimulation with LPS or IL4 resulted in significantly increased expression of iNOS or Arg1, respectively, compared to cells stimulated for the first time, indicating that prior treatment with IFNγ or IL4 boosted the responses to the subsequent exposures**.** However, if the cells were concomitantly treated with emodin during the first IFNγ or IL4 treatment, their responses to the second treatment were significantly diminished;

particularly in the case of IL4 treatment, their response to a second IL4 treatment was even lower than their first exposure (Figs. 2.9B and C**)**. After 5 days of wash-out period, there was no significant difference in the nuclear STAT1 or STAT6 in IFNγ or IL4 pretreated cells, respectively, regardless if the cells were also treated with emodin (Figs. 2.9F and G). The lack of differences in the STAT1 and STAT6 signaling pathway prior to re-stimulation indicates that emodin may regulate macrophage memory through epigenetic modification of the key genes in macrophage activation.

2.4 DISCUSSION

Taken together, these results reveal the ability of emodin to inhibit both M1 and M2 polarization of macrophages through transcriptional and epigenetic regulation. LPS and Th1 cytokine IFNγ stimulate macrophages to adopt an M1 pro-inflammatory phenotype, while Th2 cytokine IL4 induces macrophages to an M2 anti-inflammatory phenotype. Gene expression analysis of emodin treated macrophages revealed that emodin attenuated the transcriptional changes in 60% of genes altered by IL4 and 31% of the genes altered by LPS/IFNγ. Emodin mostly targeted different transcriptional networks in the two different stimulation settings, indicating emodin's ability to differentially affect a broad-spectrum of signaling pathways depending on the microenvironment. Further analysis revealed that emodin inversely regulated a subset of genes including Mrc1, YM1, TNFα, CXCL2, and CXCL10 in LPS/IFNγ or IL4 treated macrophages. Emodin inhibited macrophage migration and phagocytosis regardless of the stimuli by suppressing common pathways in the two different settings. Emodin was able to inhibit numerous signaling pathways including NFκB, STAT1, and IRF5 following LPS/IFNγ stimulation, and STAT6 signaling triggered by IL4 stimulation.

Emodin also inhibited IRF4 production by increasing H3K27m3 on its promoter region. Finally our data showed that emodin was able to inhibit the ability of macrophage training/memory. When administered along with the initial stimuli (IL4 or IFNγ), emodin diminished the response to a second stimuli (IL4 or LPS, respectively). Taken together, our data show that emodin has great potential as a treatment for pathologies driven by an imbalance in macrophage activation and polarization.

It has been implied in literature that emodin may have different effects on macrophages depending on the environment of the cells being studied. The majority of studies performed on emodin have focused on its ability to shift the Th1 inflammatory response to Th2 (125). Emodin inhibits inflammatory cytokine production in a variety of settings, often through blocking NFκB and MAP kinase signaling. Emodin has also been shown to promote expression of M2 associated molecules TGFβ and PPARγ (125,142). On the other hand, there have been a few studies which have implied that emodin may also be capable of suppressing Th2 responses. Emodin significantly inhibited the secretion of Th2 cytokines IL4, IL5, and IL13 in the lungs of mice challenged with OVA (145,179). Further, our lab has found that emodin is able to inhibit breast cancer metastasis to the lungs in mice by reducing macrophage infiltration and M2 polarization through inhibiting STAT6 and C/EBPβ signaling (148). But the interesting dual effects of emodin on macrophages have not been comprehensively studied.

Based on our data, we suggest that emodin is a bi-directional regulator of macrophage activation, and that it is able to target multiple signaling pathways in macrophages to return their phenotype to the homeostatic center between the extremes of M1 or M2 activation in various environmental settings. Our results show that emodin is

able to effectively inhibit macrophage response to both LPS/IFNγ and IL4. In agreement with previous studies, emodin was able to inhibit proinflammatory cytokine/chemokines expression through blocking NFκB signaling in response; however, we also found that emodin was able to inhibit STAT1 signaling as well. Under IL4 stimulation, emodin inhibited M2 activation markers through blocking STAT6 signaling. Emodin's ability to inhibit STAT signaling in macrophages is in agreement with previous studies which have shown that emodin can interfere with the JAK-STAT signaling pathway in human cancer cells. Muto and colleagues found that emodin could block STAT3 phosphorylation and activation in response to IL6 by inhibiting the activation of JAK2 in multiple myeloma cells (158). Similarly, Zheng et al. showed that emodin could inhibit JAK1/2 activation and subsequently block phosphorylation of STAT1, 3, and 5 in response to Oncostatin M and IFNγ in several human cancer cell lines (180). In hepatocarcinoma cells emodin inhibited JAK1/2 activation by inducing the expression of SHP-1 phosphatase (181).

For the first time our results show that emodin is also able to regulate the IRF signaling pathways. IRF4 and 5 have been shown to be inversely regulated, pushing macrophages toward an M2 or M1 phenotype, respectively (14,27). IRF5 is activated by TLR4 ligation and promotes the transcription of pro-inflammatory genes (e.g. IL12b) while also suppressing the expression of anti-inflammatory genes (e.g. IL10) (16). IRF4 competitively binds to MyD88 and is a negative regulator of IRF5 signaling. IRF4 helps to fine tune the M2 phenotype in response to parasite infections, and is regulated through the removal of H3K27m3 by the histone demethylase JMJD3 (22,27,182). Our results show that emodin is able to inhibit both IRF4 (which was the most downregulated gene under IL4 stimulation) and IRF5 signaling. Also, for the first time, we showed that

emodin can inversely regulate the expression of several key M1 and M2 markers. Emodin inhibited the expression of pro-inflammatory cytokines/chemokines TNFα, CXCL2, CXCL10 in macrophages under LPS/IFNγ stimulation while increasing the expression of M2 markers YM1 and Mrc1 which were suppressed by LPS/IFNγ. Similarly, emodin inhibited the expression of M2 markers Mrc1 and YM1 in macrophages exposed to IL4 but increased the expression of pro-inflammatory TNFα, CXCL2, and CXCL10 which were downregulated by IL4. These findings are in agreement with previous studies in our lab showing that pro-inflammatory cytokines are decreased by emodin treatment in the serum of mice with a Th1/M1 driven pathology (High fat diet fed mice treated with LPS) (133), but the levels of proinflammatory cytokines TNFα, IL12, and IL17 are all increased by emodin treatment in the serum of mice with a Th2 driven pathology (148). Taken together, these data indicate that emodin is able to target multiple antagonistic signaling pathways (STAT1 vs. STAT6, IRF5 vs. IRF4) to inhibit macrophage activation and return them to a homoeostatic state which gives emodin great potential as a therapy to target diseases in which imbalanced macrophage activation plays a major role.

Macrophages can retain a memory of signals that they are exposed to which helps to shape their response to future stimulation (27, 28, 90). This memory is predominately regulated by epigenetic mechanisms, especially histone modifications. Cytokines such as IFNγ can prime genes for increased expression by the recruitment of transcription promoting histone markers (such as H3K4m3, H3K9m3 and H3K27ac) to the promoter or enhancer regions (32). Similarly pro-longed exposure to foreign molecular patterns could lead to increased or decreased immune response (for examples, β-glucan or LPS, respectively) (178). The microarray revealed that emodin significantly changed the

expression of several histone modifying enzymes, particularly those responsible for regulating H3K27 tri-methylation and acetylation. However, emodin had no effects on genome wide levels of H3K27ac and H3K27m3; instead, it significantly increased H3K27m3 levels while decreasing H3K27ac levels on the promoters of many M1 genes and M2 associated genes. Our data revealed that emodin was able to modulate macrophage memory. Pre-stimulation of macrophages with IFNγ or IL4 resulted in exaggerated M1 or M2 responses to subsequent stimulation with LPS or IL4, respectively, up to 5 days later. Emodin treatment during the pre-stimulation stage significantly diminished the exaggerated responses, even though prior to second stimulation expression of iNOS or Arg1 were back to similar levels regardless of emodin pretreatment. Similarly, there was no difference in STAT1 or STAT6 activation prior to second stimulation. Therefore, these data suggest that at least part of emodin's effects on macrophage activation and memory could be attributed to gene specific epigenetic modifications.

In summary, emodin effectively inhibited macrophage activation in response to both M1 and M2 stimuli by suppressing the activation of multiple signaling pathways including NFκB, IRF5, MAPK, STAT1 or STAT6 and IRF4 depending on the environmental settings. Emodin thus regulated a subset of genes depending on whether the cell was exposed to M1 or M2 stimuli, pushing the phenotype of the cell back toward the center of the two poles. This phenomenon opens the possibility that emodin may exert very different homeostasis maintaining effects on macrophages in different locations and thus target two very different pathologies within a same individual. Finally we showed for the first time that emodin is able to modulate macrophage activation and memory

through increasing H3K27m3 and decreasing H3K27ac on promoters of M1 or M2 associated genes. Taken together, our data show the potential of emodin to be used as a therapy for the numerous pathologies which are driven by an imbalance of macrophage phenotypes.

Table 2.1 Antibodies used for western blots and ChIP procedures.

Antibodies	Procedure	Product #	Company
p65	Western	8242	Cell Signaling
STAT1	Western	sc-346	Santa Cruz
STAT6	Western	9362	Cell Signaling
IRF4	Western	sc-6059	Santa Cruz
IRF5	Western	4950	Cell Signaling
Actin	Western	A2066	Sigma
TBP	Western	ab51841	Abcam
H3K27m3	ChIP	ab6002	Abcam
H3K27m3	Western	07-449	Millipore
H3K27ac	Western/Chip	AB4729	Abcam
H3	Western	05-928	Millipore
Anti-rabbit HRP	Western	sc-2004	Santa Cruz
Anti-Mouse HRP	Western	sc-2005	Santa Cruz
Anti-goat HRP	Western	sc-2024	Santa Cruz

Table 2.2 Primers for RT-qPCR

Primers	Forward	Reverse
18s	CGCGGTTCTATTTTGTTGGT	AGTCGGCATCGTTTATGGTC
TNF	CGT CAG CCG ATT TGC TAT CT	CGGACTCCGCAAAGTCTAAG
CXCL2	CGCTGTCAATGCCTGAAG	GGCGTCACACTCAAGCTCT
CXCL10	TGAATCCGGAATCTAAGACCATCAA	AGGACTAGCCATCCACTGGGTAAAG
MRC1	TGGATGGATGGGAGCAAAGT	AATGCCAACCTTCCTTGCAG
IRF5	CAGGTGAACAGCTGCCAGTA	CTCATCCACCCCTTCAGTGT
SOCS1	TTAACCCGGTACTCCGTGAC	GAGGTCTCCAGCCAGAAGTG
CCL2	CAGGTCCCTGTCATGCTTCT	TCTGGACCCATTCCTTCTTG
IL1b	GCCCATCCTCTGTGACTCAT	AGGCCACAGGTATTTTGTCG
INOS	CACCTTGGAGTTCACCCAGT	ACCACTCGTACTTGGGATGC
IL6	AGTTGCCTTCTTGGGACTGA	TCCACGATTTCCCAGAGAAC
TLR4	GCTTTCACCTCTGCCTTCAC	GAAACTGCCATGTTTGAGCA
MMP2	ACACTGGGACCTGTCACTCC	GCGAAGAACACAGCCTTCTC
MMP9	CATTCGCGTGGATAAGGAGT	ACCTGGTTCACCTCATGGTC
Arg1	TTTTTCCAGCAGACCAGCTT	GGAACCCAGAGAGAGCATGA
Chi3l3	TGGAATTGGTGCCCCTACAA	CCACGGCACCTCCTAAATTG
IRF4	GCAGCTCACTTTGGATGACA	CCAAACGTCACAGGACATTG
CSFr1	TTGGACTGGCTAGGGACATC	GGTTCAGACCAAGCGAGAAG
CDKNn1a	CAAAGTGTGCCGTTGTCTCT	AGGAAGTACTGGGCCTCTTG

Table 2.3 Primers for ChIP-PCR.

	Forward	Reverse	Region	IP
INOS-1	TCCCTAGTGAGTCCCAGTTTTGA	CTGGTCGCCCGTCCAAGG	P	H3K27m3
INOS-2	GCGCTCTAGTGAAGCAAAGG	TCTTAGTGGCCCAGGACAAG	CpG	H3K27ac
TNF	AGGAGAAGGCTTGTGAGGTC	GAGTTGGGAAGTGTGCATGG	P	H3K27m3
IL6	AGGAGTGTGAGGCAGAGAGC	GTCTCCTCTCCGGACTTGTG	Intron	H3K27m3
IRF4	CACGTGATGGTCTCTGGTTG	TCATCCCACTTTTCCCTCAC	P	H3K27m3, H3K27ac
ARG1-1	TGAACAGGCTGTATTAGCCAACA	AGCACCCTCAACCCAAAGTG	P	H3K27m3
ARG1-2	AGTTCCTCTGATGGGGAGGT	TCATGCTCTCTCTGGGTTCC	P	H3K27ac
YM1	ACTTGCAACTACTCTGCACT	ACACCCCTGAGCTTTGGTAA	P	H3K27m3, H3K27ac

P=promoter

Table 2.4 Genes that were inversely regulated by emodin under the two different treatments.

Gene	Em+LPS vs LPS/IFN	Em+IL4 vs IL4	Gene	Em+LPS vs LPS/IFN	Em+IL4 vs IL4
Rab3il1	2.66	-16.18	D230044B12Rik	2.39	-2.3
Mrgprg	2.18	-16.05	Mrc1	8.72	-2.29
Gprc5c	3.74	-8.77	Rassf2	2.62	-2.29
Ikzf2	3.42	-6.36	Acp5	2.02	-2.22
Kctd12b	3.62	-5.06	Inpp5j	5.52	-2.21
Ear1	2.04	-4.71	AA914427	3.21	-2.2
Jakmip1	9.59	-4.67	A430110L20Rik	2.47	-2.19
Trim45	4	-4.6	Metrnl	2.02	-2.19
Snn	2.13	-4.52	Gm9484	3.19	-2.13
Chi3l3	2.04	-4.24	Gdf3	3.34	-2.12
Cmbl	5.87	-4.21	Selp	3.09	-2.08
Ubtf	2.47	-4.2	Ier5l	3.05	-2.04
Xpo7	2.41	-4	Cdk14	-2.71	2.03
Ear2	2.03	-4	3930401B19Rik	-2.72	2.04
Gpr77	3.05	-3.71	Tgfbi	-3.22	2.06
Mnt	2.31	-3.7	Cpd	-2.21	2.06
Gm4610	8.8	-3.53	Fzd1	-2.45	2.08
Igf1	2.12	-3.47	Klra2	-14.35	2.1
Armcx6	2.81	-3.43	Prkar2b	-4.32	2.12
S100a4	3.02	-3.36	Apol9a	-4.48	2.16
Islr2	3.58	-3.34	Chpt1	-4.06	2.2
Sult1a1	2.95	-3.15	Ass1	-6.11	2.22
9230110K08Rik	3.15	-2.88	Slc7a3	-3.03	2.23
Senp8	2.13	-2.88	Gm20186	-2.65	2.26
Zfp473	3.06	-2.82	Procr	-2.07	2.38
Itga4	4.86	-2.82	Ppap2b	-2.13	2.55
Cables1	3.87	-2.76	Ptgs2	-3.99	2.56
Klf11	2.47	-2.74	Tnf	-2.01	2.69
A930006K02Rik	2.18	-2.72	Clec4n	-2.63	2.94
BC031361	2.05	-2.68	Smtnl2	-4.06	2.96
6430531B16Rik	2.25	-2.65	Thbs1	-6.51	3.22
Taf6l	2.04	-2.62	Jag1	-11.28	3.54
Nudt16l1	2.01	-2.59	Dusp14	-3.14	3.62

Tbc1d16	3.26	-2.57	Hmga2	-2.02	3.79
Scgb2b27	2.23	-2.56	Pla2g5	-4.28	4.26
BC025920	2.91	-2.51	Flrt3	-4.09	4.37
Ccl9	5.28	-2.48	Cck	-25.26	4.53
Bcl9	2.64	-2.43	Serpine1	-23.78	6.13
1700097N02Rik	2.01	-2.42	Clec9a	-4.62	7.13
Gzmm	3.64	-2.4	Cxcl3	-37.91	7.37
Ear11	3.2	-2.39	Tnfaip6	-16.37	9.27
Hfe	3.09	-2.36	Cxcl10	-10.31	15.05
AW555355	2.31	-2.34	Cxcl2	-2.47	60.63

Table 2.5 Histone modifying enzymes significantly changed by emodin compared to LPS/IFNγ (left) or IL4 (right) treatment.

Histone modifying enzymes changed by emodin					
	LPS	**LPS+Em**		**IL4**	**IL4+Em**
EZH1	N.C.	6.63	EZH1	N.C.	-6.26
EZH2	N.C.	2.73	EZH2	N.C.	-2.04
Hdac1	N.C.	-2.3	Hdac1	N.C.	2.32
Hdac8	N.C.	-4.08	Hdac8	N.C.	2.33
KAT2B	2.33	-4.69	Hdac9	N.C.	4.39
KAT6B	-2.41	3.65	KAT2B	N.C.	3.81
KDM3B	N.C.	2.12	KAT6B	N.C.	-2.7
KDM4A	N.C.	9.21	KDM2A	N.C.	2.04
NCOA3	N.C.	2.58	KDM4A	N.C.	-7.58
NSD1	-2.06	2.46	KDM4B	N.C.	2.11
PHF8	-2.35	3.62	KDM5B	N.C.	-2.13
PRDM2	2.18	3.78	KDM6B	-2.2	1.91
SETD1B	N.C.	2.09	Mll1	N.C.	-2.2
SETD7	N.C.	2.06	Mll2	N.C.	-2.64
Sirt5	-2.06	-4.41	NCOA2	N.C.	2.6
Sirt7	N.C.	2.06	PHF8	N.C.	-5.6
SMYD2	N.C.	-3.02	PRDM2	N.C.	-2.26
SUV420H1	N.C.	3.06	Sirt7	N.C.	-2.3
Mll1	N.C.	3.09	SMYD3	N.C.	-2.79
			SUV420H1	N.C.	-2.46

Figures

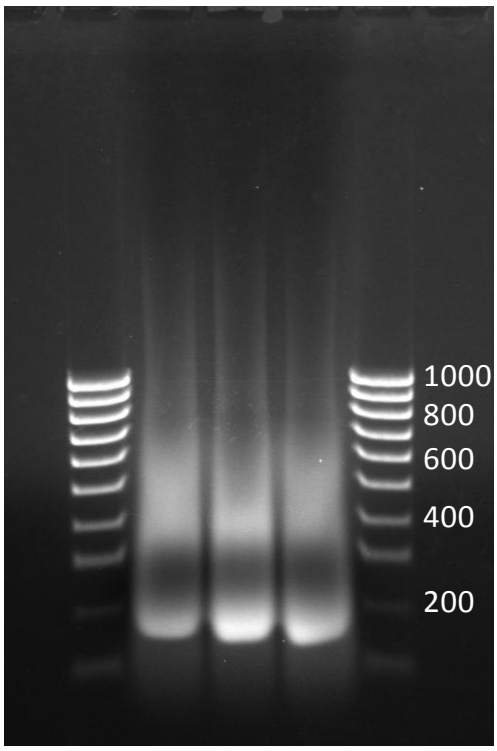

Figure 2.1 DNA fragmentation for ChIP assays. Samples were run on a 1% agarose gel along with a 100 base pair ladder and stained with ethidium bromide.

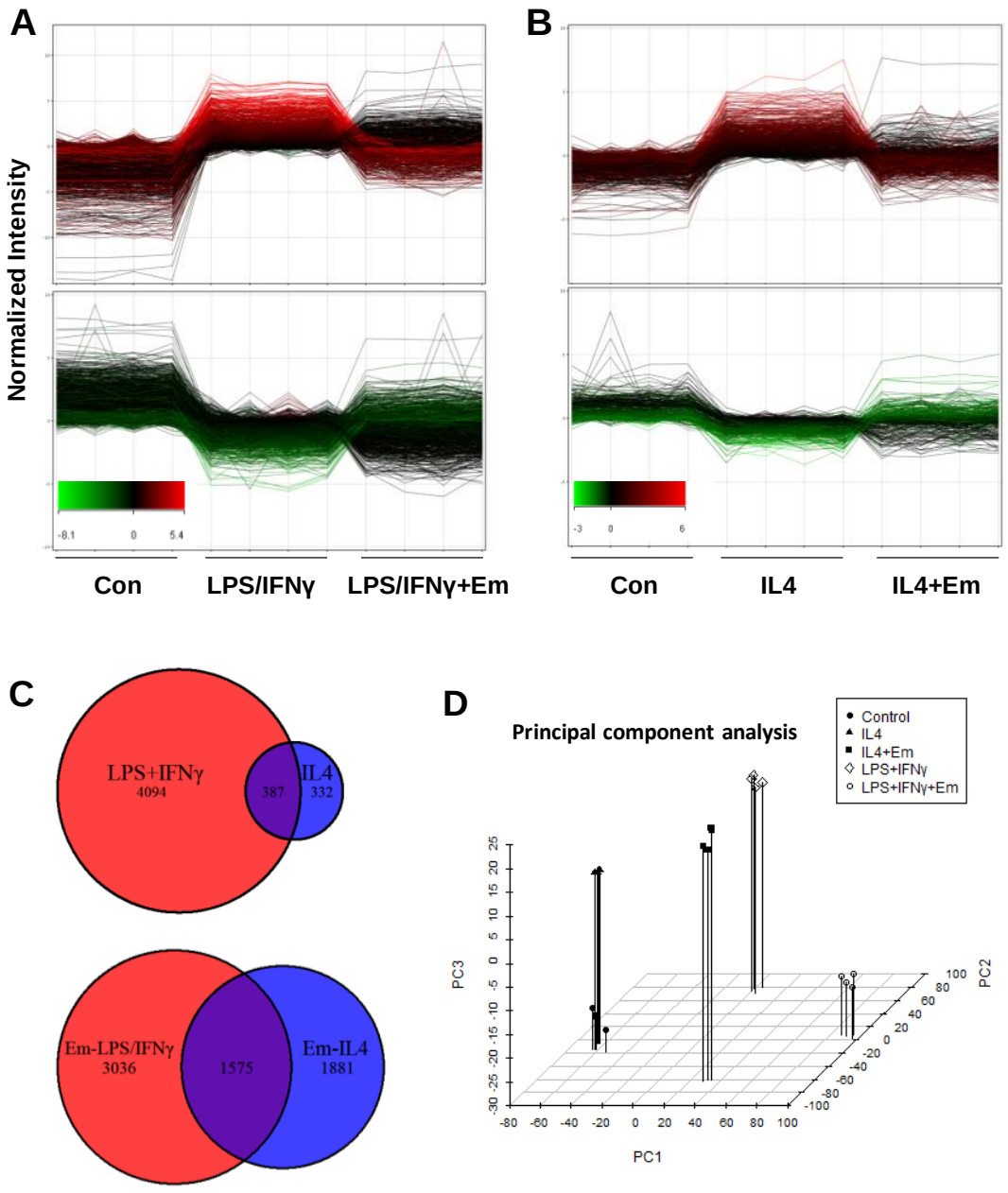

Figure 2.2 Emodin inhibits LPS/IFNγ and IL4 induced transcriptional changes in macrophages. Mouse peritoneal macrophages were stimulated with LPS (100 ng/ml) and IFNγ (20 ng/ml) for 24 h (A) or IL4 (10 ng/ml) for 6 h (B) with or without emodin (50 μM). Gene expression was then detected using a whole genome microarray. ***A*** *and* ***B***, Genes significantly increased (top panel) or decreased (bottom panel) by LPS/IFNγ or IL4, respectively. Y-axis corresponds to normalized intensity values for gene expression and the x-axis to treatments. Each line represents one gene and the red and green colors mark high and low expression of genes, respectively, in the LPS/IFNγ or IL4 treatment groups. ***C***, Venn diagrams showing genes significantly changed by LPS/IFNγ or IL4 and by emodin under LPS/IFNγ or IL4 stimulation. ***D***, Principle component analysis of genes significantly changed in one of the treatment groups.

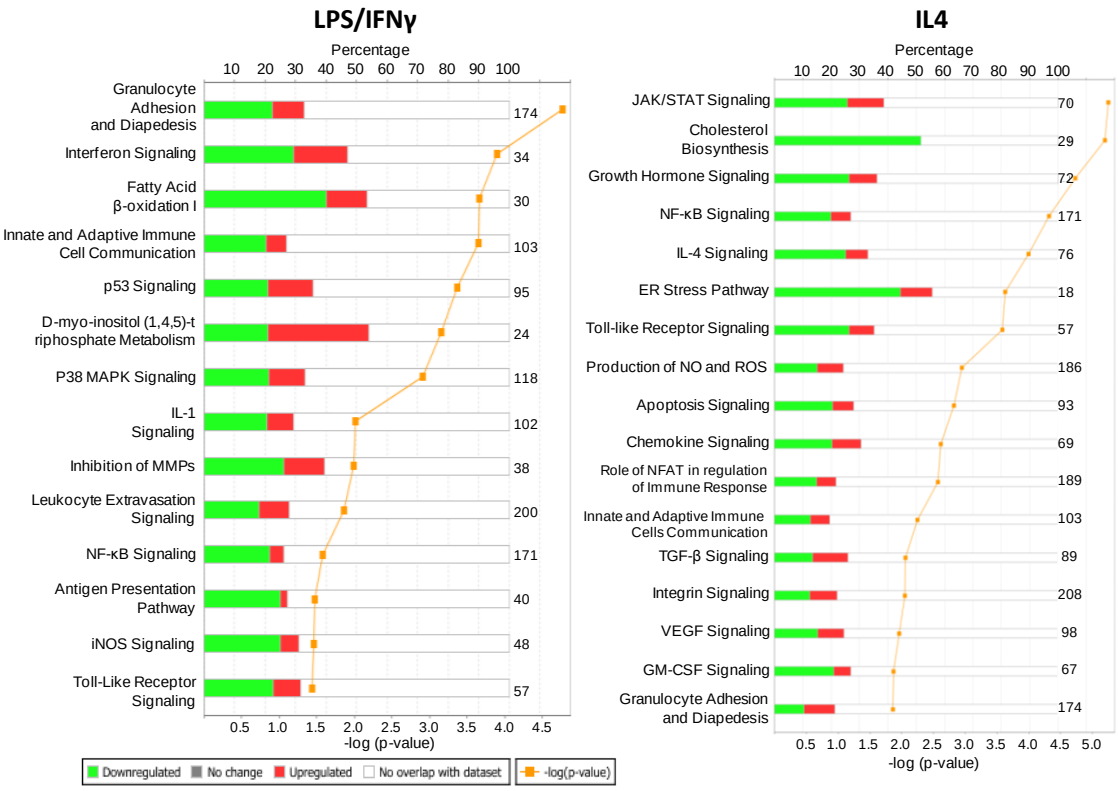

Figure 2.3 Emodin inhibits the induction of signaling pathways associated with macrophage polarization and function. Most significantly affected pathways relevant for macrophage activation determined by Ingenuity IPA canonical pathway analyses.

A

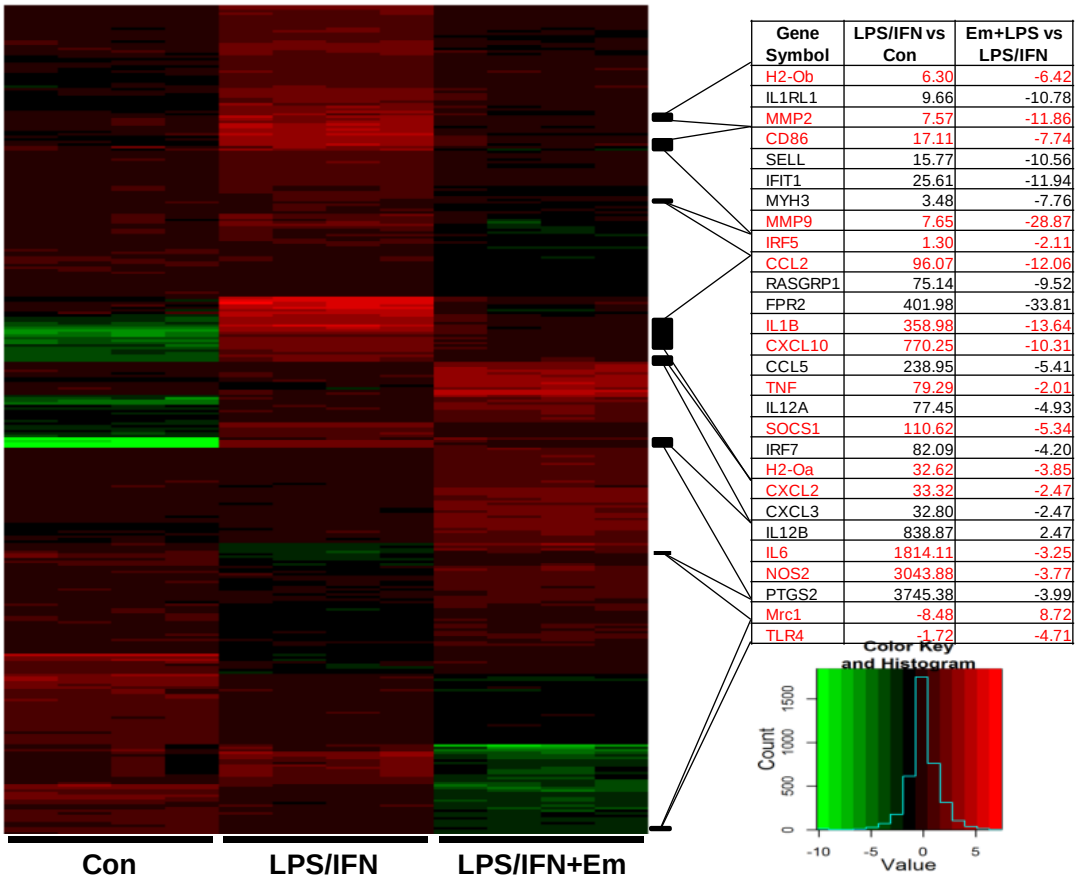

Gene Symbol	LPS/IFN vs Con	Em+LPS vs LPS/IFN
H2-Ob	6.30	-6.42
IL1RL1	9.66	-10.78
MMP2	7.57	-11.86
CD86	17.11	-7.74
SELL	15.77	-10.56
IFIT1	25.61	-11.94
MYH3	3.48	-7.76
MMP9	7.65	-28.87
IRF5	1.30	-2.11
CCL2	96.07	-12.06
RASGRP1	75.14	-9.52
FPR2	401.98	-33.81
IL1B	358.98	-13.64
CXCL10	770.25	-10.31
CCL5	238.95	-5.41
TNF	79.29	-2.01
IL12A	77.45	-4.93
SOCS1	110.62	-5.34
IRF7	82.09	-4.20
H2-Oa	32.62	-3.85
CXCL2	33.32	-2.47
CXCL3	32.80	-2.47
IL12B	838.87	2.47
IL6	1814.11	-3.25
NOS2	3043.88	-3.77
PTGS2	3745.38	-3.99
Mrc1	-8.48	8.72
TLR4	-1.72	-4.71

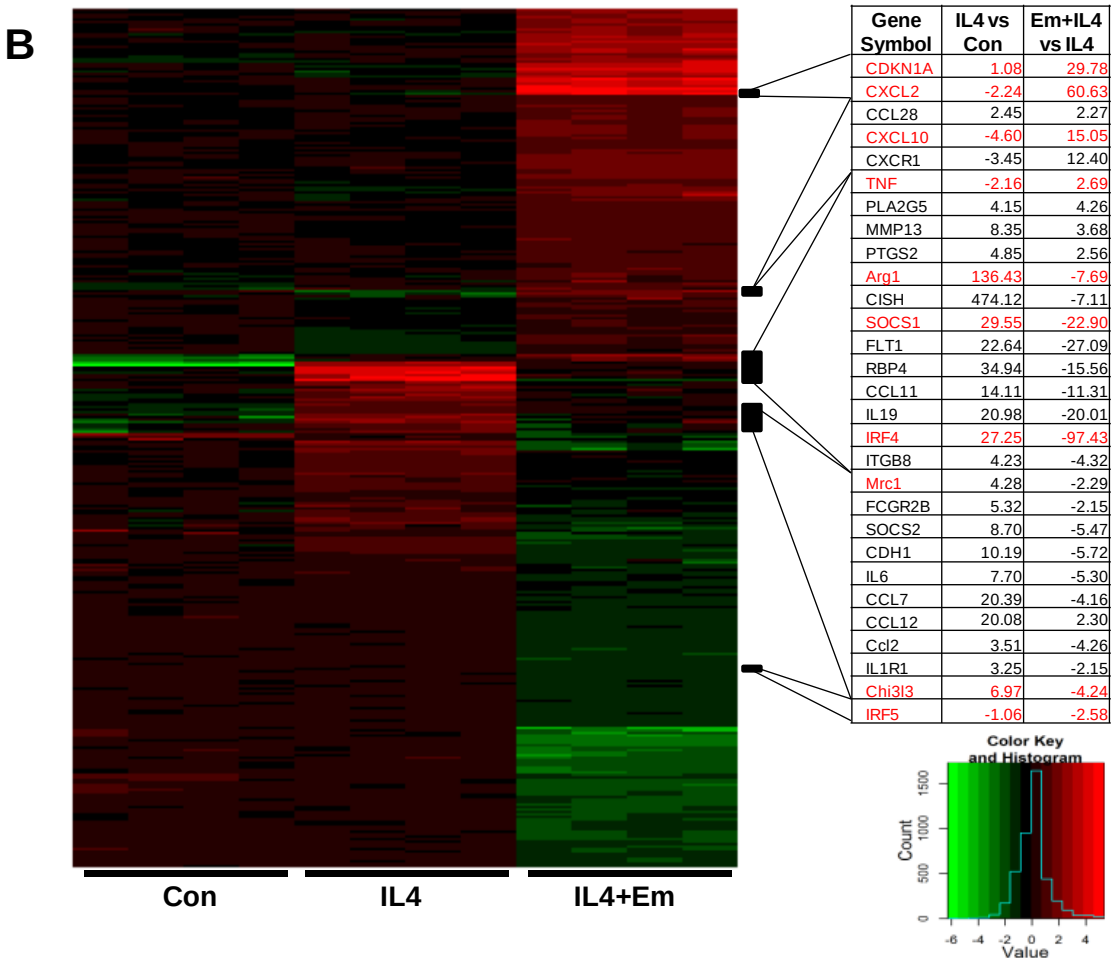

Gene Symbol	IL4 vs Con	Em+IL4 vs IL4
CDKN1A	1.08	29.78
CXCL2	-2.24	60.63
CCL28	2.45	2.27
CXCL10	-4.60	15.05
CXCR1	-3.45	12.40
TNF	-2.16	2.69
PLA2G5	4.15	4.26
MMP13	8.35	3.68
PTGS2	4.85	2.56
Arg1	136.43	-7.69
CISH	474.12	-7.11
SOCS1	29.55	-22.90
FLT1	22.64	-27.09
RBP4	34.94	-15.56
CCL11	14.11	-11.31
IL19	20.98	-20.01
IRF4	27.25	-97.43
ITGB8	4.23	-4.32
Mrc1	4.28	-2.29
FCGR2B	5.32	-2.15
SOCS2	8.70	-5.47
CDH1	10.19	-5.72
IL6	7.70	-5.30
CCL7	20.39	-4.16
CCL12	20.08	2.30
Ccl2	3.51	-4.26
IL1R1	3.25	-2.15
Chi3l3	6.97	-4.24
IRF5	-1.06	-2.58

Figure 2.4 Effects of emodin on the expression of genes that regulate macrophage activation. ***A*** and ***B***, heat maps showing expression of genes associated with the most significantly affected macrophage canonical signaling pathways. Tables on the right show the fold changes of genes caused by LPS/IFNγ or IL4 treatment compared to control and emodin treatment compared to LPS/IFN or IL4 for select macrophage activation genes.

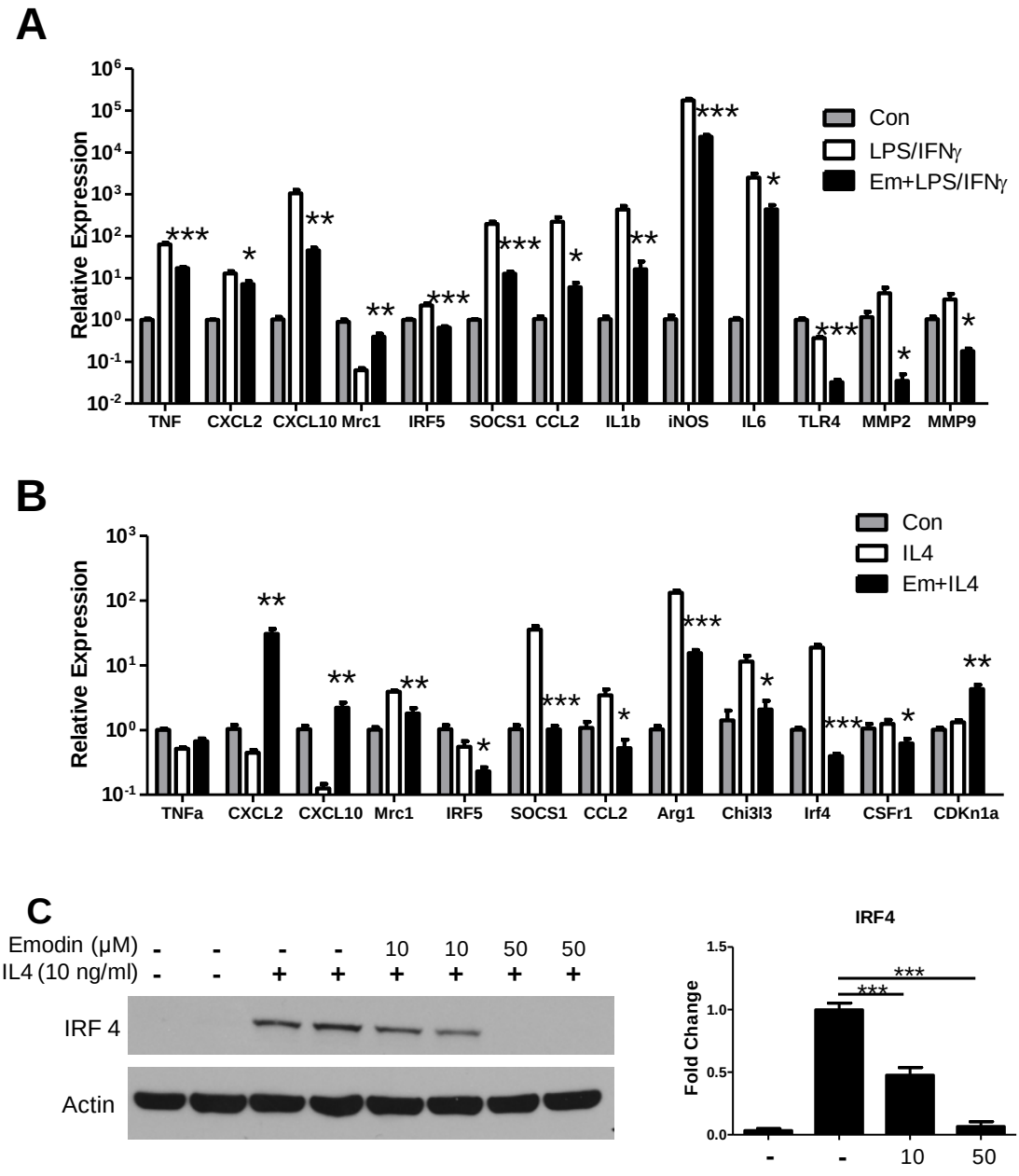

Figure 2.5 Emodin inhibits expression of M1 and M2 genes. ***A*** and ***B***, qPCR was performed to verify the microarray results for select M1 and M2 genes. *Bars* represent the mean ± S.E. For each treatment, $n = 4$. ***C***, Macrophages were stimulated with IL4 with or without emodin (0-50 μM) for 6 h. The cells were lysed and IRF4 protein levels were detected by western blotting. Results are shown as the means ± S.E. for two independent experiments (n=4) * $p<0.05$, ** $p<0.01$, *** $p<0.001$.

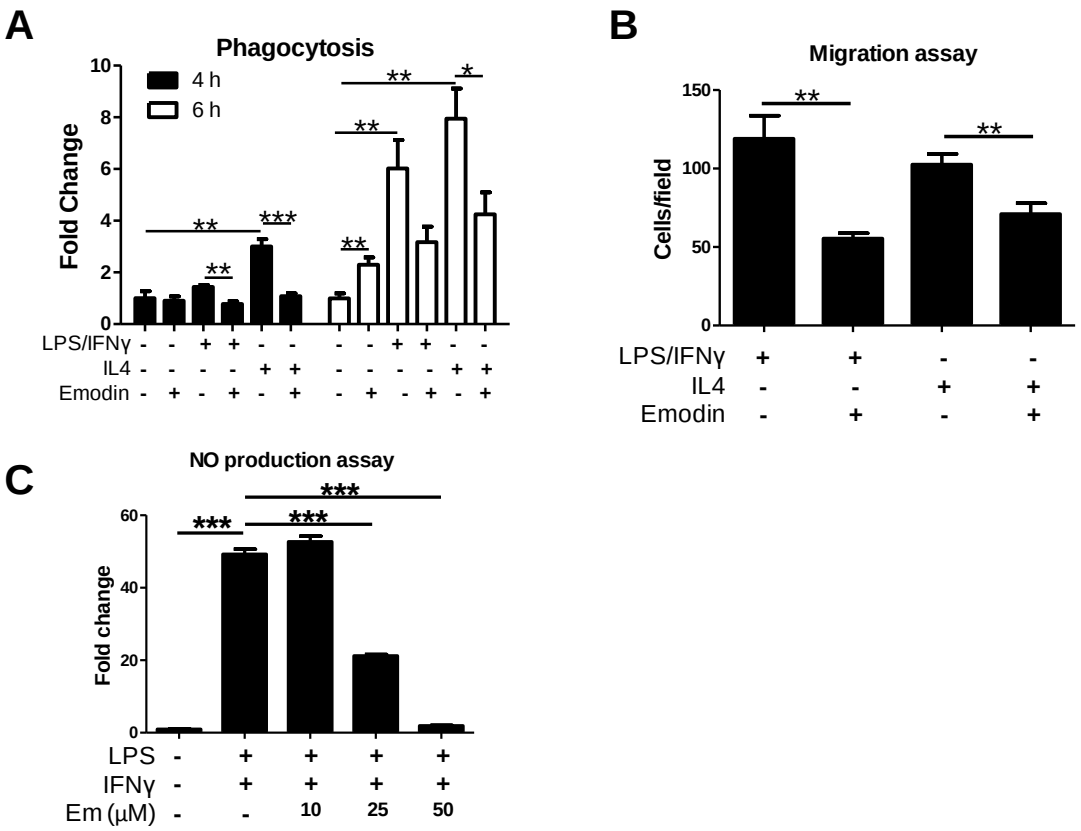

Figure 2.6 Emodin modulates functions of activated macrophages. Mouse peritoneal macrophages were stimulated with LPS (100 ng/ml) and IFNγ (20 ng/ml) or IL4 (10 ng/ml) with or without emodin (50 μM) for 24 h. ***A***, Macrophages were washed and the cells were incubated with FITC labeled *E. coli* bioparticles for 4-6 h. Fluorescence was detected with a microplate reader as an indicator of phagocytosis. Results are shown as the means ± SE (n=4). ***B***, Macrophages were seeded into the top chamber of a transwell insert in DMEM, and DMEM with MCP1 (20 ng/ml) was placed in the bottom of the well. After 4 h, cells were fixed, stained with Dapi, and imaged with 5 fields of view at 20x magnification per membrane. Results are shown as the means ± SE for two independent experiments (n=3). ***C***, Macrophages were incubated with LPS/IFNγ with emodin at various concentrations. After 24 h the media was collected and NO content was detected. Results are shown as the means ± SE (n=4).* $p<0.05$, ** $p<0.01$, *** $p<0.001$.

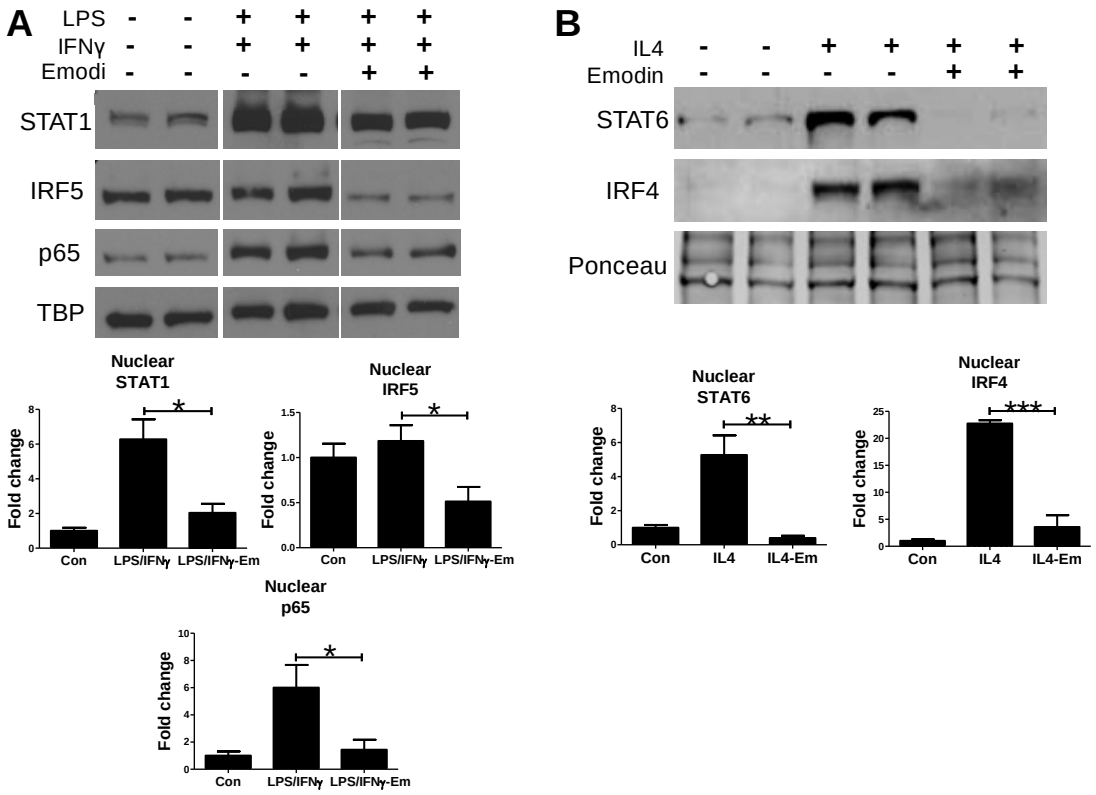

Figure 2.7 Emodin inhibits LPS/IFNγ and IL4 induced activation of signaling pathways. Macrophages were stimulated with (***A)*** LPS (100 ng/ml) and IFNγ (20 ng/ml) or (***B)*** IL4 (10 ng/ml) with or without emodin (50 μM) for 24 h. Cells were lysed and cytoplasmic and nuclear fractions were collected. Transcription factors were then detected in the nuclear fraction using western blotting. Bottom panels, quantification of blots normalized to loading controls TBP or Ponceau S. Results are shown as the means ± SE for two independent experiments (n=4). * $p<0.05$, ** $p<0.01$, *** $p<0.001$.

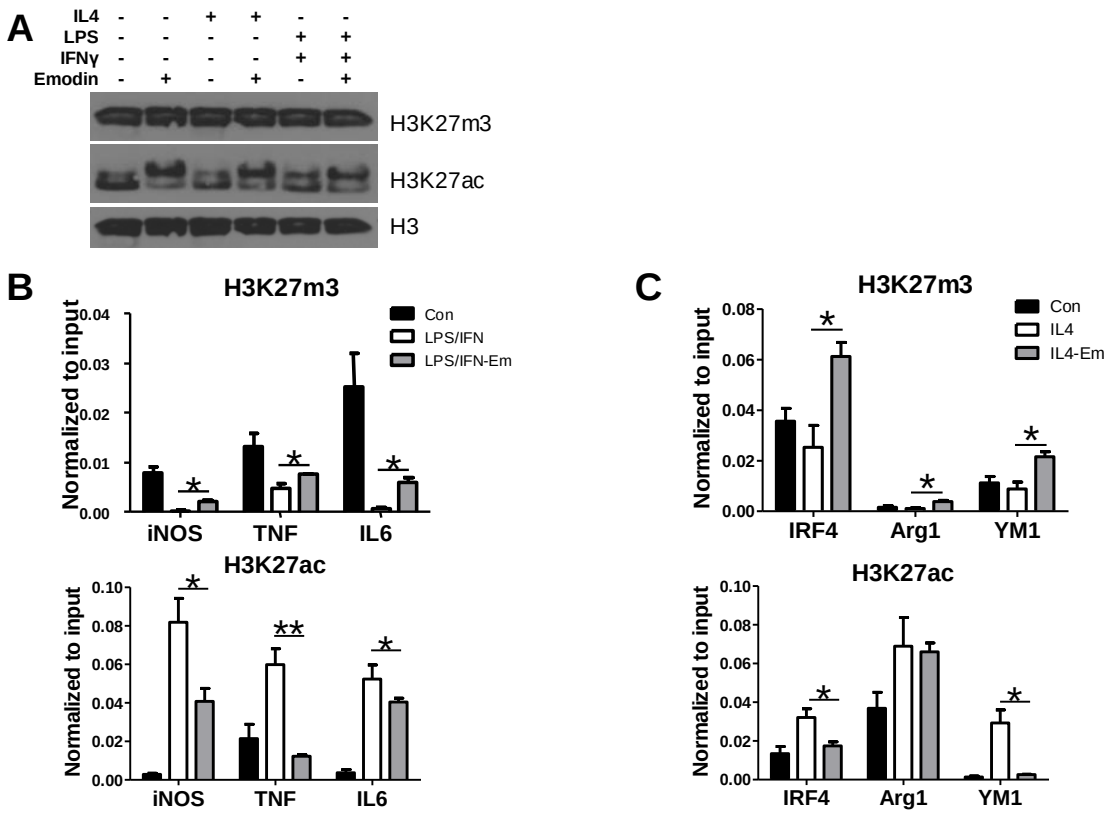

Figure 2.8 Emodin inhibits LPS/IFNγ and IL4 induced histone modifications in macrophages. Macrophages were stimulated with LPS (100 ng/ml) and IFNγ (20 ng/ml) or IL4 (10 ng/ml) with or without emodin (50 μM) for 24 h. ***A***, Global histone modification levels were detected using western blotting. Experiment was performed in triplicate (n=3). ***B*** and ***C***, ChIP-PCR was used to detect gene specific changes in histone modifications. Results are shown as the means ± SE (n=3). *$p \leq 0.05$; **$p \leq 0.01$.

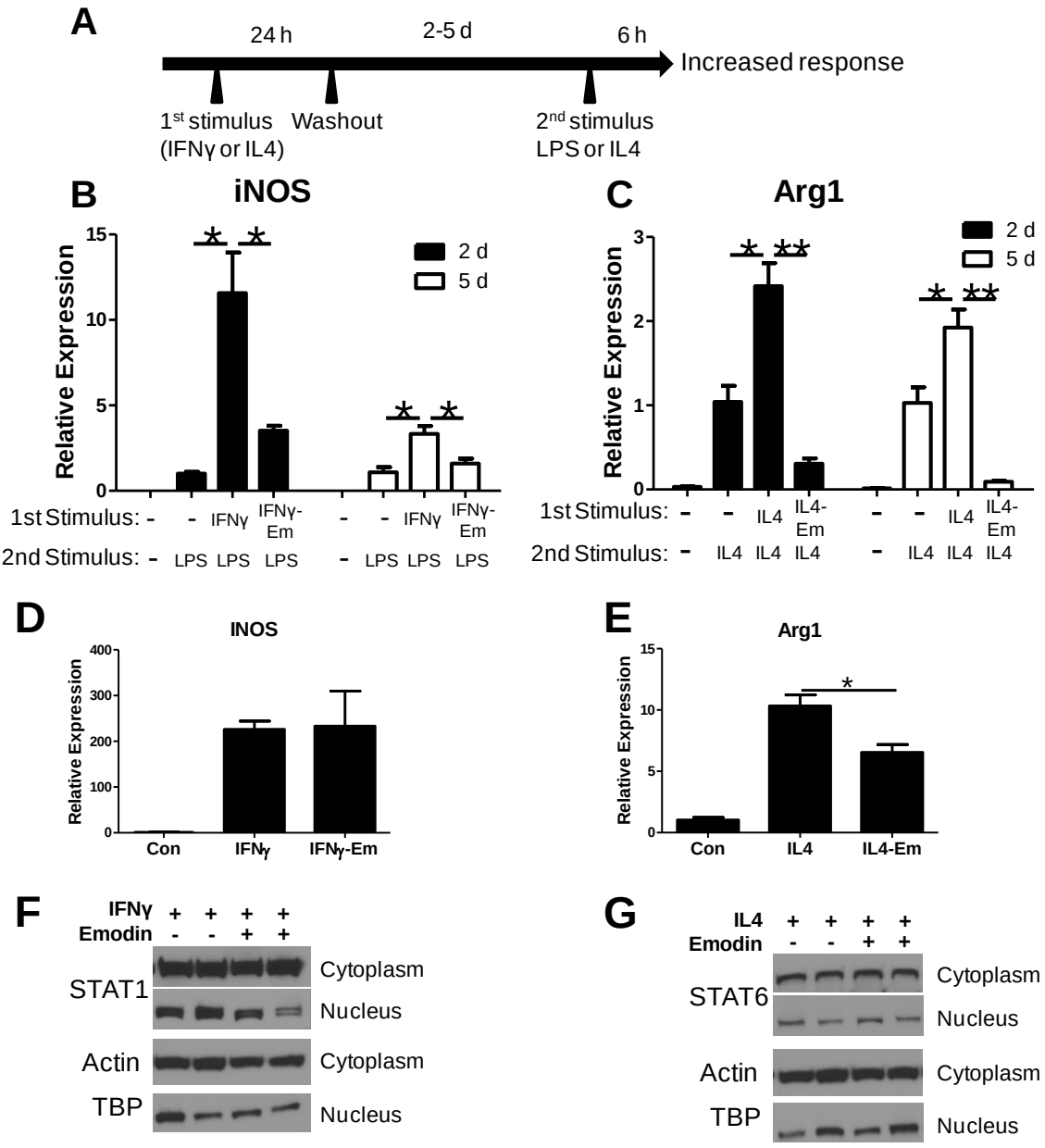

Figure 2.9 Emodin inhibits macrophage memory. *A,* Diagram of macrophage treatments for macrophage training experiments. *B and C,* Macrophages were incubated with IFNγ (20 ng/ml) or IL4 (10 ng/ml) with or without emodin (50 μM) for 24 h. Then the cells were washed and incubated for 2 or 5d. The macrophages were then stimulated with either IL4 or LPS for 6 h and the gene expression was analyzed with qPCR. Results are shown as the means ± SE for two independent experiments (n=3). *D and E,* Gene expression in macrophages after the 2 d rest period. *F and G,* Macrophages were lysed after the 5 d rest period and cytoplasmic and nuclear protein fractions were collected and analyzed via western blotting. *$p \leq 0.05$; **$p \leq 0.01$

CHAPTER 3

EMODIN INHIBITS BREAST CANCER GROWTH BY MODULATING THE TUMOR MICROENVIRONMENT

3.1 BACKGROUND

Since emodin's ability to regulate macrophage polarization was established, we then sought to investigate its therapeutic potential in a disease model dependent on macrophages for progression. In spite of the many advances that have been made, breast cancer is still the second leading cause of cancer deaths among women (183). Tumor growth and metastasis depend on the support from stromal cells including macrophages, fibroblasts, and myeloid derived suppressor cells (MDSCs) in the tumor microenvironment (TME) which promote angiogenesis, matrix remodeling, and immunosuppression (56,184). Recently there has been interest in immunotherapies for the treatment of breast cancer because of their low toxicity and extended duration of action (185,186). However, the immunosuppressive microenvironment of tumors greatly diminishes the effectiveness of these therapies (187,188). MDSCs, M2-like tumor associated macrophages (TAMs), and regulatory T cells have all been shown to repress an effective anti-tumor immune response through the production of anti-inflammatory cytokines and growth factors such as IL10 and TGFβ. Therapies targeting the immunosuppressive microenvironment have shown great potential on their own or in combination with other therapies in experimental models (92,189,190).

Therefore, we investigated emodin's ability to inhibit breast cancer growth through modulating the tumor microenvironment (TME). Emodin treatment significantly reduced the size of EO771 and 4T1 breast tumors. Emodin reduced macrophage infiltration into the tumors and their M2-like activation through inhibiting STAT6, C/EBPβ, and IRF4 signaling pathways and through inhibiting changes in histone modifications. In vitro studies showed that emodin was also able to inhibit tumor cell secretion of macrophage chemoattractants and growth factors. Further, we found that emodin treatment increased T cell activation indicating that the emodin was able to inhibit the immunosuppressive environment of the tumors.

3.2 DETAILED METHODS

Tumor cell culture and conditioned medium collection

The 4T1 cells, obtained from the American Type Culture Collection (ATCC), and EO771 cells, developed from an ER+ spontaneous mammary adenocarcinoma (191,192), were grown in high-glucose Dulbecco's modified Eagle's medium (DMEM, Invitrogen, Grand Island, NY) containing 10% fetal bovine serum (FBS), 100 U/mL penicillin (Sigma-Aldrich, St. Louis, MO), and 100 µg/mL streptomycin (Sigma-Aldrich) at 37 ^{o}C in a humidified CO_2 incubator. For tumor conditioned medium collection, cells were grown until they were 80-90% confluent. Then the media was replaced with serum free (SF) DMEM and the cells were cultured for 48 h. The media was then collected and passed through a 0.45 µm filter (Millipore Corp., Bedford, MA). The media was concentrated 10:1 using centrifuge filters with a 3000 MW cutoff (Millipore) and stored at -80^{o}C. Before use the media was diluted 1:2 with fresh SF DMEM so that the final concentration of the TCM was 5x.

Tumor models

C57BL/6 and BALB/c mice (8-12 week, female) were purchased from Jackson Labs (Bar Harbor, Maine). They were housed at the University of South Carolina Animal research facility and all procedures were approved by the Institutional Animal Care and Use Committee. EO771 or 4T1 cells ($2x10^5$) were injected in 20 µL of PBS into the fat pad of the 4^{th} pair of mammary glands on C57BL/6 mice or BALB/C, respectively, on day 0. Starting on day 1, emodin (40mg/kg) or vehicle (2% DMSO) was injected intraperitoneally in 1 mL PBS once daily until the mice were sacrificed. The tumor size was measured using calipers every 2-4 days once the tumors were large enough, and the tumor volume was calculated using a formula: V (mm^3) = L (major axis) x W^2 (minor axis)/2. Mice were sacrificed at various time points.

Isolation of tumor infiltrating cells

Macrophages or T cells were isolated from 4T1 tumors from mice sacrificed at 6 weeks post implantation or from EO771 tumors 5 weeks post implantation, using EasySep™ Mouse PE Positive Selection Kit (Stem Cell Technologies, Vancouver, BC) as previously described (193). Briefly, tumors were cut into small fragments (<3 mm) and digested in 5 mls collagenase digestion buffer (RPMI 1640 medium containing 10% FBS, Collagenase type I (4 mg/ml), Hyaluronidase (0.5 U/ml) and DNase I (20 µg/ml)) for 60 min at 37°C with continuous shaking. The cell suspensions were then passed through 70 µM cell strainers and centrifuged at 330xg for 5 min. Red blood cells were then lysed by resuspending the cells in 6 mls RBC lysis buffer (Sigma, St. Louis, MO) and incubating them for 5 min. The cells were then passed through a 70 µM strainer again and resuspended in PBS containing 2% FBS. For cell isolation, $1x10^7$-$1x10^8$ cells

were incubated with 20 µL PE conjugated anti-F4/80 (Biolegend) for macrophages or 20 µL PE conjugated anti-CD3 for T cells and 50 µL microbeads. The T cells and 2-5x10^6 macrophages were lysed in Qiazol and used for RT-PCR analysis. For ChIP assays, 5-10x10^6 macrophages were fixed in 1% formaldehyde.

Flow cytometry

The tumor draining lymph nodes and tumors of the mice were collected and cell populations were analyzed using flow cytometry as previously described (193). Briefly, lymphocytes were isolated from lymph nodes by mechanical dissociation. Tumors were cut into small fragments and incubated in collagenase digestion buffer to generate single cell suspensions. Red blood cells were then lysed by resuspending the cells in 6 mls RBC lysis buffer (Sigma, St. Louis, MO) and incubating them for 5 min. The cells were then passed through a 70 µM strainer again and resuspended in staining buffer (PBS containing 2% FBS). Cells were stained with anti-CD3 FITC, anti-CD4 APC or anti-CD8 APC, and anti-CD25 PE (Biolegend) in PBS containing 2% FBS for 30 min at 4 ^{o}C. Samples were washed twice with staining buffer and analyzed by flow cytometry using a BD FACS flow cytometer and CXP software version 2.2 (BD Biosciences, San Jose, CA). Data were collected for 20,000 live events per sample.

For Ki67 staining, 4T1 and EO771 tumor cells were seeded into 6 well plates and cultured in SF DMEM overnight. They were then treated with various concentrations of emodin (0-50 µM) for 24 h. The cells were resuspended with trypsin+EDTA and fixed with 1% paraformaldehyde for 10 min. The cells were then permeablilized with 0.25% Triton X-100 for 15 min. The cells were washed with PBS and stained with anti-Ki67 PE (Abcam). The cells were washed and incubated with goat anti-rabbit alexa 488

(Invitrogen, Eugene, OR). After washing, the samples were analyzed by flow cytometry using a BD FACS flow cytometer and CXP software version 2.2. Data were collected for 10,000 live events per sample.

Immunohistochemistry

At sacrifice, tumors were embedded in OCT. They were then cut into 8 µm thick frozen sections and placed on slides. For Immunohistochemistry (IHC) staining, the sections were fixed with 4% paraformaldehyde for 10 minutes, then blocked with 0.01 M glycine containing 0.1% Triton x-100. Next, the sections were blocked with 5% BSA. They were then incubated in primary antibody overnight at 4 ^{o}C: anti-F4/80 (1:50, Biolegend), anti-pSTAT6 (1:50, Cell Signaling), anti-C/EBPβ (1:50, Santa Cruz). The sections were washed with PBS and then incubated with secondary antibodies for 1 h at room temperature. The sections were then stained with DAPI (5 µg/mL) and coverslipped with DABCO. Slides were imaged using a Zeiss LSM 510 Confocal microscope (Zeiss, Peabody, MA). For quantitative analysis, the number of positive cells was manually counted in six random fields of view per section. CD31 staining was performed as described previously (193). Briefly, tissue sections were fixed in acetone and washed with PBS. They were then incubated with 3% hydrogen peroxide for 5 min and then blocked with normal goat serum. Next they were incubated with anti-CD31 (1:100, BD) at 4^{o}C overnight. The slides were then washed and incubated with biotin conjugated secondary antibodies and AEC chromogen/HRP substrate kit (GeneTex, Irvine, CA) according to the manufacturer's instructions. The sections were counterstained with hematoxylin and coversliped with DABCO. Slides were imaged on a Nikon ECLIPSE E600 microscope (Nikon, Melville, NY) at 200x magnification (10 fields per section).

The integrated optical density (IOD) of CD31 was quantified using Image-Pro Plus software.

Peritoneal macrophage isolation and treatment

Peritoneal macrophages were collected as described in Chapter 2. Mice were injected with 3 mls of 4% Thioglycolate solution. After 3 days, macrophages were collected by peritoneal lavage with PBS. The cells were resuspended in DMEM+10% FBS and cultured for 2 h. The non-adherent cells were then washed away and the remaining cells were cultured overnight in SF DMEM. The cells were then treated with tumor conditioned medium (TCM) with or without emodin.

Quantitative real-time PCR (qPCR)

For qPCR, cells were lysed with Qiazol and RNA was extracted using Zymo research Direct-zol RNA isolation kit. cDNA was then made from 1 µg of RNA using iScript cDNA Synthesis Kit (Bio-Rad Life Science, Hercules, CA). Primers are listed in Tables 2.1 and 3.1; run conditions were 95 ^{o}C for 10 s, 58 ^{o}C for 15 s, 70 ^{o}C for 15 s. Samples were run in duplicate on a Bio-rad CFX Real Time thermocycler. Relative expression was determined using the ΔΔCt method.

Chromatin immunoprecipitation and global histone analysis

ChIP assays were performed as described in chapter 2 with few modifications. Macrophages were fixed in 1% formaldehyde. Excess formaldehyde was quenched with glycine and the cells were collected in PBS by scraping. The cells were lysed and the nuclei were resuspended in nuclear lysis buffer. The DNA was sheared by sonication using a Diagenode Bioruptor Pico (Diagenode, Denville, NJ) for 25 cycles of 30 s on/30 s off. Then 8 µg chromatin was diluted 1:10 and 2% of the input was removed from each

sample and saved for analysis. Anti-H3K27m3 (Abcam) was added to each sample along with 20 µL of protein A+G magnetic beads (Millipore), and the samples were incubated overnight at 4 °C. The beads were washed with low salt, high salt, LiCl, and TE wash buffers sequentially and the DNA was eluted off the beads with Proteinase K at 62 °C for 2 h. The DNA was then analyzed by real time PCR using primers listed in Table 2.3.

In order to detect genome wide levels of histone H3 modifications, histones were isolated from macrophages treated with TCM with or without emodin for 24 h using EpiQuik total histone extraction kits (Epigentek, Farmingdale, NY) according to the manufacturer's directions. Briefly, macrophages were washed with PBS following treatments and collected by scraping. Macrophages were resuspended in pre-lysis buffer and incubated on ice for 10 min. The nuclei was then pelleted by centrifugation and resuspended in approximately 40µl lysis buffer and incubated on ice for 30 min. The lysate was centrifuged at 20,000xg for 5 min and the supernatant was collected. The lysate was then neutralized with balance buffer and quantified using a BioRad DC protein assay. Histones (100 ng) were then analyzed using an EpiQuik Histone H3 modification kits (EpiGentek) according to the manufacturer's instructions. The colormetric reaction was detected on a Spectra Max M5 Microplate Reader (Molecular Devices, Sunnyvale, CA).

T cell proliferation and activation assays

Peritoneal macrophages were isolated from C57BL/6 mice as described previously. Cells were seeded into 10 cm plates and treated with EO771 conditioned medium with or without emodin for 24 h. The cells were then washed with PBS and resuspended by scraping. T cells were isolated from the spleens of C57BL/6 mice using

EasySep T cell isolation kit (Stem Cell Technologies) according to the manufacturer's instructions. For the proliferation assay, T cells were labeled with CSFE (Biolegend). T cells were suspended in 1 ml PBS and were added to 1 ml of 10 µM CSFE in PBS and incubated in the dark at 37°C for 10 min. The CSFE labeled cells were then wash with RPMI1640 media containing 10% FBS. T cells were added then mixed with macrophages and CD3/CD28 DYNA beads (ThermoFisher Scientific) in a 1:1:1 ratio and added to 12 well plates in triplicate and cultured in RPMI1640 containing 10% FBS, 100 U/mL penicillin, and 100 µg/mL streptomycin. For the activation assay, the T cells were collected after 24 h and stained with anti-CD3, anti-CD4, and anti-CD69 for 30 min at 4 °C. The cells were then analyzed on a BD FACS flow cytometer. For the proliferation assay, T cells were collected after 72 h and stained with anti-CD3 and anti-CD4. The cells were analyzed for CSFE depletion on a Beckman Coulter FC500.

Tumor cell viability assay

Tumor cells ($2x10^4$ EO771 or 4T1 cells) were seeded into 96 well culture plates in DMEM+10% FBS. The cells were incubated overnight at 37 °C. The media was then removed, and the cells were washed with PBS. DMEM containing varying concentrations of emodin (0-100µM) was then added to the cells in quadruplicate. Control contained an equal volume of DMSO. Plates of cells were then incubated for 24-48 hours. After the stated time, the viability of the cells was determined using a Lactate Dehydrogenase (LDH) Cytotoxicity Detection Kit (Clonetech Mountain View, CA) according the manufacturer's instructions. Briefly, the supernatant was removed from each well on the plate and placed in a new well on the same plate. An equal volume of cell lysis buffer (2% triton in DMEM) was then added to each well containing the cancer cells, and the

cells were incubated at room temperature for 15 minutes. The reaction mixture was then added to each well (cell lysate+supernatant) and incubated for 5 minutes before the stop solution (1N HCl) was added. The absorbance was measured at 490 nm on a Spectra Max M5 Microplate Reader (Molecular Devices, Sunnyvale, CA). The percent viability was then calculated as the ratio of LDH in the cell lysate to the total amount of LDH in the lysate plus the supernatant. The viability of each group was compared to the control.

Transwell migration assay

TCM was generated from tumor cells which had been pre-treated with various concentrations of emodin. The EO771 or 4T1 cells were treated with 0-50 µM emodin for 24 h. Then the cells were washed multiple times with PBS, cultured for 48 h, and TCM was collected as previously described. The TCM was placed in the bottom chamber of transwell inserts and $2x10^5$ peritoneal macrophages were seeded into the top chamber in SF DMEM. The cells were incubated at 37 ^oC with 5% CO_2 for 4 h. The membranes were then fixed with 4% paraformaldehyde for 10 min. The cells were removed from the top chamber using cotton swabs, and the cells on the bottom chamber were stained with DAPI (5 µg/mL). The inserts were then cut out, mounted onto slides, and imaged under a Nikon Eclipse E-600 fluorescence microscope (Nikon Inc. Melville, NY) at 20 × magnification (5 fields/insert). DAPI stained cells were quantified using ImagePro Plus software.

Macrophage adhesion assays

Tumor cell monolayers (80-90% confluent) and macrophages were treated with emodin (0, 10, or 25 µM) overnight. Then the cells were washed multiple times with PBS, and fresh SF DMEM was added. Macrophages were resuspended with scraping and

$5x10^5$ cells were seeded onto the tumor cell monolayers. After 1 h the non-adherent cells were washed away and the adherent cells were resuspended with Trypsin and mild scraping. The total number of cells was counted, and the cells were stained with anti-F4/80 FITC (Biolegend). The cells were analyzed on a Beckman Coulter FC500.

Statistical analysis

For all experiments, data were presented as mean ± standard error of the mean (SEM). For two-group comparison, statistical significance was calculated by 2-tailed Student's *t* test. For multiple group comparison, one-way ANOVA was used followed by Tukey multiple comparison test. All statistical analyses were performed using the GraphPad Prism statistical program (GraphPad Software Inc., San Diego, CA). $p \leq 0.05$ was considered significant.

3.3 RESULTS

Emodin inhibits breast tumor growth

In a previous study from our lab, when emodin treatment began after tumors were well established (~200 mm^3), it had no effect on the size of the primary tumor but significantly reduced lung metastasis (148). We hypothesized that emodin might be most effective in the inhibition of primary tumor growth when administered in the early stages of tumor formation. Breast cancer EO771 and 4T1 cells were injected into the mammary glands of C57Bl/6 or Balb/c mice, respectively, and emodin treatment (40 mg/kg IP once daily) began 1 day after tumor cell injection. Emodin caused a significant inhibition of primary tumor growth (Figure 3.1A) and reduced tumor size (Figure 3.1B) and tumor weight (Figure 3.1C) at the endpoints in both EO771 and 4T1 models.

Emodin inhibits macrophage infiltration and M2-like activation

Our previous study had shown that emodin could inhibit macrophage recruitment and M2-like polarization in metastatic breast cancer in the lungs. Here we investigate whether or not emodin also acts through macrophages in the inhibition of primary breast cancer growth. First we examined macrophage infiltration and phenotype in EO771 tumor bearing mice at the experimental endpoint. Immunohistochemical analysis revealed that emodin reduced the number of tumor infiltrating macrophages by 70% (Figure 3.2A). We extracted $F4/80^{+}$ cells from the tumors using magnetic beads and used qPCR to examine the expression levels of M1 or M2 macrophage markers. qPCR showed that TAMs in the emodin-treated mice had significantly lower M2 marker (Arg1 and CD206) expression but significantly higher M1 marker (iNOS) expression and also had higher expression levels of inflammatory cytokines IL1β and TNFα, although without statistical significance (Figure 3.2B).

To exclude the possibility that reduced total TAMs and M2 marker expression in emodin-treated breast cancer mice was the result of halted tumor growth instead of it being the cause, we next investigated emodin's effects on macrophages in tumors at the time point when there was no difference in the size of the tumors between the two groups. Emodin significantly reduced the number of macrophages in 4T1 tumors 26 days post implantation while the tumor size was not different between the two groups at this time point; moreover, emodin significantly reduced the fraction of macrophages positive for transcription factors pSTAT6 and C/EBPβ (Figure 3.2C and D), indicating that emodin indeed directly inhibited the macrophage infiltration and M2 polarization in the tumors independent of tumor size.

Furthermore, we isolated TAMs from 4T1 tumors at the experimental endpoint and found that TAMs in emodin-treated mice had significantly decreased expression of IRF4 compared to those in control mice (Figure 3.2E). IRF4 has previously been shown to play a major role in macrophage M2 activation and is regulated by removal of H3K27 tri-methylation (H3K27m3) by histone demethylase JMJD3 (21,22). We found that emodin significantly decreased the expression of JMJD3 in TAMs (Figure 3.2E). Therefore, we further examined emodin's effect on H3K27m3 marks using ChIP-qPCR and found that emodin significantly increased H3K27m3 levels on the IRF4 promoter (Figure 3.2F). Taken together, these results indicate that emodin inhibited M2 like polarization in TAMs through epigenetically blocking IRF4, STAT6, and C/EBPβ signaling pathways in the breast cancer TME.

Emodin inhibits macrophage response to tumor cell-derived soluble factors

Next, we examined the effects of emodin on the response of macrophages to tumor cell derived factors. Peritoneal macrophages from C57BL/6 mice were treated with EO771 TCM and gene expression was examined by qPCR. Emodin dose dependently inhibited TCM-induced expression of Arg1 and transcription factors C/EBPβ and IRF4 (Figure 3.3A). Emodin also decreased the expression of CSFr1 (Figure 3.3A), a key receptor on macrophages through which they are induced by tumor-secreted CSF1 towards M2-like activation (70,71). Moreover, emodin inhibited the expression of pro-angiogenic factors MMP2 and MMP9 (Figure 3.3A) (194,195). Interestingly, we also found that TCM treatment increased expression of ICAM1 in macrophages and the effect was dose dependently blocked by emodin, suggesting that emodin could interfere with macrophage adhesion to tumor cells. In agreement with the *in vivo* data, TCM treatment

increased the expression of JMJD3, and emodin significantly attenuated the increase (Figure 14B). Both TCM and emodin had no effects on global levels of H3K27 methylation (Figure 3.3C). However, TCM decreased H3K27m3 on the promoter of Arg1, IRF4, and C/EBPβ but emodin treatment reversed the reduction (Figure 3.3D). These results indicate that emodin epigenetically inhibits macrophage activation in response to tumor-cell derived soluble factors.

Emodin increased T cell activation and decreased angiogenesis

TAMs substantially contribute to the immunosuppressive microenvironment in tumors. Since emodin inhibited TAM infiltration and M2-like polarization, we hypothesized that emodin treatment would lead to increased T cell activation in breast tumors. T cells were detected in the draining lymph nodes of mice bearing 4T1 tumors using flow cytometry. Emodin treated mice had increased activated $CD4^+$ and $CD8^+$ T cells (Figure 3.4A). There was a similar trend of increased activated T cells in the tumors of emodin treated mice (Figure 3.4B).We then isolated $CD3^+$ cells from the tumors and analyzed them using qPCR. T cells from emodin treated mice had a two-fold increase in IFNγ expression compared to those from control mice (Figure 3.4C). Taken together, these data indicate that emodin treatment led to increased T cell activation in breast tumors.

Next we investigated whether or not emodin increased activated T cells in breast tumors through its effects on TAMs. Peritoneal macrophages were pre-treated with EO771 TCM with or without emodin for 24 h. Then the macrophages were incubated 1:1 with T cells stimulated with CD3/CD28 beads for 24 h. TCM treated macrophages reduced expression of activation marker CD69 by 70% on CD4 T cells compared to

control macrophages (Figure 3.4D); however, pre-treatment of macrophages with emodin along with TCM completely blocked the suppression of T cell activation and even increased CD69 expression on CD4 T cells above that of T cells co-cultured with control macrophages. T cell proliferation was examined after 72 h by CSFE depletion analysis and revealed that TCM and emodin co-treated macrophages restored T cell proliferation which was suppressed by TCM only-treated macrophages (Figure 3.4E).

TAMs have also been shown to promote angiogenesis in breast tumors (100,101). Therefore, we examined the effects of emodin on angiogenesis in tumors by staining tumor sections with mouse endothelial antigen CD31 to detect microvessel density. Emodin significantly decreased CD31 staining in EO771 tumors to almost 50% of that in control tumors (Figure 3.4E). Taken together these data indicate that emodin was able to increase T cell activation and suppress angiogenesis in breast cancer.

Emodin affected gene expression in breast cancer cells

Tumor cell-TAM interaction has been shown to be a complex feedback loop that leads to a pro-tumor macrophage phenotype (85,196). Our results have shown that emodin can inhibit the response of macrophages to tumor secreted signals, but it is unknown if emodin could affect the ability of tumor cells to communicate with and therefore train macrophages. EO771 and 4T1 cells were treated with emodin *in vitro* and cell viability (LDH method) and proliferation (KI67 staining) was determined and gene expression was detected. The results showed that emodin had low toxicity toward the two cell lines used. There was only a slight effect on cell viability starting at 25μM (Figures 3.5A) and no significant effect on cell proliferation at concentrations less than 50 μM (Figure 3.5B). We then examined the effect of emodin on tumor cell gene expression.

Emodin significantly inhibited the expression macrophage chemoattractant and growth factors CCL2, CSF1, and CSF2 in both 4T1 and EO771 cells (Figure 3.5C). Emodin treatment also significantly inhibited tumor cell expression of Thy1 (Figure 3.5D), which has been shown to help anchor macrophages to the tumor cells and supports juxtacrine signaling (60). These results indicate that emodin could interfere with the ability of tumor cells signal to, recruit, and polarize macrophages.

Emodin blocks macrophage-tumor cell interactions.

We examined if emodin could inhibit tumor cell induction of macrophage migration. Conditioned medium was collected from tumor cells treated with various concentrations of emodin, and its ability to induce macrophage migration as examined. There was a decrease in macrophage migration toward the TCM collected from cells treated with increasing concentrations of emodin (Figure 3.6A). These results suggest that emodin inhibits the ability of breast cancer cells to attract macrophages.

Recent studies have shown that tumor cells can use juxtacrine signaling to communicate with macrophages and induce them toward a pro-tumor phenotype (60,65,98). We therefore examined the effects of emodin on tumor cell-macrophage adhesion by pre-treating macrophages, tumor cells, or both with emodin. We found that emodin treatment of either macrophages or tumor cells significantly inhibited the adhesion of macrophages to a monolayer of tumor cells, and treatment of both macrophages and tumor cells decreased the adhesion even further (Figure 3.6B). Taken together, these data show that emodin inihibits breast cancer cell-macrophage adhesion by acting on both cell types.

3.4 DISCUSSION

Our data show that emodin significantly inhibited the growth of breast cancer by modulating the tumor microenvironment (TME). Emodin inhibited tumor cell-macrophage interactions through blocking the response of macrophages to tumor signals and by inhibiting the paracrine and juxtacrine signaling from tumor cells to macrophages. Emodin treatment inhibited macrophage infiltration and M2- polarization by blocking STAT6, C/EBPβ, and IRF4 signaling in macrophages. Emodin epigenetically regulated macrophage polarization by increasing the amount of H3K27m3 on the promoters of IRF4 and other M2 associated genes. Through its effects on TAMs, emodin effectively increased T cell activation and inhibited angiogenesis in breast tumors. In addition, emodin inhibited tumor cell-macrophage adhesion at least partially via suppressing Thy1 expression on tumor cells and ICAM1 expression on macrophages. Emodin also inhibited tumor cell secretion of macrophage chemoattractants and growth factors CCL2, CSF1, and CSF2. Taken together, these data show that emodin blocks the pro-tumor feedforward loop between cancer cells and macrophages by targeting both cell types (Figure 3.6C).

The majority of previous studies on emodin have been focused on emodin's direct toxicity to tumor cells (150,158,197). A few studies have also found that emodin could inhibit tumor growth through inhibiting angiogenesis (125,198). In this study, we administered emodin immediately following tumor cell implantation, before the tumor cells could establish their microenvironment and found that emodin significantly inhibited growth of the primary tumor. We used two well-established breast cancer cell lines, EO771 and 4T1, and corresponding syngeneic mouse models. We found that

emodin exhibited little or no direct toxicity towards either of the cell lines at concentrations lower than 25 µM. As demonstrated in our previous study, 25 µM is the highest plasma concentration of emodin we detected *in vivo* using an intraperitoneal dose of 40mg/kg (133). Furthermore, emodin had no effect on tumor cell proliferation, as shown by Ki67 staining, at doses less than 50 µM. Therefore, it is likely that emodin inhibits tumor growth predominately through modulating the tumor microenvironment in our study. Emodin decreased macrophage infiltration in the breast tumors and inhibited TAM polarization by suppressing IRF4, STAT6 and C/EBPβ signaling. Also, we are the first to report that emodin epigenetically regulated TAM polarization by inhibiting IRF4, CEBPβ, and Arg1 expression through increasing H3K27m3 on their promoter regions, likely by decreasing the expression of H3K27 demethylase JMJD3.

Emodin treatment increased T cell activation in tumors. Emodin has previously been reported to induce apoptosis in human T cells (199), and we found similar results with direct emodin treatment of T cells isolated from spleens of mice (Figure 3.7). Therefore, emodin likely activates T cells indirectly through inhibiting TAM-mediated immune suppression. TCM treated macrophages significantly inhibited T cell activation and proliferation; however, emodin treatment abrogated the suppressive ability of TCM treated macrophages. The reduced angiogenesis in tumors of emodin-treated mice may be due to several mechanisms. Emodin has previously been shown to inhibit tumor angiogenesis by inhibiting tumor cell production of MMPs and by blocking VEGF signaling (165-167). In addition, emodin could directly target endothelial cells to inhibit proliferation and vessel formation (169,170). However, we found that emodin might be able to inhibit angiogenesis through targeting TAMs. Emodin decreased breast tumor

vascularity and inhibited macrophage expression of MMP2 and MMP9 in response to tumor cell derived soluble factors.

Although emodin did not cause direct cytotoxicity to breast cancer cells at lower than 25 μM concentrations, it did significantly inhibit the ability of tumor cells to attract and polarize macrophages through blocking the secretion of MCP1 and CSF1, two chemokines that play important roles in the TME (98). In addition, emodin reduced Arg1, IRF4, and C/EBPβ expression in TAMs, which promote the immunosuppressive phenotype (182,200,201). Moreover, emodin reduced TAM expression of CSF1r. Tumor derived soluble factors decreased the expression of transcription inhibitory mark H3K27m3 at the promoters of M2 associated genes (IRF4, Arg1, CEBPβ, and YM1). Emodin prevented the loss of H3K27m3 likely by inhibiting the TCM induced expression of JMJD3. Emodin also significantly inhibited the ability of tumor cells to attract and polarize macrophages through blocking the secretion of chemoattractant CCL2 and growth factors CSF1 and CSF2**.** Therefore, our results indicate that emodin is able to inhibit both macrophage response to tumor derived signals and tumor cell expression of signaling molecules.

Juxtacrine signaling between macrophages and breast cancer cells has been shown to be important for tumor growth. Expression of adhesion protein CD90, which can interact with integrins on monocytes/macrophages, can greatly enhance breast cancer growth (22). $CD90^{hi}$ human breast cancer cells formed significantly larger and more aggressive tumors than $CD90^{lo}$ cells when injected into the mammary fat pad of Nude mice. Previous studies have shown that emodin has potential to block cell-cell interactions by inhibiting the expression or function of adhesion molecules on the surface

of cells. Liu and colleagues reported that emodin treatment could dose dependently reduce adhesion of THP-1 monocytes to fibroblast monolayers (136). Similarly emodin treatment inhibited the expression of cell surface adhesion proteins ICAM1, VCAM1, and ELAM1 in human endothelial cells (203). In agreement with these studies, our data shows that emodin is able to block tumor cell-macrophage adhesion. Emodin decreased expression of cell adhesion proteins CD90 (THY-1) on tumor cells and ICAM-1 on macrophages.

In summary our results show that emodin emodin acts on both breast cancer cells and TAMs and thus ameliorates the immunosuppressive Emodin inhibits tumor cell recruitment and education of macrophages; and transcriptionally and epigenetically inhibits the response of macrophages to tumor-secreted factors. The reduction of M2-like macrophage numbers led to increased T cell activity in tumors, reduced angiogenesis, and reduced tumor growth. Therefore, emodin may be developed as a potent therapy for breast cancer

Tables

Table 3.1 Primers for qPCR

Primers	**Forward**	**Reverse**
CD86	GCACGTCTAAGCAAGGTCAC	CATATGCCACACACCATCCG
CEBPB	CAAGCTGAGCGACGAGTACA	AGCTGCTCCACCTTCTTCTG
CSF1	CACCTTCTCCAGTGTGCTGA	GGAGTCCATAGGGAGGAAGC
CSF2	CAAAGAAGCCCTGAACCTCCTG	ATTGCCCCGTAGACCCTGCTC
IFNg	GGAACTGGCAAAAGGATGGTGA	TTGTTGCTGATGGCCTGATTGT
JMJD3	TCGCGGTACATGAGCACTAT	ATCCACACAAGGTCTCCAGG
THY-1	TGAACCAAAACCTTCGCCTG	AGTAGTCGCCCTCATCCTTG

Figures

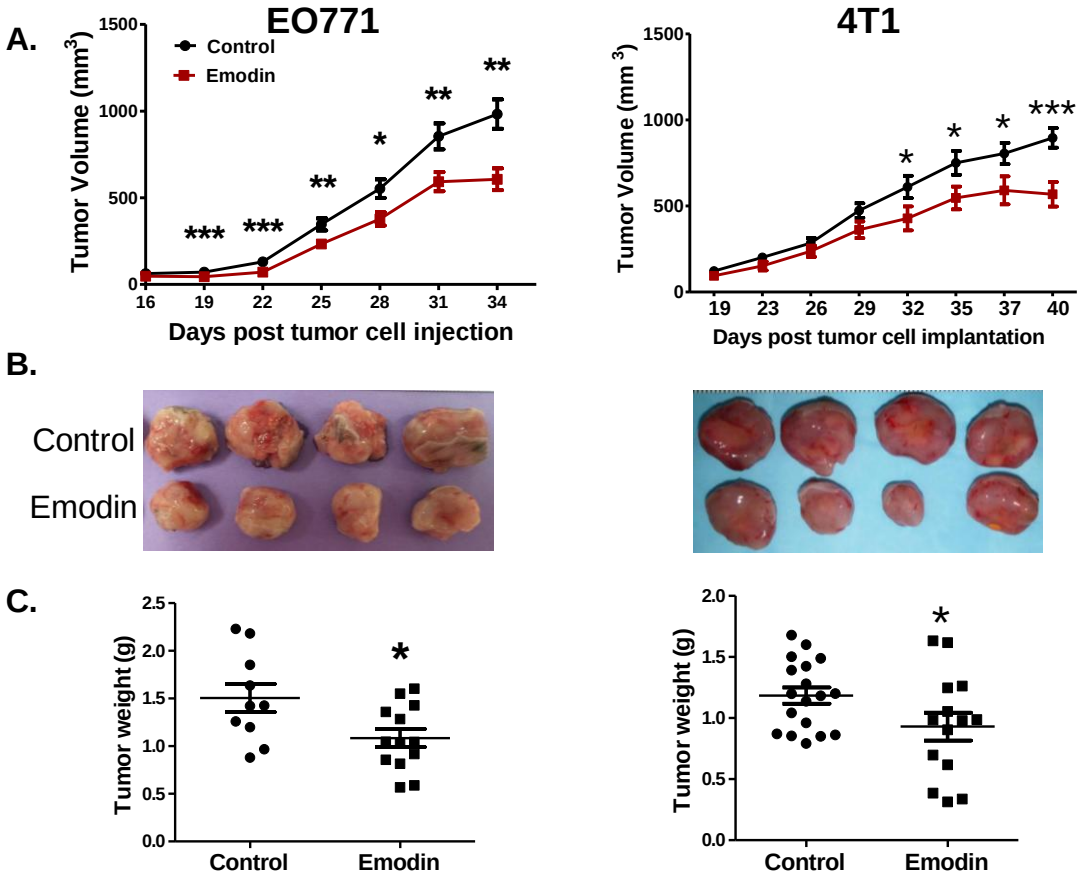

Figure 3.1 Emodin inhibits growth of breast tumors. C57BL/6 (n=7 for control, n= 8 for emodin group) or BALB/c (n=9 for control, n=7 for emodin group) were injected with $2x10^5$ EO771 or 4T1 cells respectively. Emodin treatment (40 mg/kg IP once daily) began on day 1 following tumor injection of tumor cells. **A.** Tumor size was measured with calipers and volume was calculated using the following formula: V (mm^3) = L x $W^2/2$. **B.** Representative image of tumors. **C.** Weight of tumors. *p<0.05, **p<0.01, ***p<0.001.

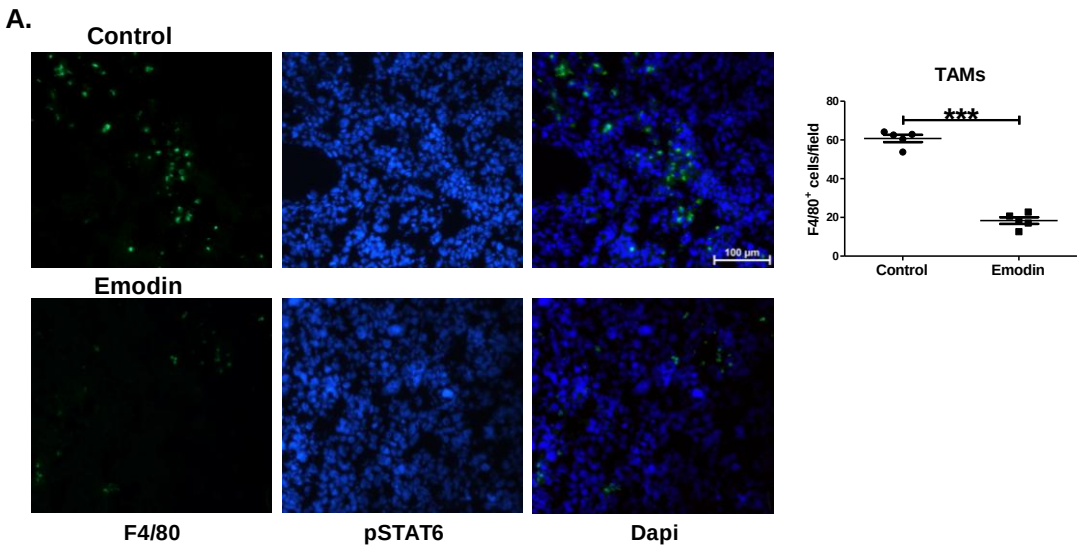

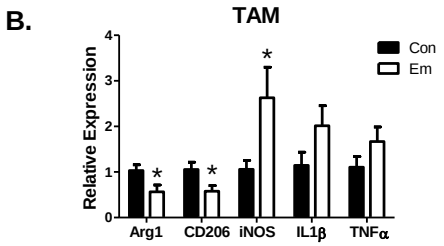

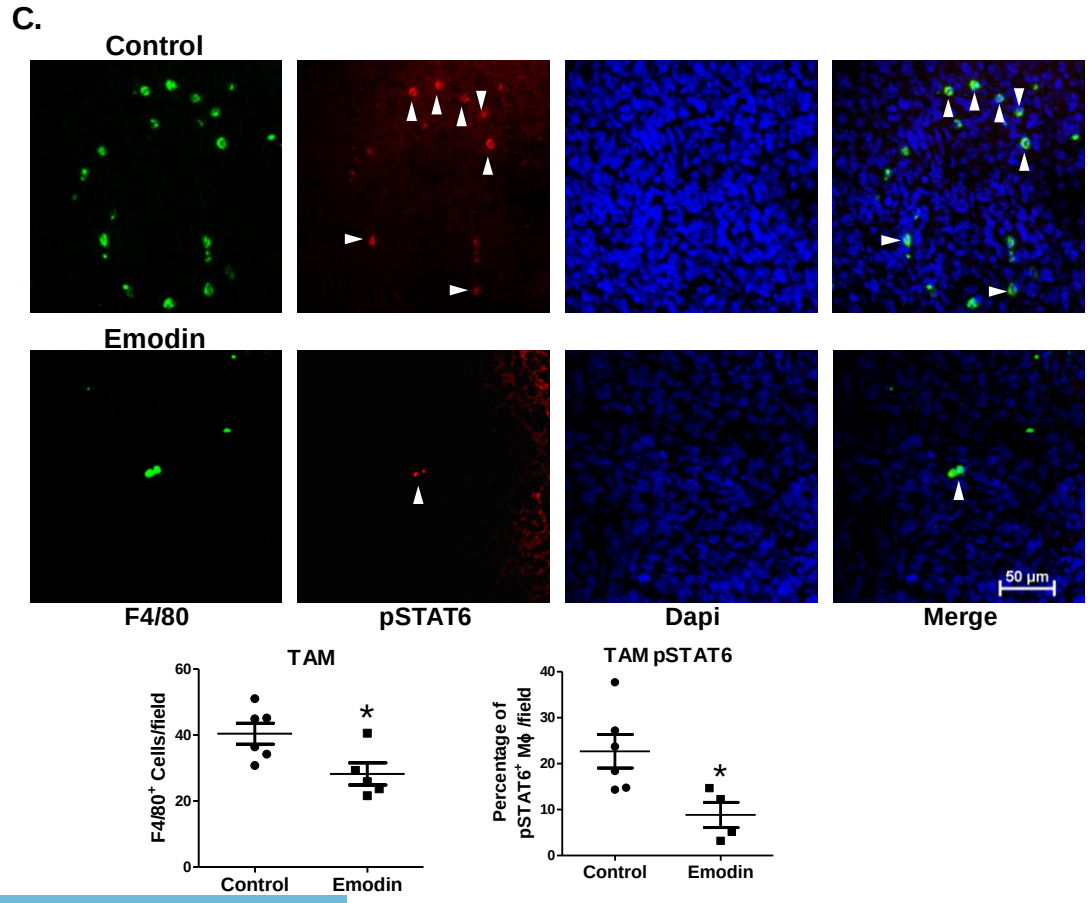

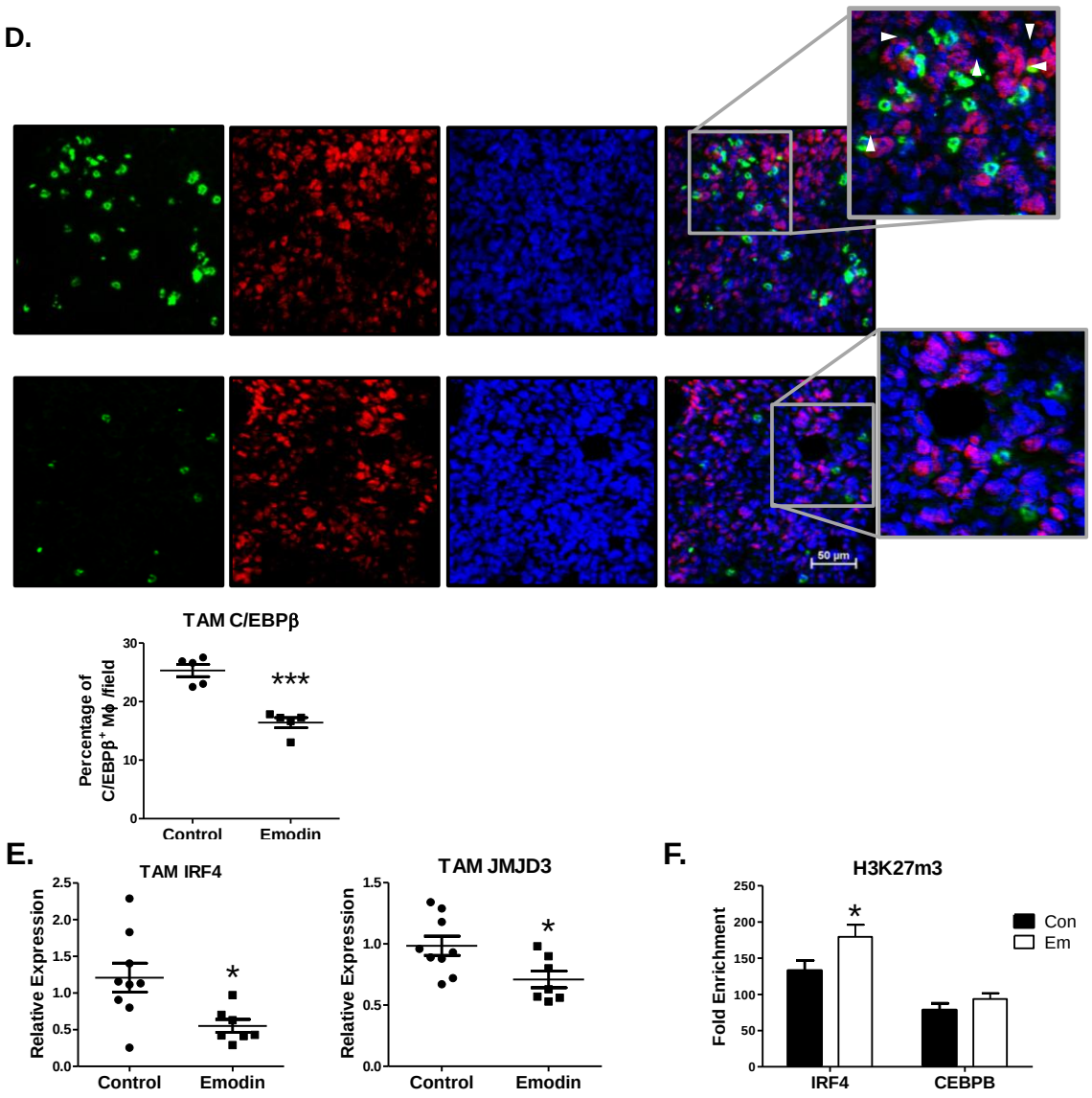

Figure 3.2 Emodin inhibits macrophage infiltration into tumors and activation. A. EO771 tumors were embedded in OCT (n=5). Tumors were cut in 8 µm sections and stained for F4/80. Sections were imaged (200x, 10 fields per section) and the number of positive cells was manually counted. Results are shown as means ± S.E. **B.** F4/80^{+} cells were isolated from the EO771 tumors of C57BL/6 mice (n=5). Gene expression was detected using RT-qPCR. **C. and D.** 4T1 tumors from mice were collected 26 days post injection and embedded in OCT (n=6 for control, n=5 for emodin group). Tumors were cut in 8 µm sections and stained for F4/80 and pSTAT6 or C/EBPβ. Sections were imaged (200x, 5 fields per section) and the number of positive cells was manually counted. Results are shown as means ± S.E. **E.** F4/80^{+} TAMs were isolated from 4T1 tumors using magnetic beads at the experimental end point. Gene expression (n=9 for control, n=7 for emodin group) was detected using RT-qPCR. **F.** A ChIP assay was used to detect H3K27m3 levels on the promoters of IRF4 and C/EBPβ (n=8 for control, n=6 for emodin group). Results are shown as means ± S.E. *p<0.05, ***p<0.001

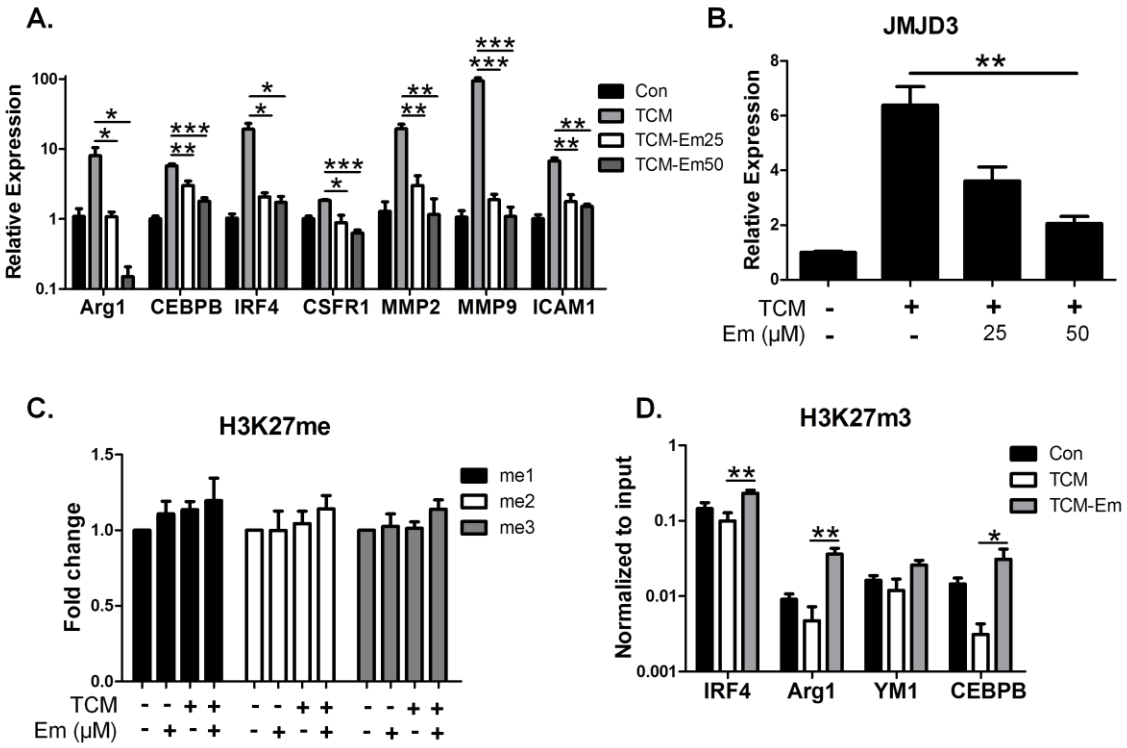

Figure 3.3 Emodin inhibits macrophage response to tumor cell secreted factors. Peritoneal macrophages were stimulated with EO771 TCM with or without emodin for 24 h. **A. and B**. Gene expression was detected using RT-qPCR, n=3. Results shown as means ± S.E of one of two independent experiments. **C.** Histones were extracted from the macrophages and histone modifications were detected using an EpiQuick histone modification kit, n=3. **D.** Gene specific H3K27m3 levels were detected using a ChIP assay. Results shown as means ± S.E. of one of two independent experiments, n=3. **p*<0.05, ***p*<0.01, ****p*<0.001

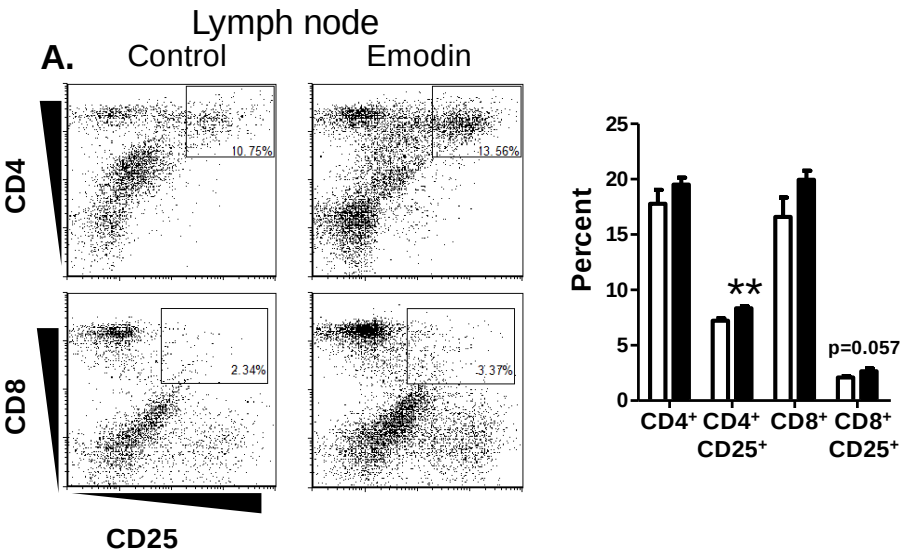

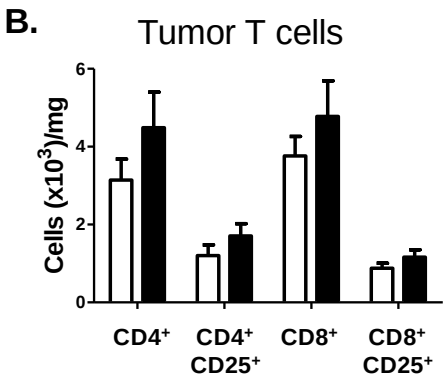

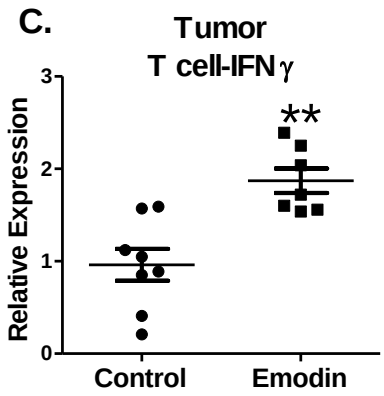

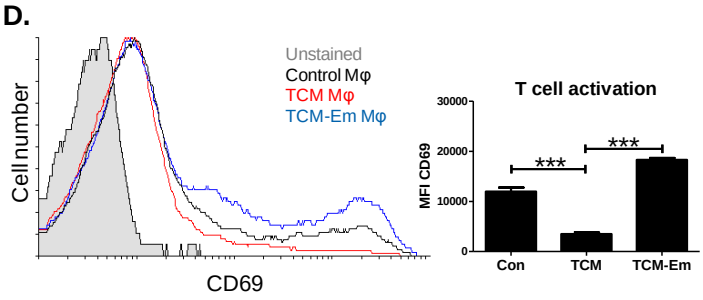

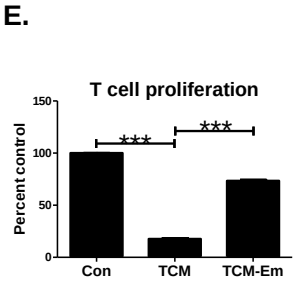

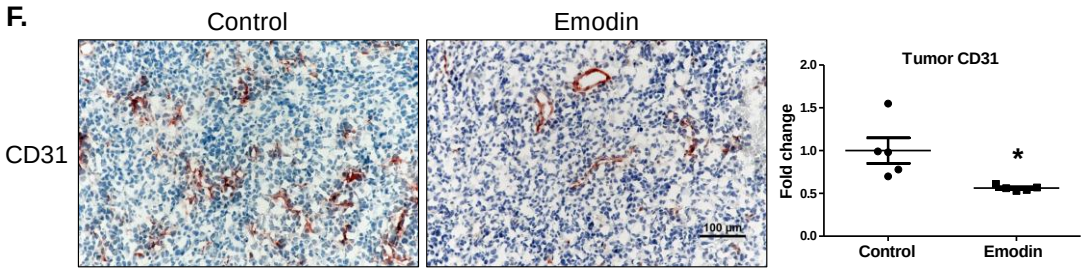

Figure 3.4 Emodin inhibits macrophage suppression of T cell activation and support of angiogenesis. A. and B. The draining lymph node and tumors from mice bearing 4T1 tumors (n=9 for control, n=7 for emodin group) was collected at experimental end point. A single cell suspension was made, and the cells were stained with CD3, CD4 or CD8, and CD25 to detect activated T cells. Cells were analyzed using flow cytometry. Right panel shows results as means ± S.E. **C.** $CD3^+$ T cells were isolated from the draining lymph node of mice bearing 4T1 tumors 6 weeks after tumor cell injections. Gene expression was detected using RT-qPCR. **D.** Peritoneal macrophages were treated with EO771 TCM with or without emodin for 24 h. They were then washed and co-cultured with T cells isolated from the spleens of mice and stimulated with CD3/CD20 microbeads at a ratio of 1:1, n=3. After 24 h, the T cells were collected and stained with CD3, CD4, and CD69 and analyzed using flow cytometry. Left panel shows representative flow cytometry results. Right panel shows results as means ± S.E. **E.** Macrophages were pre-treated with TCM with or without emodin for 24 h. Then they were washed and co-cultured with T cells labeled with CSFE and stimulated with CD3/CD20 microbeads. After 72 h, the cells were collected and stained for CD3 and CD4, and CSFE depletion was detected as a measure of proliferation. Results are shown as means ± S.E. of one of two independent experiments. **F.** EO771 tumors were collected from mice 5 weeks post injection and embedded in OCT. The tumors (n=5) were cut into 8 μm thick sections, stained with CD31, and imaged (10 fields per section at 200x). Images were quantified using ImagePro plus by calculating the IOD for CD31 positive areas. Results (right panel) are shown as means ± S.E. *p<0.05, **p<0.01, ***p<0.001.

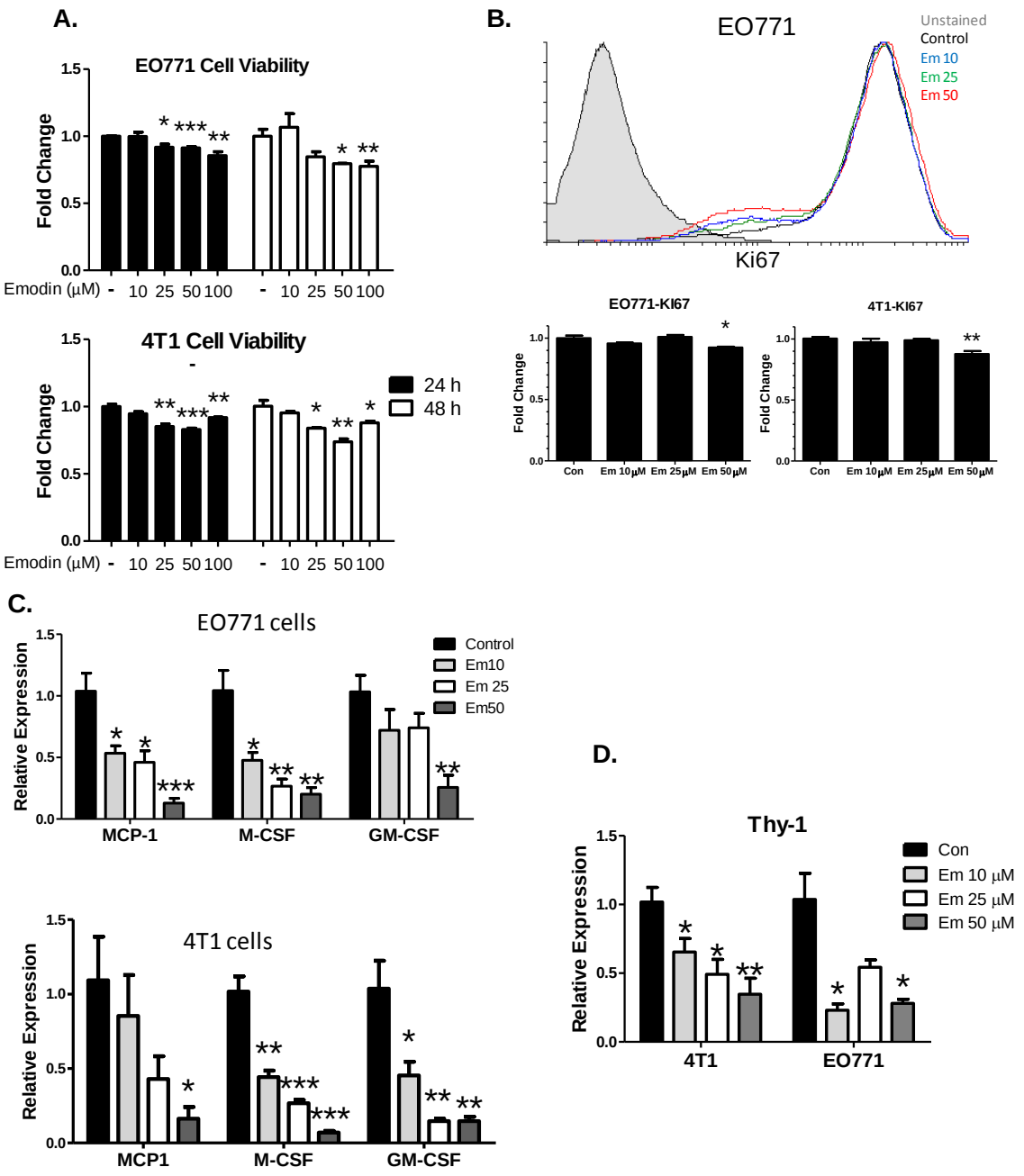

Figure 3.5 Emodin inhibits tumor cell recruitment of macrophages. Tumor cells were cultured with various concentrations of emodin (0-100 μM) for 24-48 h. **A**. Cell viability was detected using an LDH assay, n=4. Results are shown as means ± S.E. for one of two independent experiments **B**. Tumor cells were stained for Ki67 (n=3) after 24 h culture. Cells were then analyzed using flow cytometry. Results are shown as means ± S.E. **C. and D.** After 24 h, gene expression was detected using RT-qPCR (n=3). Results shown as means ± S.E. of one of two independent experiments. *p<0.05, **p<0.01, ***p<0.001.

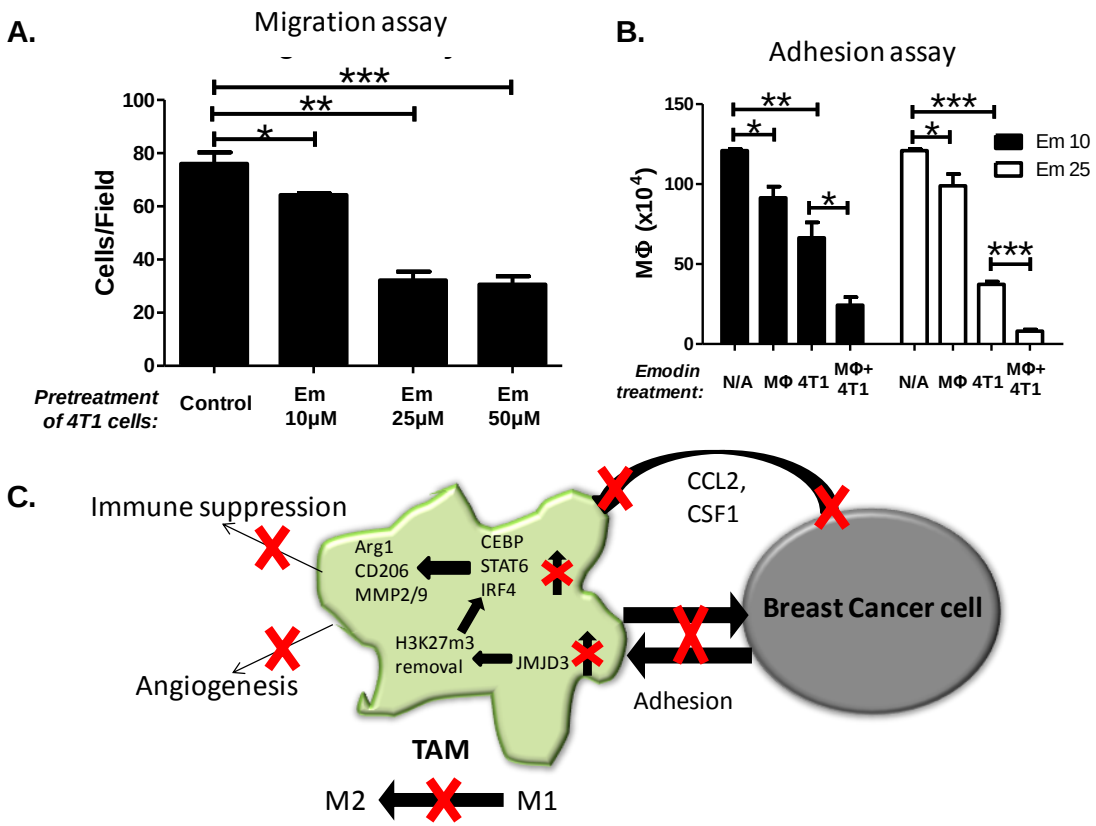

Figure 3.6 Emodin inhibits macrophage adhesion to tumor cells. A. 4T1 cells were treated with varying concentrations of emodin for 24 h. The cells were then washed and cultured in fresh medium for 48 h. Conditioned medium was collected from the cells and placed in the bottom chamber of transwell inserts. Peritoneal macrophages were placed in the top and incubated for 4 h. The cells were then fixed and the membranes were mounted onto slides and imaged (200x, 5 fields per membrane), n=3. The number of cells that migrated to the bottom chamber were counted. Results shown as means ± S.E. of one of two independent experiments. **B.** Peritoneal macrophages and/or 4T1 cells were treated with emodin for 24 h. Then the macrophages were collected and seeded onto 4T1 cell monolayers, n=3. After 1 h, non-adherent cells were washed away and the remaining cells were collected and counted. Cells were then stained with F4/80 and analyzed using flow cytometry. Results shown as means ± S.E. **C.** Illustration showing how emodin interferes with tumor cell-macrophage interactions. Red "X"s represent emodin's functions. *p<0.05, **p<0.01, ***p<0.001.

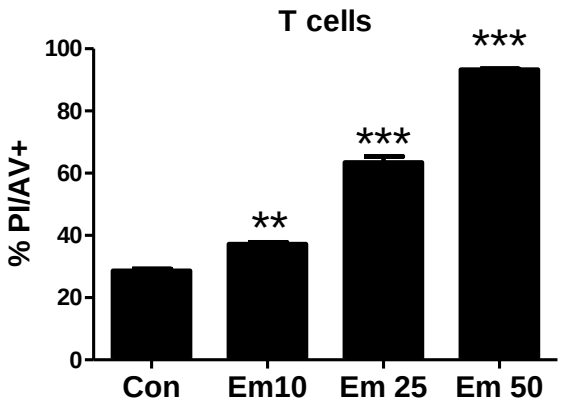

Figure 3.7 Emodin induces T cell apoptosis. $CD3^+$ cells were isolated from spleens of mice using magnetic beads. The T cells were then incubated with emodin for 24 h in DMEM+10% FBS plus IL2 (10 ng/ml). The cells were then washed and stained for Propidium Iodide and Annexin V.

CHAPTER 4

CONCLUSIONS AND FUTURE PERSPECTIVES

The discovery of the substantial role that macrophages play in a variety of diseases, especially cancer, has opened up new avenues of therapy, for these diseases. However, the diversity and plasticity of macrophages make it challenging to develop therapies to target macrophages within different pathologies. Macrophages display a variety of different phenotypes even within the same pathology depending on their location within the tissue or the stage of the disease (37,194,204). In the typical wound healing response, M1 macrophages dominate early, but after 1-2 weeks M2 macrophage become the dominate phenotype (205). Similar phenotype switching is seen in cancers with pro-inflammatory macrophages dominating early but eventually the majority of macrophages adopt an M2-like phenotype. Furthermore, macrophage phenotype varies upon location within tumors (55,79). M2-like TAMs tend to localize to hypoxic regions of tumors while more M1-like TAMs can be found in normoxic tumor areas. Varying populations of monocytes/macrophages could also be differentially recruited to the primary tumor or sites of metastasis (79). Complicating matters further, macrophage activation is regulated by many different signaling pathways which co-ordinate to fine-tune their response to environmental signals (16,173). Therefore, herb derived compounds which are capable of targeting multiple pathways have been receiving increasing attention for use alongside tradition therapies (74,120,121). The value of using combination therapies to target/manipulate the immune component of diseases is

becoming evident, particularly in cancers (185,206,207). Emodin is an active ingredient of several Chinese herbs which have been used for centuries to treat inflammatory disease (125). Many studies have been performed on emodin investigating its potent anti-inflammatory and anti-cancer mechanisms; however, its specific mechanisms of action have not been well elucidated. Emodin is able to inhibit the activity of a variety of kinases and transcription factors including: CK2, HER2/neu, JAK, STAT3, NFκB, ERK, PI3K, P38 (125). Emodin has also been reported to have varying effects on the same signaling molecules such as PPARγ, TGFβ, IL4, and TNFα (125,142,145-147,208). One explanation for these findings could be the use of different experimental models. This would indicate that emodin's function on inflammatory cells could be dependent on the environment of the cells. However, most of the studies performed on emodin have only evaluated its effects under a narrow range of conditions. Therefore, our attempt to better characterize emodin's effects on macrophages and its ability to be used as a therapy for a macrophage-driven pathology is a first of the kind.

Microarray analysis of macrophages stimulated with M1 or M2 stimulants confirmed that emodin is able to inhibit both directions of macrophage activation (Figures 2.2-2.4). Analysis of the dataset with Ingenuity IPA software was unable to identify emodin's direct target with high probability, but instead provided many different possible proteins as direct targets of emodin. These results lend support to the hypothesis that emodin can inhibit many different signaling pathways dependent on environment of the macrophages. Emodin inhibited STAT1, NFκB, and IRF5 signaling in response to LPS/IFNγ stimulation, and STAT6 and IRF4 signaling in response to IL4 stimulation

(Figure 2.7). These results showed for the first time emodin's ability to regulate the antagonistic IRF4 and IRF5 signaling pathways.

Furthermore, our results revealed that emodin could epigenetically regulate macrophage activation by regulating gene specific methylation and acetylation of histone 3 lysine 27 (Figure 2.8). Previous studies have hinted that emodin could epigenetically regulate cell responses. Emodin was reported to increase genome wide H3K27m3 in bladder cancer cells in which H3K27m3 marks are repressed (209). Another study found that emodin could inhibit the expression and activity of HDAC1 in synoviocytes (137). However, emodin's effects on gene specific histone modifications in macrophages have not been previously reported. Our results also showed for the first time the ability of emodin to regulate macrophage memory. The ability of cytokines or other environmental stimuli to alter macrophage's response to future stimuli is only recently becoming understood (210,211). Cytokines can alter histone modifications, such as H3K4m3 or H3K27ac, to prime genes for increased expression upon a second stimulation (178,212). Emodin was able to effectively block this effect likely through the regulation of histone modifications. These findings demonstrate novel functions of emodin and, while not identifying which specific proteins emodin targets, further elucidate the ability of emodin to modulate macrophage activation by targeting multiple transcriptional and epigenetic signaling pathways. Emodin is able to push the phenotype of cells from the extremes of M1 or M2 toward a more central state, which was especially evident by emodin's ability to reciprocally regulate a subset of genes under the two different conditions (Table 2.4).

The majority of studies on emodin as a cancer therapy focused on its direct toxicity toward cancer cells. A few studies have reported that emodin could inhibit

angiogenesis by preventing the release of angiogenic factors from tumor cells. Our results revealed that emodin is able to inhibit the growth of breast tumors in mice at a dose which showed little to no direct cytotoxicity towards the tumor cells (Figure 3.1 and 3.5). Emodin treatment shifted the phenotype of TAMs from an M2-like state toward an M1 phenotype which inhibited their immunosuppressive potential (Figure 3.2 and 3.4). Our results demonstrated for the first time emodin's ability to inhibit tumor cell-macrophage interactions by blocking both the ability of tumor cells to signal to macrophages and macrophages' response to tumor cells (Figure 3.3 and 3.5). Moreover, emodin was able to inhibit tumor cell-macrophage adhesion (Figure 3.6). These results demonstrate a novel mechanism by which emodin inhibits tumor growth.

There have been many obstacles for the development of cancer immunotherapies, including the ability of tumors to adapt to the immune attack, known as immunoeditting, and the ability of tumors to train stromal cells to create an immunosuppressive environment (93,213). Further, the development of TAM targeting therapies has been complicated by the diversity of TAM phenotypes within tumors (67,79,213). Emodin's ability to interfere with the communication between tumor cells and TAMs by a variety of mechanisms as demonstrated in our study confers it great therapeutic potential to overcome these obstacles. Experimental studies have demonstrated that optimal effectiveness of immunotherapies likely requires the combination of treatments that activate T cells and those that reduce the immunosuppressive microenvironment of tumors (185,213-215). The properties of emodin demonstrated in our studies hold great promise for emodin to be used to complement current T cell activating therapies, such as checkpoint inhibitors.

Our results further indicate that emodin treatment alone is most beneficial when it occurs in the early stages of tumor progression prior to the establishment of the TME. Emodin's properties give it strong potential as a therapy to block breast cancer metastasis as well as inhibit recurrence following primary tumor removal. Finally, the role of macrophage memory in the progression of pathologies is only recently becoming appreciated (216,217). Emodin's ability to regulate macrophage memory suggests that it can also be developed as a therapy to block maladaptive macrophage training.

REFERENCES

1. Chawla, A. (2010) Control of macrophage activation and function by PPARs. *Circ Res* **106**, 1559-1569
2. Mosser, D. M., and Edwards, J. P. (2008) Exploring the full spectrum of macrophage activation. *Nat Rev Immunol* **8**, 958-969
3. Swirski, F. K., Hilgendorf, I., and Robbins, C. S. (2014) From proliferation to proliferation: monocyte lineage comes full circle. *Semin Immunopathol* **36**, 137-148
4. Davies, L. C., Jenkins, S. J., Allen, J. E., and Taylor, P. R. (2013) Tissue-resident macrophages. *Nat Immunol* **14**, 986-995
5. Hashimoto, D., Chow, A., Noizat, C., Teo, P., Beasley, M. B., Leboeuf, M., Becker, C. D., See, P., Price, J., Lucas, D., Greter, M., Mortha, A., Boyer, S. W., Forsberg, E. C., Tanaka, M., van Rooijen, N., Garcia-Sastre, A., Stanley, E. R., Ginhoux, F., Frenette, P. S., and Merad, M. (2013) Tissue-resident macrophages self-maintain locally throughout adult life with minimal contribution from circulating monocytes. *Immunity* **38**, 792-804
6. Epelman, S., Lavine, K. J., Beaudin, A. E., Sojka, D. K., Carrero, J. A., Calderon, B., Brija, T., Gautier, E. L., Ivanov, S., Satpathy, A. T., Schilling, J. D., Schwendener, R., Sergin, I., Razani, B., Forsberg, E. C., Yokoyama, W. M., Unanue, E. R., Colonna, M., Randolph, G. J., and Mann, D. L. (2014) Embryonic and adult-derived resident cardiac macrophages are maintained through distinct mechanisms at steady state and during inflammation. *Immunity* **40**, 91-104
7. Panni, R. Z., Linehan, D. C., and DeNardo, D. G. Targeting tumor-infiltrating macrophages to combat cancer. *Immunotherapy* **5**, 1075-1087
8. Davies, L. C., Rosas, M., Jenkins, S. J., Liao, C. T., Scurr, M. J., Brombacher, F., Fraser, D. J., Allen, J. E., Jones, S. A., and Taylor, P. R. (2013) Distinct bone marrow-derived and tissue-resident macrophage lineages proliferate at key stages during inflammation. *Nat Commun* **4**, 1886
9. Casano, A. M., and Peri, F. (2015) Microglia: multitasking specialists of the brain. *Dev Cell* **32**, 469-477
10. Martinez, F. O., Helming, L., and Gordon, S. (2009) Alternative activation of macrophages: an immunologic functional perspective. *Annu Rev Immunol* **27**, 451-483
11. Gordon, S., and Martinez, F. O. (2010) Alternative activation of macrophages: mechanism and functions. *Immunity* **32**, 593-604
12. Gordon, S. (2003) Alternative activation of macrophages. *Nat Rev Immunol* **3**, 23-35
13. Sica, A., and Mantovani, A. (2012) Macrophage plasticity and polarization: in vivo veritas. *J Clin Invest* **122**, 787-795

14. Zhou, D., Huang, C., Lin, Z., Zhan, S., Kong, L., Fang, C., and Li, J. (2014) Macrophage polarization and function with emphasis on the evolving roles of coordinated regulation of cellular signaling pathways. *Cell Signal* **26**, 192-197
15. Mills, C. D. (2012) M1 and M2 Macrophages: Oracles of Health and Disease. *Crit Rev Immunol* **32**, 463-488
16. Lawrence, T., and Natoli, G. (2011) Transcriptional regulation of macrophage polarization: enabling diversity with identity. *Nat Rev Immunol* **11**, 750-761
17. Murray, P. J., Allen, J. E., Biswas, S. K., Fisher, E. A., Gilroy, D. W., Goerdt, S., Gordon, S., Hamilton, J. A., Ivashkiv, L. B., Lawrence, T., Locati, M., Mantovani, A., Martinez, F. O., Mege, J. L., Mosser, D. M., Natoli, G., Saeij, J. P., Schultze, J. L., Shirey, K. A., Sica, A., Suttles, J., Udalova, I., van Ginderachter, J. A., Vogel, S. N., and Wynn, T. A. (2014) Macrophage activation and polarization: nomenclature and experimental guidelines. *Immunity* **41**, 14-20
18. Wang, N., Liang, H., and Zen, K. (2014) Molecular mechanisms that influence the macrophage m1-m2 polarization balance. *Front Immunol* **5**, 614
19. Fernando, M. R., Reyes, J. L., Iannuzzi, J., Leung, G., and McKay, D. M. (2014) The pro-inflammatory cytokine, interleukin-6, enhances the polarization of alternatively activated macrophages. *PLoS One* **9**, e94188
20. Jenkins, S. J., Ruckerl, D., Thomas, G. D., Hewitson, J. P., Duncan, S., Brombacher, F., Maizels, R. M., Hume, D. A., and Allen, J. E. (2013) IL-4 directly signals tissue-resident macrophages to proliferate beyond homeostatic levels controlled by CSF-1. *J Exp Med* **210**, 2477-2491
21. El Chartouni, C., Schwarzfischer, L., and Rehli, M. (2010) Interleukin-4 induced interferon regulatory factor (Irf) 4 participates in the regulation of alternative macrophage priming. *Immunobiology* **215**, 821-825
22. Satoh, T., Takeuchi, O., Vandenbon, A., Yasuda, K., Tanaka, Y., Kumagai, Y., Miyake, T., Matsushita, K., Okazaki, T., Saitoh, T., Honma, K., Matsuyama, T., Yui, K., Tsujimura, T., Standley, D. M., Nakanishi, K., Nakai, K., and Akira, S. (2010) The Jmjd3-Irf4 axis regulates M2 macrophage polarization and host responses against helminth infection. *Nat Immunol* **11**, 936-944
23. Ishii, M., Wen, H., Corsa, C. A., Liu, T., Coelho, A. L., Allen, R. M., Carson, W. F. t., Cavassani, K. A., Li, X., Lukacs, N. W., Hogaboam, C. M., Dou, Y., and Kunkel, S. L. (2009) Epigenetic regulation of the alternatively activated macrophage phenotype. *Blood* **114**, 3244-3254
24. Ohmori, Y., and Hamilton, T. A. (1997) IL-4-induced STAT6 suppresses IFN-gamma-stimulated STAT1-dependent transcription in mouse macrophages. *J Immunol* **159**, 5474-5482
25. Ohmori, Y., and Hamilton, T. A. (2000) Interleukin-4/STAT6 represses STAT1 and NF-kappa B-dependent transcription through distinct mechanisms. *J Biol Chem* **275**, 38095-38103
26. Krausgruber, T., Blazek, K., Smallie, T., Alzabin, S., Lockstone, H., Sahgal, N., Hussell, T., Feldmann, M., and Udalova, I. A. (2011) IRF5 promotes inflammatory macrophage polarization and TH1-TH17 responses. *Nat Immunol* **12**, 231-238

27. Negishi, H., Ohba, Y., Yanai, H., Takaoka, A., Honma, K., Yui, K., Matsuyama, T., Taniguchi, T., and Honda, K. (2005) Negative regulation of Toll-like-receptor signaling by IRF-4. *Proc Natl Acad Sci U S A* **102**, 15989-15994
28. Deng, H., Maitra, U., Morris, M., and Li, L. (2012) Molecular mechanism responsible for the priming of macrophage activation. *J Biol Chem* **288**, 3897-3906
29. Saeed, S., Quintin, J., Kerstens, H. H., Rao, N. A., Aghajanirefah, A., Matarese, F., Cheng, S. C., Ratter, J., Berentsen, K., van der Ent, M. A., Sharifi, N., Janssen-Megens, E. M., Ter Huurne, M., Mandoli, A., van Schaik, T., Ng, A., Burden, F., Downes, K., Frontini, M., Kumar, V., Giamarellos-Bourboulis, E. J., Ouwehand, W. H., van der Meer, J. W., Joosten, L. A., Wijmenga, C., Martens, J. H., Xavier, R. J., Logie, C., Netea, M. G., and Stunnenberg, H. G. Epigenetic programming of monocyte-to-macrophage differentiation and trained innate immunity. *Science* **345**, 1251086
30. Ifrim, D. C., Quintin, J., Joosten, L. A., Jacobs, C., Jansen, T., Jacobs, L., Gow, N. A., Williams, D. L., van der Meer, J. W., and Netea, M. G. (2014) Trained immunity or tolerance: opposing functional programs induced in human monocytes after engagement of various pattern recognition receptors. *Clin Vaccine Immunol* **21**, 534-545
31. Ivashkiv, L. B. (2013) Epigenetic regulation of macrophage polarization and function. *Trends Immunol* **34**, 216-223
32. Qiao, Y., Giannopoulou, E. G., Chan, C. H., Park, S. H., Gong, S., Chen, J., Hu, X., Elemento, O., and Ivashkiv, L. B. (2013) Synergistic activation of inflammatory cytokine genes by interferon-gamma-induced chromatin remodeling and toll-like receptor signaling. *Immunity* **39**, 454-469
33. Alvarez-Errico, D., Vento-Tormo, R., Sieweke, M., and Ballestar, E. (2015) Epigenetic control of myeloid cell differentiation, identity and function. *Nat Rev Immunol* **15**, 7-17
34. Wynn, T. A., Chawla, A., and Pollard, J. W. (2013) Macrophage biology in development, homeostasis and disease. *Nature* **496**, 445-455
35. Murray, P. J., and Wynn, T. A. (2011) Protective and pathogenic functions of macrophage subsets. *Nat Rev Immunol* **11**, 723-737
36. Pollard, J. W. (2009) Trophic macrophages in development and disease. *Nat Rev Immunol* **9**, 259-270
37. Shechter, R., and Schwartz, M. (2013) Harnessing monocyte-derived macrophages to control central nervous system pathologies: no longer 'if' but 'how'. *J Pathol* **229**, 332-346
38. Karsdal, M. A., Woodworth, T., Henriksen, K., Maksymowych, W. P., Genant, H., Vergnaud, P., Christiansen, C., Schubert, T., Qvist, P., Schett, G., Platt, A., and Bay-Jensen, A. C. (2011) Biochemical markers of ongoing joint damage in rheumatoid arthritis--current and future applications, limitations and opportunities. *Arthritis Res Ther* **13**, 215
39. Wicks, K., Torbica, T., and Mace, K. A. (2014) Myeloid cell dysfunction and the pathogenesis of the diabetic chronic wound. *Semin Immunol* **26**, 341-353
40. Nahrendorf, M., and Swirski, F. K. (2013) Monocyte and macrophage heterogeneity in the heart. *Circ Res* **112**, 1624-1633

41. van Nieuwenhoven, F. A., and Turner, N. A. (2012) The role of cardiac fibroblasts in the transition from inflammation to fibrosis following myocardial infarction. *Vascul Pharmacol* **58**, 182-188
42. Yellon, D. M., and Hausenloy, D. J. (2007) Myocardial reperfusion injury. *N Engl J Med* **357**, 1121-1135
43. McNelis, J. C., and Olefsky, J. M. Macrophages, immunity, and metabolic disease. *Immunity* **41**, 36-48
44. MacNeill, B. D., Jang, I. K., Bouma, B. E., Iftimia, N., Takano, M., Yabushita, H., Shishkov, M., Kauffman, C. R., Houser, S. L., Aretz, H. T., DeJoseph, D., Halpern, E. F., and Tearney, G. J. (2004) Focal and multi-focal plaque macrophage distributions in patients with acute and stable presentations of coronary artery disease. *J Am Coll Cardiol* **44**, 972-979
45. Hermansson, C., Lundqvist, A., Magnusson, L. U., Ullstrom, C., Bergstrom, G., and Hulten, L. M. (2014) Macrophage CD14 expression in human carotid plaques is associated with complicated lesions, correlates with thrombosis, and is reduced by angiotensin receptor blocker treatment. *Int Immunopharmacol* **22**, 318-323
46. Le, K. A., Mahurkar, S., Alderete, T. L., Hasson, R. E., Adam, T. C., Kim, J. S., Beale, E., Xie, C., Greenberg, A. S., Allayee, H., and Goran, M. I. (2011) Subcutaneous adipose tissue macrophage infiltration is associated with hepatic and visceral fat deposition, hyperinsulinemia, and stimulation of NF-kappaB stress pathway. *Diabetes* **60**, 2802-2809
47. Qian, B. Z., and Pollard, J. W. Macrophage diversity enhances tumor progression and metastasis. *Cell* **141**, 39-51
48. Kundu, J. K., and Surh, Y. J. (2008) Inflammation: gearing the journey to cancer. *Mutat Res* **659**, 15-30
49. Sun, B., and Karin, M. (2014) The therapeutic value of targeting inflammation in gastrointestinal cancers. *Trends Pharmacol Sci* **35**, 349-357
50. Swann, J. B., Vesely, M. D., Silva, A., Sharkey, J., Akira, S., Schreiber, R. D., and Smyth, M. J. (2008) Demonstration of inflammation-induced cancer and cancer immunoediting during primary tumorigenesis. *Proc Natl Acad Sci U S A* **105**, 652-656
51. Lauzon-Joset, J. F., Marsolais, D., Langlois, A., and Bissonnette, E. Y. (2014) Dysregulation of alveolar macrophages unleashes dendritic cell-mediated mechanisms of allergic airway inflammation. *Mucosal Immunol* **7**, 155-164
52. Xue, J., Sharma, V., Hsieh, M. H., Chawla, A., Murali, R., Pandol, S. J., and Habtezion, A. (2015) Alternatively activated macrophages promote pancreatic fibrosis in chronic pancreatitis. *Nat Commun* **6**, 7158
53. Wynn, T. A., and Barron, L. (2010) Macrophages: master regulators of inflammation and fibrosis. *Semin Liver Dis* **30**, 245-257
54. Zhang, Y., Cheng, S., Zhang, M., Zhen, L., Pang, D., Zhang, Q., and Li, Z. High-infiltration of tumor-associated macrophages predicts unfavorable clinical outcome for node-negative breast cancer. *PLoS One* **8**, e76147
55. Schmieder, A., Michel, J., Schonhaar, K., Goerdt, S., and Schledzewski, K. (2012) Differentiation and gene expression profile of tumor-associated macrophages. *Semin Cancer Biol* **22**, 289-297

56. Rudnick, J. A., and Kuperwasser, C. (2012) Stromal biomarkers in breast cancer development and progression. *Clin Exp Metastasis* **29**, 663-672
57. Galdiero, M. R., Garlanda, C., Jaillon, S., Marone, G., and Mantovani, A. (2013) Tumor associated macrophages and neutrophils in tumor progression. *J Cell Physiol* **228**, 1404-1412
58. Linde, N., Lederle, W., Depner, S., van Rooijen, N., Gutschalk, C. M., and Mueller, M. M. (2012) Vascular endothelial growth factor-induced skin carcinogenesis depends on recruitment and alternative activation of macrophages. *J Pathol* **227**, 17-28
59. Komohara, Y., Jinushi, M., and Takeya, M. Clinical significance of macrophage heterogeneity in human malignant tumors. *Cancer Sci* **105**, 1-8
60. Lu, H., Clauser, K. R., Tam, W. L., Frose, J., Ye, X., Eaton, E. N., Reinhardt, F., Donnenberg, V. S., Bhargava, R., Carr, S. A., and Weinberg, R. A. (2014) A breast cancer stem cell niche supported by juxtacrine signalling from monocytes and macrophages. *Nat Cell Biol* **16**, 1105-1117
61. Doedens, A. L., Stockmann, C., Rubinstein, M. P., Liao, D., Zhang, N., DeNardo, D. G., Coussens, L. M., Karin, M., Goldrath, A. W., and Johnson, R. S. (2010) Macrophage expression of hypoxia-inducible factor-1 alpha suppresses T-cell function and promotes tumor progression. *Cancer Res* **70**, 7465-7475
62. Casey, S. C., Amedei, A., Aquilano, K., Azmi, A. S., Benencia, F., Bhakta, D., Bilsland, A. E., Boosani, C. S., Chen, S., Ciriolo, M. R., Crawford, S., Fujii, H., Georgakilas, A. G., Guha, G., Halicka, D., Helferich, W. G., Heneberg, P., Honoki, K., Keith, W. N., Kerkar, S. P., Mohammed, S. I., Niccolai, E., Nowsheen, S., Vasantha Rupasinghe, H. P., Samadi, A., Singh, N., Talib, W. H., Venkateswaran, V., Whelan, R. L., Yang, X., and Felsher, D. W. Cancer prevention and therapy through the modulation of the tumor microenvironment. *Semin Cancer Biol* **35 Suppl**, S199-223
63. Biswas, S. K., and Mantovani, A. (2010) Macrophage plasticity and interaction with lymphocyte subsets: cancer as a paradigm. *Nat Immunol* **11**, 889-896
64. Quail, D. F., and Joyce, J. A. (2013) Microenvironmental regulation of tumor progression and metastasis. *Nat Med* **19**, 1423-1437
65. Pignatelli, J., Goswami, S., Jones, J. G., Rohan, T. E., Pieri, E., Chen, X., Adler, E., Cox, D., Maleki, S., Bresnick, A., Gertler, F. B., Condeelis, J. S., and Oktay, M. H. Invasive breast carcinoma cells from patients exhibit MenaINV- and macrophage-dependent transendothelial migration. *Sci Signal* **7**, ra112
66. Qian, B., Deng, Y., Im, J. H., Muschel, R. J., Zou, Y., Li, J., Lang, R. A., and Pollard, J. W. (2009) A distinct macrophage population mediates metastatic breast cancer cell extravasation, establishment and growth. *PLoS One* **4**, e6562
67. Panni, R. Z., Linehan, D. C., and DeNardo, D. G. (2013) Targeting tumor-infiltrating macrophages to combat cancer. *Immunotherapy* **5**, 1075-1087
68. Faxon, D. P., Gibbons, R. J., Chronos, N. A., Gurbel, P. A., and Sheehan, F. (2002) The effect of blockade of the CD11/CD18 integrin receptor on infarct size in patients with acute myocardial infarction treated with direct angioplasty: the results of the HALT-MI study. *J Am Coll Cardiol* **40**, 1199-1204
69. Tabas, I., and Glass, C. K. (2013) Anti-inflammatory therapy in chronic disease: challenges and opportunities. *Science* **339**, 166-172

70. Strachan, D. C., Ruffell, B., Oei, Y., Bissell, M. J., Coussens, L. M., Pryer, N., and Daniel, D. CSF1R inhibition delays cervical and mammary tumor growth in murine models by attenuating the turnover of tumor-associated macrophages and enhancing infiltration by CD8 T cells. *Oncoimmunology* **2**, e26968
71. Zhu, Y., Knolhoff, B. L., Meyer, M. A., Nywening, T. M., West, B. L., Luo, J., Wang-Gillam, A., Goedegebuure, S. P., Linehan, D. C., and DeNardo, D. G. (2014) CSF1/CSF1R blockade reprograms tumor-infiltrating macrophages and improves response to T-cell checkpoint immunotherapy in pancreatic cancer models. *Cancer Res* **74**, 5057-5069
72. Heninger, E., Krueger, T. E., and Lang, J. M. (2015) Augmenting antitumor immune responses with epigenetic modifying agents. *Front Immunol* **6**, 29
73. Cantley, M. D., and Haynes, D. R. (2013) Epigenetic regulation of inflammation: progressing from broad acting histone deacetylase (HDAC) inhibitors to targeting specific HDACs. *Inflammopharmacology* **21**, 301-307
74. Gupta, S. C., Tyagi, A. K., Deshmukh-Taskar, P., Hinojosa, M., Prasad, S., and Aggarwal, B. B. (2014) Downregulation of tumor necrosis factor and other proinflammatory biomarkers by polyphenols. *Arch Biochem Biophys*
75. Shehzad, A., Rehman, G., and Lee, Y. S. (2013) Curcumin in inflammatory diseases. *Biofactors* **39**, 69-77
76. Wang, Q., and Li, X. K. (2011) Immunosuppressive and anti-inflammatory activities of sinomenine. *Int Immunopharmacol* **11**, 373-376
77. Liang, Q., Wu, Q., Jiang, J., Duan, J., Wang, C., Smith, M. D., Lu, H., Wang, Q., Nagarkatti, P., and Fan, D. (2011) Characterization of sparstolonin B, a Chinese herb-derived compound, as a selective Toll-like receptor antagonist with potent anti-inflammatory properties. *J Biol Chem* **286**, 26470-26479
78. Roca, H., Varsos, Z. S., Sud, S., Craig, M. J., Ying, C., and Pienta, K. J. (2009) CCL2 and interleukin-6 promote survival of human CD11b+ peripheral blood mononuclear cells and induce M2-type macrophage polarization. *J Biol Chem* **284**, 34342-34354
79. Schouppe, E., De Baetselier, P., Van Ginderachter, J. A., and Sarukhan, A. (2012) Instruction of myeloid cells by the tumor microenvironment: Open questions on the dynamics and plasticity of different tumor-associated myeloid cell populations. *Oncoimmunology* **1**, 1135-1145
80. Lu, H., Clauser, K. R., Tam, W. L., Frose, J., Ye, X., Eaton, E. N., Reinhardt, F., Donnenberg, V. S., Bhargava, R., Carr, S. A., and Weinberg, R. A. A breast cancer stem cell niche supported by juxtacrine signalling from monocytes and macrophages. *Nat Cell Biol* **16**, 1105-1117
81. Marigo, I., Bosio, E., Solito, S., Mesa, C., Fernandez, A., Dolcetti, L., Ugel, S., Sonda, N., Bicciato, S., Falisi, E., Calabrese, F., Basso, G., Zanovello, P., Cozzi, E., Mandruzzato, S., and Bronte, V. Tumor-induced tolerance and immune suppression depend on the C/EBPbeta transcription factor. *Immunity* **32**, 790-802
82. Williams, L., Bradley, L., Smith, A., and Foxwell, B. (2004) Signal transducer and activator of transcription 3 is the dominant mediator of the anti-inflammatory effects of IL-10 in human macrophages. *J Immunol* **172**, 567-576
83. Alvaro, T., Lejeune, M., Camacho, F. I., Salvado, M. T., Sanchez, L., Garcia, J. F., Lopez, C., Jaen, J., Bosch, R., Pons, L. E., Bellas, C., and Piris, M. A. (2006)

The presence of STAT1-positive tumor-associated macrophages and their relation to outcome in patients with follicular lymphoma. *Haematologica* **91**, 1605-1612
84. Hix, L. M., Karavitis, J., Khan, M. W., Shi, Y. H., Khazaie, K., and Zhang, M. (2013) Tumor STAT1 transcription factor activity enhances breast tumor growth and immune suppression mediated by myeloid-derived suppressor cells. *J Biol Chem* **288**, 11676-11688
85. Su, S., Liu, Q., Chen, J., Chen, F., He, C., Huang, D., Wu, W., Lin, L., Huang, W., Zhang, J., Cui, X., Zheng, F., Li, H., Yao, H., Su, F., and Song, E. (2014) A positive feedback loop between mesenchymal-like cancer cells and macrophages is essential to breast cancer metastasis. *Cancer Cell* **25**, 605-620
86. Van Overmeire, E., Laoui, D., Keirsse, J., Van Ginderachter, J. A., and Sarukhan, A. (2014) Mechanisms driving macrophage diversity and specialization in distinct tumor microenvironments and parallelisms with other tissues. *Front Immunol* **5**, 127
87. de Vos van Steenwijk, P. J., Ramwadhdoebe, T. H., Goedemans, R., Doorduijn, E. M., van Ham, J. J., Gorter, A., van Hall, T., Kuijjer, M. L., van Poelgeest, M. I., van der Burg, S. H., and Jordanova, E. S. (2013) Tumor-infiltrating CD14-positive myeloid cells and CD8-positive T-cells prolong survival in patients with cervical carcinoma. *Int J Cancer* **133**, 2884-2894
88. Ohri, C. M., Shikotra, A., Green, R. H., Waller, D. A., and Bradding, P. (2009) Macrophages within NSCLC tumour islets are predominantly of a cytotoxic M1 phenotype associated with extended survival. *Eur Respir J* **33**, 118-126
89. Tagliabue, A., Mantovani, A., Kilgallen, M., Herberman, R. B., and McCoy, J. L. (1979) Natural cytotoxicity of mouse monocytes and macrophages. *J Immunol* **122**, 2363-2370
90. Urban, J. L., Shepard, H. M., Rothstein, J. L., Sugarman, B. J., and Schreiber, H. (1986) Tumor necrosis factor: a potent effector molecule for tumor cell killing by activated macrophages. *Proc Natl Acad Sci U S A* **83**, 5233-5237
91. Yuan, X., Li, W., Cui, Y., Zhan, Q., Zhang, C., Yang, Z., Li, X., Li, S., Guan, Q., and Sun, X. (2015) Specific cellular immune response elicited by the necrotic tumor cell-stimulated macrophages. *Int Immunopharmacol* **27**, 171-176
92. Guiducci, C., Vicari, A. P., Sangaletti, S., Trinchieri, G., and Colombo, M. P. (2005) Redirecting in vivo elicited tumor infiltrating macrophages and dendritic cells towards tumor rejection. *Cancer Res* **65**, 3437-3446
93. Tveita, A. A., Schjesvold, F., Haabeth, O. A., Fauskanger, M., and Bogen, B. (2015) Tumors Escape CD4+ T-cell-Mediated Immunosurveillance by Impairing the Ability of Infiltrating Macrophages to Indirectly Present Tumor Antigens. *Cancer Res* **75**, 3268-3278
94. van der Sluis, T. C., Sluijter, M., van Duikeren, S., West, B. L., Melief, C. J., Arens, R., van der Burg, S. H., and van Hall, T. (2015) Therapeutic Peptide Vaccine-Induced CD8 T Cells Strongly Modulate Intratumoral Macrophages Required for Tumor Regression. *Cancer Immunol Res* **3**, 1042-1051
95. Shi, Y., Fan, X., Deng, H., Brezski, R. J., Rycyzyn, M., Jordan, R. E., Strohl, W. R., Zou, Q., Zhang, N., and An, Z. (2015) Trastuzumab triggers phagocytic killing of high HER2 cancer cells in vitro and in vivo by interaction with Fcgamma receptors on macrophages. *J Immunol* **194**, 4379-4386

96. Gul, N., Babes, L., Siegmund, K., Korthouwer, R., Bogels, M., Braster, R., Vidarsson, G., ten Hagen, T. L., Kubes, P., and van Egmond, M. (2014) Macrophages eliminate circulating tumor cells after monoclonal antibody therapy. *J Clin Invest* **124**, 812-823
97. van der Bij, G. J., Bogels, M., Otten, M. A., Oosterling, S. J., Kuppen, P. J., Meijer, S., Beelen, R. H., and van Egmond, M. (2010) Experimentally induced liver metastases from colorectal cancer can be prevented by mononuclear phagocyte-mediated monoclonal antibody therapy. *J Hepatol* **53**, 677-685
98. Komohara, Y., Jinushi, M., and Takeya, M. (2014) Clinical significance of macrophage heterogeneity in human malignant tumors. *Cancer Sci* **105**, 1-8
99. Medrek, C., Ponten, F., Jirstrom, K., and Leandersson, K. (2012) The presence of tumor associated macrophages in tumor stroma as a prognostic marker for breast cancer patients. *BMC Cancer* **12**, 306
100. Leek, R. D., Lewis, C. E., Whitehouse, R., Greenall, M., Clarke, J., and Harris, A. L. (1996) Association of macrophage infiltration with angiogenesis and prognosis in invasive breast carcinoma. *Cancer Res* **56**, 4625-4629
101. Ueno, T., Toi, M., Saji, H., Muta, M., Bando, H., Kuroi, K., Koike, M., Inadera, H., and Matsushima, K. (2000) Significance of macrophage chemoattractant protein-1 in macrophage recruitment, angiogenesis, and survival in human breast cancer. *Clin Cancer Res* **6**, 3282-3289
102. DeNardo, D. G., Brennan, D. J., Rexhepaj, E., Ruffell, B., Shiao, S. L., Madden, S. F., Gallagher, W. M., Wadhwani, N., Keil, S. D., Junaid, S. A., Rugo, H. S., Hwang, E. S., Jirstrom, K., West, B. L., and Coussens, L. M. (2011) Leukocyte complexity predicts breast cancer survival and functionally regulates response to chemotherapy. *Cancer Discov* **1**, 54-67
103. Gyorki, D. E., Asselin-Labat, M. L., van Rooijen, N., Lindeman, G. J., and Visvader, J. E. (2009) Resident macrophages influence stem cell activity in the mammary gland. *Breast Cancer Res* **11**, R62
104. Lin, E. Y., Nguyen, A. V., Russell, R. G., and Pollard, J. W. (2001) Colony-stimulating factor 1 promotes progression of mammary tumors to malignancy. *J Exp Med* **193**, 727-740
105. Cho, H. J., Jung, J. I., Lim do, Y., Kwon, G. T., Her, S., and Park, J. H. (2012) Bone marrow-derived, alternatively activated macrophages enhance solid tumor growth and lung metastasis of mammary carcinoma cells in a Balb/C mouse orthotopic model. *Breast Cancer Res* **14**, R81
106. Galmbacher, K., Heisig, M., Hotz, C., Wischhusen, J., Galmiche, A., Bergmann, B., Gentschev, I., Goebel, W., Rapp, U. R., and Fensterle, J. (2010) Shigella mediated depletion of macrophages in a murine breast cancer model is associated with tumor regression. *PLoS One* **5**, e9572
107. Pignatelli, J., Goswami, S., Jones, J. G., Rohan, T. E., Pieri, E., Chen, X., Adler, E., Cox, D., Maleki, S., Bresnick, A., Gertler, F. B., Condeelis, J. S., and Oktay, M. H. (2014) Invasive breast carcinoma cells from patients exhibit MenaINV- and macrophage-dependent transendothelial migration. *Sci Signal* **7**, ra112
108. Shirato, K., Kizaki, T., Sakurai, T., Ogasawara, J. E., Ishibashi, Y., Iijima, T., Okada, C., Noguchi, I., Imaizumi, K., Taniguchi, N., and Ohno, H. (2009)

Hypoxia-inducible factor-1alpha suppresses the expression of macrophage scavenger receptor 1. *Pflugers Arch* **459**, 93-103
109. Mantovani, A., and Allavena, P. (2015) The interaction of anticancer therapies with tumor-associated macrophages. *J Exp Med* **212**, 435-445
110. Shiao, S. L., Ruffell, B., DeNardo, D. G., Faddegon, B. A., Park, C. C., and Coussens, L. M. (2015) TH2-Polarized CD4(+) T Cells and Macrophages Limit Efficacy of Radiotherapy. *Cancer Immunol Res* **3**, 518-525
111. Noy, R., and Pollard, J. W. (2014) Tumor-associated macrophages: from mechanisms to therapy. *Immunity* **41**, 49-61
112. Beatty, G. L., Torigian, D. A., Chiorean, E. G., Saboury, B., Brothers, A., Alavi, A., Troxel, A. B., Sun, W., Teitelbaum, U. R., Vonderheide, R. H., and O'Dwyer, P. J. (2013) A phase I study of an agonist CD40 monoclonal antibody (CP-870,893) in combination with gemcitabine in patients with advanced pancreatic ductal adenocarcinoma. *Clin Cancer Res* **19**, 6286-6295
113. Beatty, G. L., Chiorean, E. G., Fishman, M. P., Saboury, B., Teitelbaum, U. R., Sun, W., Huhn, R. D., Song, W., Li, D., Sharp, L. L., Torigian, D. A., O'Dwyer, P. J., and Vonderheide, R. H. (2011) CD40 agonists alter tumor stroma and show efficacy against pancreatic carcinoma in mice and humans. *Science* **331**, 1612-1616
114. Tseng, D., Volkmer, J. P., Willingham, S. B., Contreras-Trujillo, H., Fathman, J. W., Fernhoff, N. B., Seita, J., Inlay, M. A., Weiskopf, K., Miyanishi, M., and Weissman, I. L. (2013) Anti-CD47 antibody-mediated phagocytosis of cancer by macrophages primes an effective antitumor T-cell response. *Proc Natl Acad Sci U S A* **110**, 11103-11108
115. Coscia, M., Quaglino, E., Iezzi, M., Curcio, C., Pantaleoni, F., Riganti, C., Holen, I., Monkkonen, H., Boccadoro, M., Forni, G., Musiani, P., Bosia, A., Cavallo, F., and Massaia, M. (2010) Zoledronic acid repolarizes tumour-associated macrophages and inhibits mammary carcinogenesis by targeting the mevalonate pathway. *J Cell Mol Med* **14**, 2803-2815
116. Rietkotter, E., Menck, K., Bleckmann, A., Farhat, K., Schaffrinski, M., Schulz, M., Hanisch, U. K., Binder, C., and Pukrop, T. (2013) Zoledronic acid inhibits macrophage/microglia-assisted breast cancer cell invasion. *Oncotarget* **4**, 1449-1460
117. Ottewell, P. D., Woodward, J. K., Lefley, D. V., Evans, C. A., Coleman, R. E., and Holen, I. (2009) Anticancer mechanisms of doxorubicin and zoledronic acid in breast cancer tumor growth in bone. *Mol Cancer Ther* **8**, 2821-2832
118. Gnant, M., Mlineritsch, B., Schippinger, W., Luschin-Ebengreuth, G., Postlberger, S., Menzel, C., Jakesz, R., Seifert, M., Hubalek, M., Bjelic-Radisic, V., Samonigg, H., Tausch, C., Eidtmann, H., Steger, G., Kwasny, W., Dubsky, P., Fridrik, M., Fitzal, F., Stierer, M., Rucklinger, E., Greil, R., and Marth, C. (2009) Endocrine therapy plus zoledronic acid in premenopausal breast cancer. *N Engl J Med* **360**, 679-691
119. Gnant, M., Mlineritsch, B., Luschin-Ebengreuth, G., Kainberger, F., Kassmann, H., Piswanger-Solkner, J. C., Seifert, M., Ploner, F., Menzel, C., Dubsky, P., Fitzal, F., Bjelic-Radisic, V., Steger, G., Greil, R., Marth, C., Kubista, E., Samonigg, H., Wohlmuth, P., Mittlbock, M., and Jakesz, R. (2008) Adjuvant

endocrine therapy plus zoledronic acid in premenopausal women with early-stage breast cancer: 5-year follow-up of the ABCSG-12 bone-mineral density substudy. *Lancet Oncol* **9**, 840-849
120. Tan, W., Lu, J., Huang, M., Li, Y., Chen, M., Wu, G., Gong, J., Zhong, Z., Xu, Z., Dang, Y., Guo, J., Chen, X., and Wang, Y. (2011) Anti-cancer natural products isolated from chinese medicinal herbs. *Chin Med* **6**, 27
121. Mohd Fauzi, F., Koutsoukas, A., Lowe, R., Joshi, K., Fan, T. P., Glen, R. C., and Bender, A. (2013) Chemogenomics approaches to rationalizing the mode-of-action of traditional Chinese and Ayurvedic medicines. *J Chem Inf Model* **53**, 661-673
122. Li, J. W., and Vederas, J. C. (2009) Drug discovery and natural products: end of an era or an endless frontier? *Science* **325**, 161-165
123. Schmidt, B. M., Ribnicky, D. M., Lipsky, P. E., and Raskin, I. (2007) Revisiting the ancient concept of botanical therapeutics. *Nat Chem Biol* **3**, 360-366
124. Huang, S., and Chang, W. H. (2009) Advantages of nanotechnology-based Chinese herb drugs on biological activities. *Curr Drug Metab* **10**, 905-913
125. Shrimali, D., Shanmugam, M. K., Kumar, A. P., Zhang, J., Tan, B. K., Ahn, K. S., and Sethi, G. (2013) Targeted abrogation of diverse signal transduction cascades by emodin for the treatment of inflammatory disorders and cancer. *Cancer Lett* **341**, 139-149
126. (2001) NTP Toxicology and Carcinogenesis Studies of EMODIN (CAS NO. 518-82-1) Feed Studies in F344/N Rats and B6C3F1 Mice. *Natl Toxicol Program Tech Rep Ser* **493**, 1-278
127. Hwang, J. K., Noh, E. M., Moon, S. J., Kim, J. M., Kwon, K. B., Park, B. H., You, Y. O., Hwang, B. M., Kim, H. J., Kim, B. S., Lee, S. J., Kim, J. S., and Lee, Y. R. (2013) Emodin suppresses inflammatory responses and joint destruction in collagen-induced arthritic mice. *Rheumatology (Oxford)* **52**, 1583-1591
128. Wu, Y., Tu, X., Lin, G., Xia, H., Huang, H., Wan, J., Cheng, Z., Liu, M., Chen, G., Zhang, H., Fu, J., Liu, Q., and Liu, D. X. (2007) Emodin-mediated protection from acute myocardial infarction via inhibition of inflammation and apoptosis in local ischemic myocardium. *Life Sci* **81**, 1332-1338
129. Xiao, M., Zhu, T., Zhang, W., Wang, T., Shen, Y. C., Wan, Q. F., and Wen, F. Q. (2014) Emodin ameliorates LPS-induced acute lung injury, involving the inactivation of NF-kappaB in mice. *Int J Mol Sci* **15**, 19355-19368
130. Li, Y., Xiong, W., Yang, J., Zhong, J., Zhang, L., Zheng, J., Liu, H., Zhang, Q., Ouyang, X., Lei, L., and Yu, X. (2015) Attenuation of Inflammation by Emodin in Lipopolysaccharide-induced Acute Kidney Injury via Inhibition of Toll-like Receptor 2 Signal Pathway. *Iran J Kidney Dis* **9**, 202-208
131. Liu, Y., Chen, X., Qiu, M., Chen, W., Zeng, Z., and Chen, Y. (2014) Emodin ameliorates ethanol-induced fatty liver injury in mice. *Pharmacology* **94**, 71-77
132. Xue, J., Chen, F., Wang, J., Wu, S., Zheng, M., Zhu, H., Liu, Y., He, J., and Chen, Z. (2015) Emodin protects against concanavalin A-induced hepatitis in mice through inhibiting activation of the p38 MAPK-NF-kappaB signaling pathway. *Cell Physiol Biochem* **35**, 1557-1570
133. Jia, X., Iwanowycz, S., Wang, J., Saaoud, F., Yu, F., Wang, Y., Hu, J., Chatterjee, S., Wang, Q., and Fan, D. (2014) Emodin attenuates systemic and liver

inflammation in hyperlipidemic mice administrated with lipopolysaccharides. *Exp Biol Med (Maywood)* **239**, 1025-1035
134. Cozza, G., Mazzorana, M., Papinutto, E., Bain, J., Elliott, M., di Maira, G., Gianoncelli, A., Pagano, M. A., Sarno, S., Ruzzene, M., Battistutta, R., Meggio, F., Moro, S., Zagotto, G., and Pinna, L. A. (2009) Quinalizarin as a potent, selective and cell-permeable inhibitor of protein kinase CK2. *Biochem J* **421**, 387-395
135. Yang, Y., Shang, W., Zhou, L., Jiang, B., Jin, H., and Chen, M. (2007) Emodin with PPARgamma ligand-binding activity promotes adipocyte differentiation and increases glucose uptake in 3T3-Ll cells. *Biochem Biophys Res Commun* **353**, 225-230
136. Liu, C. (2015) Inhibition of mechanical stress-induced hypertrophic scar inflammation by emodin. *Mol Med Rep* **11**, 4087-4092
137. Ha, M. K., Song, Y. H., Jeong, S. J., Lee, H. J., Jung, J. H., Kim, B., Song, H. S., Huh, J. E., and Kim, S. H. (2011) Emodin inhibits proinflammatory responses and inactivates histone deacetylase 1 in hypoxic rheumatoid synoviocytes. *Biol Pharm Bull* **34**, 1432-1437
138. Meng, G., Liu, Y., Lou, C., and Yang, H. (2010) Emodin suppresses lipopolysaccharide-induced pro-inflammatory responses and NF-kappaB activation by disrupting lipid rafts in CD14-negative endothelial cells. *Br J Pharmacol* **161**, 1628-1644
139. Lu, Y., Yang, J. H., Li, X., Hwangbo, K., Hwang, S. L., Taketomi, Y., Murakami, M., Chang, Y. C., Kim, C. H., Son, J. K., and Chang, H. W. (2011) Emodin, a naturally occurring anthraquinone derivative, suppresses IgE-mediated anaphylactic reaction and mast cell activation. *Biochem Pharmacol* **82**, 1700-1708
140. Han, J. W., Shim, D. W., Shin, W. Y., Heo, K. H., Kwak, S. B., Sim, E. J., Jeong, J. H., Kang, T. B., and Lee, K. H. (2015) Anti-Inflammatory Effect of Emodin via Attenuation of NLRP3 Inflammasome Activation. *International Journal of Molecular Sciences* **16**, 8102-8109
141. Tong, H. F., Chen, K. J., Chen, H., Wu, H. Y., Lin, H. D., Ni, Z. L., and Lin, S. Z. (2011) Emodin Prolongs Recipient Survival Time After Orthotopic Liver Transplantation in Rats by Polarizing the Th1/Th2 Paradigm to Th2. *Anatomical Record-Advances in Integrative Anatomy and Evolutionary Biology* **294**, 445-452
142. Fu, X., Xu, A. G., Yao, M. Y., Guo, L., and Zhao, L. S. (2014) Emodin enhances cholesterol efflux by activating peroxisome proliferator-activated receptor-gamma in oxidized low density lipoprotein-loaded THP1 macrophages. *Clin Exp Pharmacol Physiol* **41**, 679-684
143. Lou, K. X., Gong, Z. H., and Yuan, Y. Z. (2001) [Study on effect of emodin on TGF beta 1 expression in pancreatic tissue of rats suffering from acute pancreatitis]. *Zhongguo Zhong Xi Yi Jie He Za Zhi* **21**, 433-436
144. Zhou, M., Xu, H., Pan, L., Wen, J., Guo, Y., and Chen, K. (2008) Emodin promotes atherosclerotic plaque stability in fat-fed apolipoprotein E-deficient mice. *Tohoku J Exp Med* **215**, 61-69
145. Chu, X., Wei, M., Yang, X., Cao, Q., Xie, X., Guan, M., Wang, D., and Deng, X. (2012) Effects of an anthraquinone derivative from Rheum officinale Baill,

emodin, on airway responses in a murine model of asthma. *Food Chem Toxicol* **50**, 2368-2375
146. Yang, F., Yuan, P. W., Hao, Y. Q., and Lu, Z. M. (2014) Emodin enhances osteogenesis and inhibits adipogenesis. *BMC Complement Altern Med* **14**, 74
147. Yang, J., Zeng, Z., Wu, T., Yang, Z., Liu, B., and Lan, T. (2013) Emodin attenuates high glucose-induced TGF-beta1 and fibronectin expression in mesangial cells through inhibition of NF-kappaB pathway. *Exp Cell Res* **319**, 3182-3189
148. Jia, X., Yu, F., Wang, J., Iwanowycz, S., Saaoud, F., Wang, Y., Hu, J., Wang, Q., and Fan, D. (2014) Emodin suppresses pulmonary metastasis of breast cancer accompanied with decreased macrophage recruitment and M2 polarization in the lungs. *Breast Cancer Res Treat* **148**, 291-302
149. Wei, W. T., Lin, S. Z., Liu, D. L., and Wang, Z. H. (2013) The distinct mechanisms of the antitumor activity of emodin in different types of cancer (Review). *Oncol Rep* **30**, 2555-2562
150. Chang, Y. C., Lai, T. Y., Yu, C. S., Chen, H. Y., Yang, J. S., Chueh, F. S., Lu, C. C., Chiang, J. H., Huang, W. W., Ma, C. Y., and Chung, J. G. (2011) Emodin Induces Apoptotic Death in Murine Myelomonocytic Leukemia WEHI-3 Cells In Vitro and Enhances Phagocytosis in Leukemia Mice In Vivo. *Evid Based Complement Alternat Med* **2011**, 523596
151. Kuo, T. C., Yang, J. S., Lin, M. W., Hsu, S. C., Lin, J. J., Lin, H. J., Hsia, T. C., Liao, C. L., Yang, M. D., Fan, M. J., Wood, W. G., and Chung, J. G. (2009) Emodin has cytotoxic and protective effects in rat C6 glioma cells: roles of Mdr1a and nuclear factor kappaB in cell survival. *J Pharmacol Exp Ther* **330**, 736-744
152. Huang, Z., Chen, G., and Shi, P. (2009) Effects of emodin on the gene expression profiling of human breast carcinoma cells. *Cancer Detect Prev* **32**, 286-291
153. Jing, Y., Yang, J., Wang, Y., Li, H., Chen, Y., Hu, Q., Shi, G., Tang, X., and Yi, J. (2006) Alteration of subcellular redox equilibrium and the consequent oxidative modification of nuclear factor kappaB are critical for anticancer cytotoxicity by emodin, a reactive oxygen species-producing agent. *Free Radic Biol Med* **40**, 2183-2197
154. Yang, J., Tang, X. M., Li, H., Shi, G. Y., Zhu, P., Jin, H. F., and Yi, J. (2003) [Emodin sensitizes HeLa cell to arsenic trioxide induced apoptosis via the reactive oxygen species-mediated signaling pathways]. *Shi Yan Sheng Wu Xue Bao* **36**, 465-475
155. Liu, A., Chen, H., Wei, W., Ye, S., Liao, W., Gong, J., Jiang, Z., Wang, L., and Lin, S. (2011) Antiproliferative and antimetastatic effects of emodin on human pancreatic cancer. *Oncol Rep* **26**, 81-89
156. Fu, J. M., Zhou, J., Shi, J., Xie, J. S., Huang, L., Yip, A. Y., Loo, W. T., Chow, L. W., and Ng, E. L. (2012) Emodin affects ERCC1 expression in breast cancer cells. *J Transl Med* **10 Suppl 1**, S7
157. Yu, J. Q., Bao, W., and Lei, J. C. (2013) Emodin regulates apoptotic pathway in human liver cancer cells. *Phytother Res* **27**, 251-257
158. Muto, A., Hori, M., Sasaki, Y., Saitoh, A., Yasuda, I., Maekawa, T., Uchida, T., Asakura, K., Nakazato, T., Kaneda, T., Kizaki, M., Ikeda, Y., and Yoshida, T.

(2007) Emodin has a cytotoxic activity against human multiple myeloma as a Janus-activated kinase 2 inhibitor. *Mol Cancer Ther* **6**, 987-994
159. Chen, R. S., Jhan, J. Y., Su, Y. J., Lee, W. T., Cheng, C. M., Ciou, S. C., Lin, S. T., Chuang, S. M., Ko, J. C., and Lin, Y. W. (2009) Emodin enhances gefitinib-induced cytotoxicity via Rad51 downregulation and ERK1/2 inactivation. *Exp Cell Res* **315**, 2658-2672
160. Sun, Y., Wang, X., Zhou, Q., Lu, Y., Zhang, H., Chen, Q., Zhao, M., and Su, S. (2015) Inhibitory effect of emodin on migration, invasion and metastasis of human breast cancer MDA-MB-231 cells in vitro and in vivo. *Oncol Rep* **33**, 338-346
161. Zhang, L., Lau, Y. K., Xi, L., Hong, R. L., Kim, D. S., Chen, C. F., Hortobagyi, G. N., Chang, C., and Hung, M. C. (1998) Tyrosine kinase inhibitors, emodin and its derivative repress HER-2/neu-induced cellular transformation and metastasis-associated properties. *Oncogene* **16**, 2855-2863
162. Ueno, N., Kiyokawa, N., and Hung, M. (1996) Growth suppression of low HER-2/neu-expressing breast cancer cell line MDA-MB-435 by tyrosine kinase inhibitor emodin. *Oncol Rep* **3**, 509-511
163. Huang, Z., Chen, G., and Shi, P. (2008) Emodin-induced apoptosis in human breast cancer BCap-37 cells through the mitochondrial signaling pathway. *Arch Pharm Res* **31**, 742-748
164. Fu, J. M., Zhou, J., Shi, J., Xie, J. S., Huang, L., Yip, A. Y., Loo, W. T., Chow, L. W., and Ng, E. L. Emodin affects ERCC1 expression in breast cancer cells. *J Transl Med* **10 Suppl 1**, S7
165. Lin, S. Z., Wei, W. T., Chen, H., Chen, K. J., Tong, H. F., Wang, Z. H., Ni, Z. L., Liu, H. B., Guo, H. C., and Liu, D. L. Antitumor activity of emodin against pancreatic cancer depends on its dual role: promotion of apoptosis and suppression of angiogenesis. *PLoS One* **7**, e42146
166. Damodharan, U., Ganesan, R., and Radhakrishnan, U. C. (2011) Expression of MMP2 and MMP9 (gelatinases A and B) in human colon cancer cells. *Appl Biochem Biotechnol* **165**, 1245-1252
167. Lu, Y., Zhang, J., and Qian, J. (2008) The effect of emodin on VEGF receptors in human colon cancer cells. *Cancer Biother Radiopharm* **23**, 222-228
168. Chen, Y. Y., Chiang, S. Y., Lin, J. G., Ma, Y. S., Liao, C. L., Weng, S. W., Lai, T. Y., and Chung, J. G. (2010) Emodin, aloe-emodin and rhein inhibit migration and invasion in human tongue cancer SCC-4 cells through the inhibition of gene expression of matrix metalloproteinase-9. *Int J Oncol* **36**, 1113-1120
169. Kaneshiro, T., Morioka, T., Inamine, M., Kinjo, T., Arakaki, J., Chiba, I., Sunagawa, N., Suzui, M., and Yoshimi, N. (2006) Anthraquinone derivative emodin inhibits tumor-associated angiogenesis through inhibition of extracellular signal-regulated kinase 1/2 phosphorylation. *Eur J Pharmacol* **553**, 46-53
170. Kwak, H. J., Park, M. J., Park, C. M., Moon, S. I., Yoo, D. H., Lee, H. C., Lee, S. H., Kim, M. S., Lee, H. W., Shin, W. S., Park, I. C., Rhee, C. H., and Hong, S. I. (2006) Emodin inhibits vascular endothelial growth factor-A-induced angiogenesis by blocking receptor-2 (KDR/Flk-1) phosphorylation. *Int J Cancer* **118**, 2711-2720

171. Tong, H., Chen, K., Chen, H., Wu, H., Lin, H., Ni, Z., and Lin, S. Emodin prolongs recipient survival time after orthotopic liver transplantation in rats by polarizing the Th1/Th2 paradigm to Th2. *Anat Rec (Hoboken)* **294**, 445-452
172. Tomar, S., Graves, C. A., Altomare, D., Kowli, S., Kassler, S., Sutkowski, N., Gillespie, M. B., Creek, K. E., and Pirisi, L. (2015) Human papillomavirus status and gene expression profiles of oropharyngeal and oral cancers from European American and African American patients. *Head Neck*
173. Martinez, F. O., Gordon, S., Locati, M., and Mantovani, A. (2006) Transcriptional profiling of the human monocyte-to-macrophage differentiation and polarization: new molecules and patterns of gene expression. *J Immunol* **177**, 7303-7311
174. Whyte, C. S., Bishop, E. T., Ruckerl, D., Gaspar-Pereira, S., Barker, R. N., Allen, J. E., Rees, A. J., and Wilson, H. M. (2011) Suppressor of cytokine signaling (SOCS)1 is a key determinant of differential macrophage activation and function. *J Leukoc Biol* **90**, 845-854
175. Xaus, J., Cardo, M., Valledor, A. F., Soler, C., Lloberas, J., and Celada, A. (1999) Interferon gamma induces the expression of p21waf-1 and arrests macrophage cell cycle, preventing induction of apoptosis. *Immunity* **11**, 103-113
176. Lloberas, J., and Celada, A. (2009) p21(waf1/CIP1), a CDK inhibitor and a negative feedback system that controls macrophage activation. *Eur J Immunol* **39**, 691-694
177. Ni, Q., Sun, K., Chen, G., and Shang, D. In vitro effects of emodin on peritoneal macrophages that express membrane-bound CD14 protein in a rat model of severe acute pancreatitis/systemic inflammatory response syndrome. *Mol Med Rep* **9**, 355-359
178. Saeed, S., Quintin, J., Kerstens, H. H., Rao, N. A., Aghajanirefah, A., Matarese, F., Cheng, S. C., Ratter, J., Berentsen, K., van der Ent, M. A., Sharifi, N., Janssen-Megens, E. M., Ter Huurne, M., Mandoli, A., van Schaik, T., Ng, A., Burden, F., Downes, K., Frontini, M., Kumar, V., Giamarellos-Bourboulis, E. J., Ouwehand, W. H., van der Meer, J. W., Joosten, L. A., Wijmenga, C., Martens, J. H., Xavier, R. J., Logie, C., Netea, M. G., and Stunnenberg, H. G. (2014) Epigenetic programming of monocyte-to-macrophage differentiation and trained innate immunity. *Science* **345**, 1251086
179. Wang, T., Zhong, X. G., Li, Y. H., Jia, X., Zhang, S. J., Gao, Y. S., Liu, M., and Wu, R. H. (2014) Protective effect of emodin against airway inflammation in the ovalbumin-induced mouse model. *Chin J Integr Med*
180. Zheng, Y., Qin, H., Frank, S. J., Deng, L., Litchfield, D. W., Tefferi, A., Pardanani, A., Lin, F. T., Li, J., Sha, B., and Benveniste, E. N. (2011) A CK2-dependent mechanism for activation of the JAK-STAT signaling pathway. *Blood* **118**, 156-166
181. Subramaniam, A., Shanmugam, M. K., Ong, T. H., Li, F., Perumal, E., Chen, L., Vali, S., Abbasi, T., Kapoor, S., Ahn, K. S., Kumar, A. P., Hui, K. M., and Sethi, G. (2013) Emodin inhibits growth and induces apoptosis in an orthotopic hepatocellular carcinoma model by blocking activation of STAT3. *Br J Pharmacol* **170**, 807-821

182. El Chartouni, C., Schwarzfischer, L., and Rehli, M. Interleukin-4 induced interferon regulatory factor (Irf) 4 participates in the regulation of alternative macrophage priming. *Immunobiology* **215**, 821-825
183. DeSantis, C., Ma, J., Bryan, L., and Jemal, A. (2013) Breast cancer statistics, 2013. *CA Cancer J Clin* **64**, 52-62
184. Schouppe, E., De Baetselier, P., Van Ginderachter, J. A., and Sarukhan, A. Instruction of myeloid cells by the tumor microenvironment: Open questions on the dynamics and plasticity of different tumor-associated myeloid cell populations. *Oncoimmunology* **1**, 1135-1145
185. Tang, H., Qiao, J., and Fu, Y. X. (2016) Immunotherapy and tumor microenvironment. *Cancer Lett* **370**, 85-90
186. Weber, J. S., Yang, J. C., Atkins, M. B., and Disis, M. L. (2015) Toxicities of Immunotherapy for the Practitioner. *J Clin Oncol* **33**, 2092-2099
187. Gabrilovich, D. I., Ostrand-Rosenberg, S., and Bronte, V. (2012) Coordinated regulation of myeloid cells by tumours. *Nat Rev Immunol* **12**, 253-268
188. Stagg, J., and Allard, B. (2013) Immunotherapeutic approaches in triple-negative breast cancer: latest research and clinical prospects. *Ther Adv Med Oncol* **5**, 169-181
189. Singh, M., Ramos, I., Asafu-Adjei, D., Quispe-Tintaya, W., Chandra, D., Jahangir, A., Zang, X., Aggarwal, B. B., and Gravekamp, C. Curcumin improves the therapeutic efficacy of Listeria(at)-Mage-b vaccine in correlation with improved T-cell responses in blood of a triple-negative breast cancer model 4T1. *Cancer Med* **2**, 571-582
190. Kim, K., Skora, A. D., Li, Z., Liu, Q., Tam, A. J., Blosser, R. L., Diaz, L. A., Jr., Papadopoulos, N., Kinzler, K. W., Vogelstein, B., and Zhou, S. (2014) Eradication of metastatic mouse cancers resistant to immune checkpoint blockade by suppression of myeloid-derived cells. *Proc Natl Acad Sci U S A* **111**, 11774-11779
191. Casey, A. E., Laster, W. R., Jr., and Ross, G. L. (1951) Sustained enhanced growth of carcinoma EO771 in C57 black mice. *Proc Soc Exp Biol Med* **77**, 358-362
192. Nachat-Kappes, R., Pinel, A., Combe, K., Lamas, B., Farges, M. C., Rossary, A., Goncalves-Mendes, N., Caldefie-Chezet, F., Vasson, M. P., and Basu, S. (2012) Effects of enriched environment on COX-2, leptin and eicosanoids in a mouse model of breast cancer. *PLoS One* **7**, e51525
193. Wang, J., Yu, F., Jia, X., Iwanowycz, S., Wang, Y., Huang, S., Ai, W., and Fan, D. MicroRNA-155 deficiency enhances the recruitment and functions of myeloid-derived suppressor cells in tumor microenvironment and promotes solid tumor growth. *Int J Cancer* **136**, E602-613
194. Qian, B. Z., and Pollard, J. W. (2010) Macrophage diversity enhances tumor progression and metastasis. *Cell* **141**, 39-51
195. Casey, S. C., Amedei, A., Aquilano, K., Azmi, A. S., Benencia, F., Bhakta, D., Bilsland, A. E., Boosani, C. S., Chen, S., Ciriolo, M. R., Crawford, S., Fujii, H., Georgakilas, A. G., Guha, G., Halicka, D., Helferich, W. G., Heneberg, P., Honoki, K., Keith, W. N., Kerkar, S. P., Mohammed, S. I., Niccolai, E., Nowsheen, S., Vasantha Rupasinghe, H. P., Samadi, A., Singh, N., Talib, W. H.,

Venkateswaran, V., Whelan, R. L., Yang, X., and Felsher, D. W. (2015) Cancer prevention and therapy through the modulation of the tumor microenvironment. *Semin Cancer Biol*

196. Chaturvedi, P., Gilkes, D. M., Wong, C. C., Luo, W., Zhang, H., Wei, H., Takano, N., Schito, L., Levchenko, A., and Semenza, G. L. (2013) Hypoxia-inducible factor-dependent breast cancer-mesenchymal stem cell bidirectional signaling promotes metastasis. *J Clin Invest* **123**, 189-205
197. Wei, W. T., Lin, S. Z., Liu, D. L., and Wang, Z. H. The distinct mechanisms of the antitumor activity of emodin in different types of cancer (Review). *Oncol Rep* **30**, 2555-2562
198. Lin, S. Z., Wei, W. T., Chen, H., Chen, K. J., Tong, H. F., Wang, Z. H., Ni, Z. L., Liu, H. B., Guo, H. C., and Liu, D. L. (2012) Antitumor activity of emodin against pancreatic cancer depends on its dual role: promotion of apoptosis and suppression of angiogenesis. *PLoS One* **7**, e42146
199. Qu, K., Shen, N. Y., Xu, X. S., Su, H. B., Wei, J. C., Tai, M. H., Meng, F. D., Zhou, L., Zhang, Y. L., and Liu, C. (2013) Emodin induces human T cell apoptosis in vitro by ROS-mediated endoplasmic reticulum stress and mitochondrial dysfunction. *Acta Pharmacol Sin* **34**, 1217-1228
200. Schmieder, A., Michel, J., Schonhaar, K., Goerdt, S., and Schledzewski, K. Differentiation and gene expression profile of tumor-associated macrophages. *Semin Cancer Biol* **22**, 289-297
201. Marigo, I., Bosio, E., Solito, S., Mesa, C., Fernandez, A., Dolcetti, L., Ugel, S., Sonda, N., Bicciato, S., Falisi, E., Calabrese, F., Basso, G., Zanovello, P., Cozzi, E., Mandruzzato, S., and Bronte, V. (2010) Tumor-induced tolerance and immune suppression depend on the C/EBPbeta transcription factor. *Immunity* **32**, 790-802
202. Huang, Q., Shen, H. M., Shui, G., Wenk, M. R., and Ong, C. N. (2006) Emodin inhibits tumor cell adhesion through disruption of the membrane lipid Raft-associated integrin signaling pathway. *Cancer Res* **66**, 5807-5815
203. Kumar, A., Dhawan, S., and Aggarwal, B. B. (1998) Emodin (3-methyl-1,6,8-trihydroxyanthraquinone) inhibits TNF-induced NF-kappaB activation, IkappaB degradation, and expression of cell surface adhesion proteins in human vascular endothelial cells. *Oncogene* **17**, 913-918
204. Mantovani, A., Garlanda, C., and Locati, M. (2009) Macrophage diversity and polarization in atherosclerosis: a question of balance. *Arterioscler Thromb Vasc Biol* **29**, 1419-1423
205. Troidl, C., Mollmann, H., Nef, H., Masseli, F., Voss, S., Szardien, S., Willmer, M., Rolf, A., Rixe, J., Troidl, K., Kostin, S., Hamm, C., and Elsasser, A. (2009) Classically and alternatively activated macrophages contribute to tissue remodelling after myocardial infarction. *J Cell Mol Med* **13**, 3485-3496
206. Vinogradov, S., Warren, G., and Wei, X. (2014) Macrophages associated with tumors as potential targets and therapeutic intermediates. *Nanomedicine (Lond)* **9**, 695-707
207. Zanardi, E., Bregni, G., de Braud, F., and Di Cosimo, S. (2015) Better Together: Targeted Combination Therapies in Breast Cancer. *Semin Oncol* **42**, 887-895
208. Lin, S. Z., Chen, K. J., Tong, H. F., Jing, H., Li, H., and Zheng, S. S. (2010) Emodin attenuates acute rejection of liver allografts by inhibiting hepatocellular

apoptosis and modulating the Th1/Th2 balance in rats. *Clin Exp Pharmacol Physiol* **37**, 790-794
209. Cha, T. L., Chuang, M. J., Tang, S. H., Wu, S. T., Sun, K. H., Chen, T. T., Sun, G. H., Chang, S. Y., Yu, C. P., Ho, J. Y., Liu, S. Y., Huang, S. M., and Yu, D. S. (2013) Emodin modulates epigenetic modifications and suppresses bladder carcinoma cell growth. *Mol Carcinog* **54**, 167-177
210. Netea, M. G., Quintin, J., and van der Meer, J. W. Trained immunity: a memory for innate host defense. *Cell Host Microbe* **9**, 355-361
211. Blok, B. A., Arts, R. J., van Crevel, R., Benn, C. S., and Netea, M. G. Trained innate immunity as underlying mechanism for the long-term, nonspecific effects of vaccines. *J Leukoc Biol* **98**, 347-356
212. Cheng, S. C., Quintin, J., Cramer, R. A., Shepardson, K. M., Saeed, S., Kumar, V., Giamarellos-Bourboulis, E. J., Martens, J. H., Rao, N. A., Aghajanirefah, A., Manjeri, G. R., Li, Y., Ifrim, D. C., Arts, R. J., van der Veer, B. M., Deen, P. M., Logie, C., O'Neill, L. A., Willems, P., van de Veerdonk, F. L., van der Meer, J. W., Ng, A., Joosten, L. A., Wijmenga, C., Stunnenberg, H. G., Xavier, R. J., and Netea, M. G. (2014) mTOR- and HIF-1alpha-mediated aerobic glycolysis as metabolic basis for trained immunity. *Science* **345**, 1250684
213. Long, K. B., and Beatty, G. L. (2013) Harnessing the antitumor potential of macrophages for cancer immunotherapy. *Oncoimmunology* **2**, e26860
214. Singh, M., Ramos, I., Asafu-Adjei, D., Quispe-Tintaya, W., Chandra, D., Jahangir, A., Zang, X., Aggarwal, B. B., and Gravekamp, C. (2013) Curcumin improves the therapeutic efficacy of Listeria(at)-Mage-b vaccine in correlation with improved T-cell responses in blood of a triple-negative breast cancer model 4T1. *Cancer Med* **2**, 571-582
215. Fridlender, Z. G., Jassar, A., Mishalian, I., Wang, L. C., Kapoor, V., Cheng, G., Sun, J., Singhal, S., Levy, L., and Albelda, S. M. (2013) Using macrophage activation to augment immunotherapy of established tumours. *Br J Cancer* **108**, 1288-1297
216. Bekkering, S., Joosten, L. A., van der Meer, J. W., Netea, M. G., and Riksen, N. P. (2015) The epigenetic memory of monocytes and macrophages as a novel drug target in atherosclerosis. *Clin Ther* **37**, 914-923
217. Netea, M. G., Latz, E., Mills, K. H., and O'Neill, L. A. (2015) Innate immune memory: a paradigm shift in understanding host defense. *Nat Immunol* **16**, 675-679